Type 3 Innate Lymphoid Cells Acquire a Cytotoxic Program upon Stimulation with Interleukins 12 and 15

Dissertation

zur
Erlangung der naturwissenschaftlichen Doktorwürde
(Dr. sc. nat.)

vorgelegt der
Mathematisch-naturwissenschaftlichen Fakultät
der
Universität Zürich
von

Ana Raykova

aus
Bulgarien

Promotionskommission

Prof. Dr. Christian Münz
(Vorsitz un Leitung der Dissertation)
Prof. Dr. Burkhard Becher
Prof. Dr. Maries van den Broek

Zürich, 2017

Table of Contents

Table of Contents **1**
Figures and Tables **2**
Zusammenfassung **3**
Summary **5**
Introduction **7**
I. Human immune system overview 7
II. Innate lymphoid cells overview 7
III. ILC development 9
A. In mice 9
1. Development 9
2. Cytokine requirements 13
B. In humans 15
1. Development 15
2. Cytokine requirements 19
IV. ILC subsets and their characteristics 20
A. Group 1 ILCs 20
1. NK cells 20
2. Helper ILC1s cells 24
B. Group 2 ILCs 26
C. Group 3 ILCs 26
V. Role of ILC1s and ILC3s at steady state and disease 27
A. Role of NK cells 27
B. Role of hILC1s 28
C. Role of ILC3s 29
VI. Plasticity of hILCs 32
A. In mice 32
B. In humans 32
VII. Mice reconstituted with human immune system components 35
VIII. EBV 36
Aim of the study **38**
Results **39**
I. ILC3s in tonsils and humanized mouse tissues 39
II. ILC3s up-regulate NK cell markers in response to IL-12 and/or IL-15 41
III. Transcriptional profile of NKp44$^+$ ILC3s upon IL-12 and IL-15 culture is reminiscent of early differentiated NK cells 47
IV. Stimulation with IL-12 and IL-15 induces a functional program of NK cells in ILC3s 52
A. Acquisition of an ILC1 cytokine profile upon IL-12 and IL-15 stimulation 52
B. Up-regulation of cytotoxic molecules and degranulation in response to classical NK cell targets upon IL-12 and IL-15 exposure 54
C. Cytotoxicity of IL-12 and IL-15 cultured ILC3s towards classical NK cell targets and correlation with NK-related markers 56
V. NKp44$^+$ ILC3s might differentiate into CD94-expressing cells *in vivo* 62
VI. NKp44$^+$ ILC3s seem not to affect EBV disease progression *in vivo* 64
Discussion **66**
Materials and Methods **73**
Appendix **85**
Abbreviations **88**
Declaration **90**
References **91**
Acknowledgements **102**

Figures and Tables

Figure A Simplified overview of human ILC subset characteristics 8
Figure B Model of murine ILC development 11
Figure C Model of human ILC development 17
Figure 1 ILC3 cells in tonsils and humanized mouse tissues 40
Figure 2 IL-12 induces expression of NK cell markers in IL-2 and IL-7 expanded tonsil-derived NKp44^{+} ILC3s 42
Figure 3 Plasticity of NKp44^{+} ILC3s 43
Figure 4 IL-12 and IL-15 promote expression of phenotypic NK cell markers on ILC3s 44
Figure 5 Transcriptional profile of NKp44^{+} ILC3s upon IL-12 and IL-15 culture is reminiscent of early differentiated NK cells 49
Figure 6 Acquisition of an ILC1 cytokine profile in spleen-derived NKp44^{+} ILC3s upon IL-12 and IL-15 stimulation 53
Figure 7 Up-regulation of cytotoxic machinery in spleen-derived NKp44^{+} ILC3s upon IL-12 and IL-15 exposure and degranulation in response to classical NK cell targets K562 55
Figure 8 Cytotoxicity of IL-12 and IL-15 cultured ILC3s towards classical NK cell targets K562 and correlation with differentiated ILC3s 58
Figure 9 NKp44^{+} ILC3s might differentiate into CD94-expressing cells *in vivo* 63
Figure 10 NKp44^{+} ILC3s seem not to affect EBV disease progression *in vivo* 65
Figure 11 Reconstitution of human immune system components in huNSG and HLA-A2 huNSG used for ILC3 purification. 76
Figure 12 Reconstitution and group distribution of humanized mice used for adoptive transfer EBV experiments 74
Table 1 Tonsil samples details 75
Table 2 Humanized mouse samples details 79
Table 3 List of antibodies used in flow cytometry 79
Figure 13 Expression of lineage-specific transcription factors in the purified ILC populations 85
Figure 14 Frequency of CD16^{+}CD56^{+} among Eomes-expressing CD94^{+} or CD94^{-} cells 85
Figure 15 GSEA analysis for tonsillar NKp44^{+} ILC3s 86
Figure 16 Analysis of putative ILC1s 87

Zusammenfassung

Typ 3 natürliche lymphoide Zellen (type 3 innate lymphoid cells, ILC3s) unterstützen sowohl Gewebshomöostase als auch -schutz, massgeblich an Schleimhautoberflächen. Ihr Profil wird eng vom Gewebeumfeld kontrolliert und kann durch ein Entzündungsmilieu zur Produktion des Typ 1 Zytokins IFNg angeregt werden. Wahrscheinlich weil in Mäusen ILC3s und natürliche Killerzellen (NK) in ihrer Entwicklung innerhalb der Familie der natürlichen Lymphozyten unterschiedlicher Abstammung sind, ist die Frage der Plastizität von ILCs bezüglich zytotoxischer Funktionen bisher vernachlässigt worden. Da RORgt exprimierende Vorläufer jedoch im Menschen zur Entstehung von NK Zellen beitragen, zielten wir in der hier vorgelegten Arbeit darauf ab, diese Wissenslücke sowohl *in vitro* als auch *in vivo*, in humanisierten Mäusen, zu schliessen.

Wir konnten zeigen, dass humane ILC3s nach Zugabe von IL-12 und IL-15 die Expression des Hauptregulators für zytotoxische Funktionen EOMES und auch, in geringerem Masse, den Typ 1 Immunitätstranskriptionfaktor T-bet, hochregulieren. Transkriptions- und durchflusszytometrische Analysen ergaben die Aneignung von NK Schlüsseleigenschaften wie der Expression von CD94, NKG2A, NKG2C, CD56 und CD16, sowie eine erhöhte Antwortbereitschaft gegenüber IL-2, IL-12 und IL-15. Funktionell erwerben expandierte ILC3s die Eigenschaft IFNg neben anderen NK Zell-assoziierten Zytokinen und Chemokinen zu produzieren. Zusätzlich exprimieren sie zytolytische Effektormoleküle wie Granzyme und Perforin, und üben eine zytotoxische Antwort gegen die klassische NK Zielzelle K562 aus. Sie zeigen im Vergleich zu konventionellen NK Zellen eine langsamere und niedrigere zytolytische Aktivität, wahrscheinlich als ein Resultat geringerer Aktivierung oder unterschiedlicher zytolytischer Mechanismen. Wichtigerweise haben wir Unterschiede im zytotoxischen Potential zwischen Mandel- und Milz-ILC3s beobachtet, die auf eine gewebsspezifische Prägung hinweisen könnten. Zusätzlich erhält ein Teil der ILC3s ihren Phänotyp trotz entzündungsbedingter Reize, was darauf

hindeutet, dass nicht alle ILC3s in der Lage sind mit einer Differenzierung auf Entzündung zu antworten.

In Anbetracht dieser Befunde und da auch $CD4^+$ Helfer-T-Zellen ein zytotoxisches Programm während symptomatischer Epstein Barr Virus (EBV) aktivieren können, haben wir ILC3s *in vivo* unter EBV induzierten entzündlichen Konditionen untersucht. Eine kurzfristige Stimulation autologer unmanipulierter ILC3s unter diesen Bedingungen schien die Expression von CD94 zu induzieren. Allerdings hatte der Transfer IL-2 und IL-7 expandierter ILC3s vor Virusgabe keine konsistenten Effekte auf die EBV Infektion und Pathogenese, was allerdings am Verlust der transferierten Zellen liegen könnte.

Da ILC3s ebenso häufig wie NK Zellen an Schleimhautoberflächen vorkommen, könnten diese eine schnelle Quelle zytotoxischer Vorläuferzellen darstellen. Diese Fähigkeit könnte für die Immuntherapie in Virusinfektionen oder Krebserkrankungen ausgenutzt werden, in Anbetracht dessen sind weitere *in vivo* Untersuchungen zum Schicksal und der funktionellen Kapazität der ILC3s während einer Entzündung notwendig.

Summary

Type 3 innate lymphoid cells (ILCs) mediate tissue homeostasis and protection, primarily at mucosal sites. Their profile is tightly controlled by the tissue microenvironment and can shift toward production of the type 1 cytokine IFNγ in an inflammatory setting. Likely because ILC3 and natural killer (NK) cells are developmentally divergent innate lymphocyte lineages in mice, the plasticity of ILC3s with respect to cytotoxic function has been neglected. Since RORγt-expressing progenitors, however, contribute to NK cell generation in humans, we aimed to address this knowledge gap both *in vitro* and *in vivo*, using humanized mice.

We could demonstrate that after exposure to IL-12 and IL-15, human ILC3s up-regulate expression of the master regulator of cytotoxic function Eomes and also the type 1 immunity associated transcription factor T-bet, albeit to a lesser extent. Transcriptional profiling and flow cytometric analysis revealed acquisition of key NK cell features like expression of CD94, NKG2A, NKG2C, CD56 and CD16 as well as enhanced responsiveness towards IL-2, IL-12 and IL-15. Functionally, expanded ILC3s gain the capacity to produce IFNγ among other NK cell-associated cytokines and chemokines. In addition, they express cytolytic effector molecules such as granzymes and perforin and mount a cytotoxic response against the classical NK target cell line K562. They show slower and lower cytolytic activity compared to conventional NK cells, likely as a result of a less potent activation or a distinct cytolytic mechanism. Importantly, we observed differences in cytotoxic potential between tonsil and spleen ILC3 subsets, which might indicate tissue-specific imprinting. In addition, a fraction of the ILC3s retains their phenotype despite the presence of inflammatory cues, which suggests that not all ILC3s are primed to respond with a differentiation program to inflammation.

In light of these findings and as helper $CD4^+$ T cells can also switch on a cytotoxic program in symptomatic Epstein Barr virus (EBV) infection, we studied ILC3s *in vivo* under EBV-driven inflammatory conditions. A short-term exposure of autologous unmanipulated ILC3s in that setting seems to induce expression of

CD94. However, transfer of IL-2 and IL-7 expanded ILC3s prior to virus inoculation had no consistent effects on EBV infection and pathogenesis, which though could be due to loss of the transferred cells over prolonged periods of time.

As ILC3s are as abundant as NK cells at mucosal sites, they could be a rapid source of cytotoxic precursors. This capacity might be exploited for immunotherapy in virus infections or cancer and hence further *in vivo* investigation into the fate and functional capacity of ILC3s during inflammation is required.

Introduction

I. Human immune system overview

Human immune responses are classically divided into two branches, innate and adaptive. The innate arm of immunity, including complement, phagocytic leukocytes and innate lymphoid cells, is rapidly mobilized, broadly specific as it relies on germ line-encoded receptors and generally short-lived. It not only serves as a first line of defense against invading pathogens but also modulates the development of an appropriate adaptive response, mediated by B and T lymphocytes. These cells undergo a process termed somatic recombination – the random gene rearrangements in the immunoglobulin and T cell receptor (TCR) loci, which create a diverse repertoire of highly specific receptors with the potential to recognize a vast array of pathogens. Adaptive immunity is thus characterized by specific antigen recognition. Moreover, it is able to generate a faster and more vigorous response upon rechallenge, i.e. to form memory (Murphy and Weaver, 2016). This view of the immune system as two separate branches however is oversimplified, as there is a constant and complex interplay between the innate and adaptive systems, whose boundaries become blurred with discoveries of lymphocytes with innate-like features like γδ T cells or studies of natural killer (NK) cells showing memory-like behavior (Lanier and Sun, 2009).

II. Innate lymphoid cells (ILCs) overview

ILCs are innate effectors with important roles in inflammation, defense against pathogens or transformed cells as well as tissue homeostasis and remodeling. They have lymphoid morphology and originate from a common lymphoid progenitor (CLP) but are independent of recombination-activating genes (RAGs) activity and are negative for lineage (Lin) markers such as CD3. The ILC family comprises NK cells and the recently identified helper populations. The latter are regarded as innate counterparts of T helper (Th) cells and based

on their cytokine profile and transcription factor expression are divided into group 1 (ILC1; Th1-like), group 2 (ILC2; Th2-like) and group 3 (ILC3; Th17/22-like). NK cells are classified as ILC1s but are segregated from the rest due to their cytotoxic properties (Figure A) (Gronke et al., 2016; Vivier et al., 2016). ILCs have strict tissue division at steady state with NK cells constituting the majority of ILCs (> 95%) in peripheral blood (PB), spleen and bone marrow (BM), whereas in barrier tissues (tonsil, adenoid, skin, but not lung) other ILCs prevail. Importantly, ILCs are highly heterogeneous in frequency as well as phenotype across tissues and individuals, indicating flexibility governed by environmental and/or genetic factors (Simoni et al., 2017).

This project focuses on ILC3 and ILC1 cell types, therefore ILC2s are not described in detail.

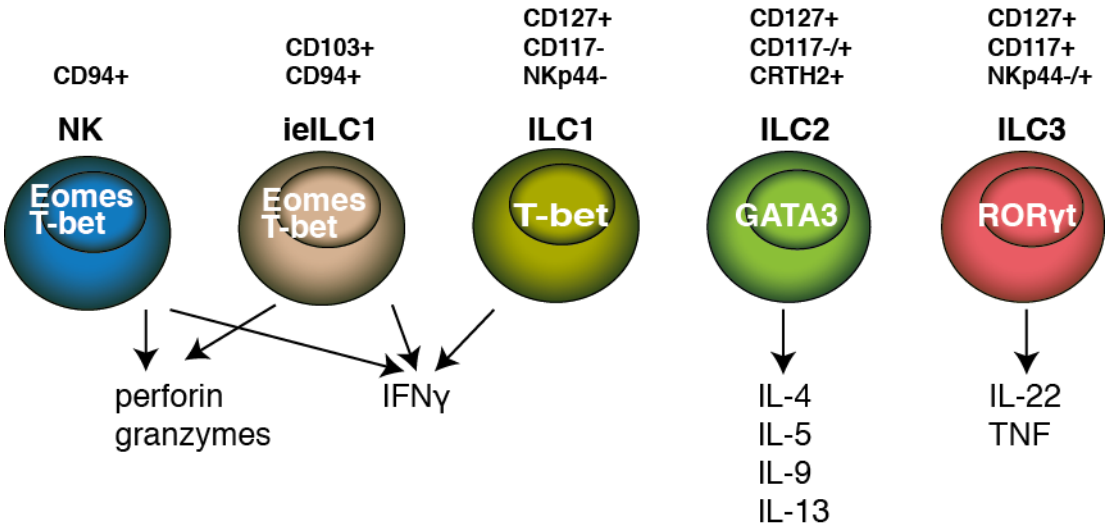

Figure A Simplified overview of human ILC subset characteristics
The ILC family is comprised of 3 subgroups. Type 1 cells are characterized by T-bet expression and secretion of the Th1 cytokine IFNγ. NK cells and intraepithelial (ie)ILC1 belong to this group, but are distinguished by their cytotoxic properties contributed to Eomes expression. Type 2 cells express GATA3 and produce Th2 cytokines. Type 3 cells express RORγt and are characterized by IL-22 secretion. Markers defining the human ILCs subsets are indicated above. Figure is based on (Mjösberg and Spits, 2016)

III. ILC development

A. In mice

1. Development

ILCs derive from hematopoietic stem cells (HSCs) through a CLP, a developmental intermediate that has lost the potential to produce myeloid or erythroid lineages. Further commitment to the ILC fate has been extensively studied in recent years and a diverging point of innate and adaptive lymphocytes has been identified in murine bone marrow (BM) among integrin $\alpha4\beta7^+$ lymphoid progenitors (αLPs), which have lost FMS-like tyrosine kinase 3 (Flt3) expression (Gronke et al., 2016). This early ILC progenitor (EILP) has high levels of T cell factor 1 (TCF-1, encoded by *Tcf7*), a protein associated so far with T cell fate specification, low or no expression of IL-7Rα (CD127) (unlike the CLP: Lin^- Sca-1^{lo}c-kit(CD117)^{lo}Flt3^+IL-$7R\alpha^+$) and many transcripts for *Nfil3* and *Tox*, encoding crucial drivers of ILC development. The EILP has no capacity for T or B cell generation but can give rise to all four ILC subsets as well as dendritic cells (DCs). Despite evidence for compensatory mechanisms, data from mixed BM chimeras with *Tcf7*$^{-/-}$ LSK (Lin^-Sca-1^+c-Kit^+) progenitors, a population that includes HSCs, suggests that the predominant pathway of ILC differentiation under steady state conditions is TCF-1–dependent (Yang et al., 2015). A separate IL-$7R\alpha^+$ ILC committed precursor has been described in mouse fetal liver (FL) and BM that through successive expression of α4β7 and CXCR6 loses B and T cell potential, respectively (Possot et al., 2011). Downstream of these progenitors, there is evidence for a branching event where the development pathways of conventional (c)NK cells, defined as cytotoxic eomesodermin $(Eomes)^+$ cells, and the rest of the ILCs diverge. For example, GATA-3 ablation within the hematopoietic system (using Vav-Cre mice) results in loss of all $CD127^+$ ILCs whereas splenic cNK cells are not significantly affected. This seems to be due to an arrest in development as αLP (but not CLP) numbers are greatly diminished in fetal liver and although all $CD127^+$ ILCs express GATA3 (albeit at different levels), its inactivation in already mature cells leads to reduction only in ILC2s, the latter demonstrating its requirement in ILC2 maintenance (Yagi et al., 2014).

Notably, the drastic effect of GATA3 on αLPs but not cNK cells (no assessment of functionality), suggests existence of an alternative pathway of NK cell development. Moreover, a common helper-like ILC precursor (CHILP) has recently been described among BM cells that is $Lin^{-}Sca\text{-}1^{lo}c\text{-}kit^{+}Flt3^{-}\alpha4\beta7^{+}IL\text{-}7R\alpha^{+}CD25^{-}CD27^{+}CD224(2B4)^{+}$ and expresses inhibitor of DNA binding 2 (Id2), a transcriptional repressor of E proteins, which control early T and B cell development. The progeny of CHILPs after adoptive transfer *in vivo* was found mainly in the small intestine and liver, consistent with its expression of the mucosal-homing integrin α4β7, and comprised all ILCs with the exception of $Eomes^{+}$ NK cells. Of note, whether the $NKp46^{+}T\text{-}bet^{+}ROR\gamma t^{-}$ population was derived from plastic ILC3s (discussed below) or represented a separate ILC1 lineage was not investigated *in vivo* but ILC1-only wells were generated in clonal cultures (3 weeks on OP9-DL1 plus IL-2, IL-7 and stem cell factor (SCF, c-kit ligand)) (unclear whether gated for Eomes) (Klose et al., 2014). Additional restriction in the helper ILC lineage choices is induced by the promyelocytic leukemia zinc finger (PLZF, encoded by *Zbtb16*), whose expression represses lymphoid tissue inducer (LTi) cell potential (Constantinides et al., 2015). Further differentiation is mediated by the expression of lineage-defining transcription factors. An overview of the described developmental stages is shown in Figure B.

Differentiation towards ILC3s is dependent on RAR-related orphan receptor gamma (RORγt). This was early demonstrated for LTis as RORγt-deficient mice lack this subset as well as lymphoid structures, such as lymph nodes (LNs) and Peyer's patches (PPs). Concurrently, during fetal life RORγt was found to be exclusively expressed in $CD127^{+}$ cells, which represent LTis or their precursors (Eberl et al., 2004). Interestingly, fetal $\alpha4\beta7^{+}ROR\gamma t^{+}$ precursors isolated from gut, in contrast to liver, already express transcripts for proteins like LTα, TRANCE, IL-17a, suggesting functional maturation within the tissues (Cherrier et al., 2012). Using an inducible RORγt fate map (fm) system, Sawa et al showed that fetal and perinatal $ROR\gamma t^{+}CD3\varepsilon^{-}$ cells could give rise to adult ILC3s, which are preferentially found in the lamina propria (LP) (Sawa et al., 2010).

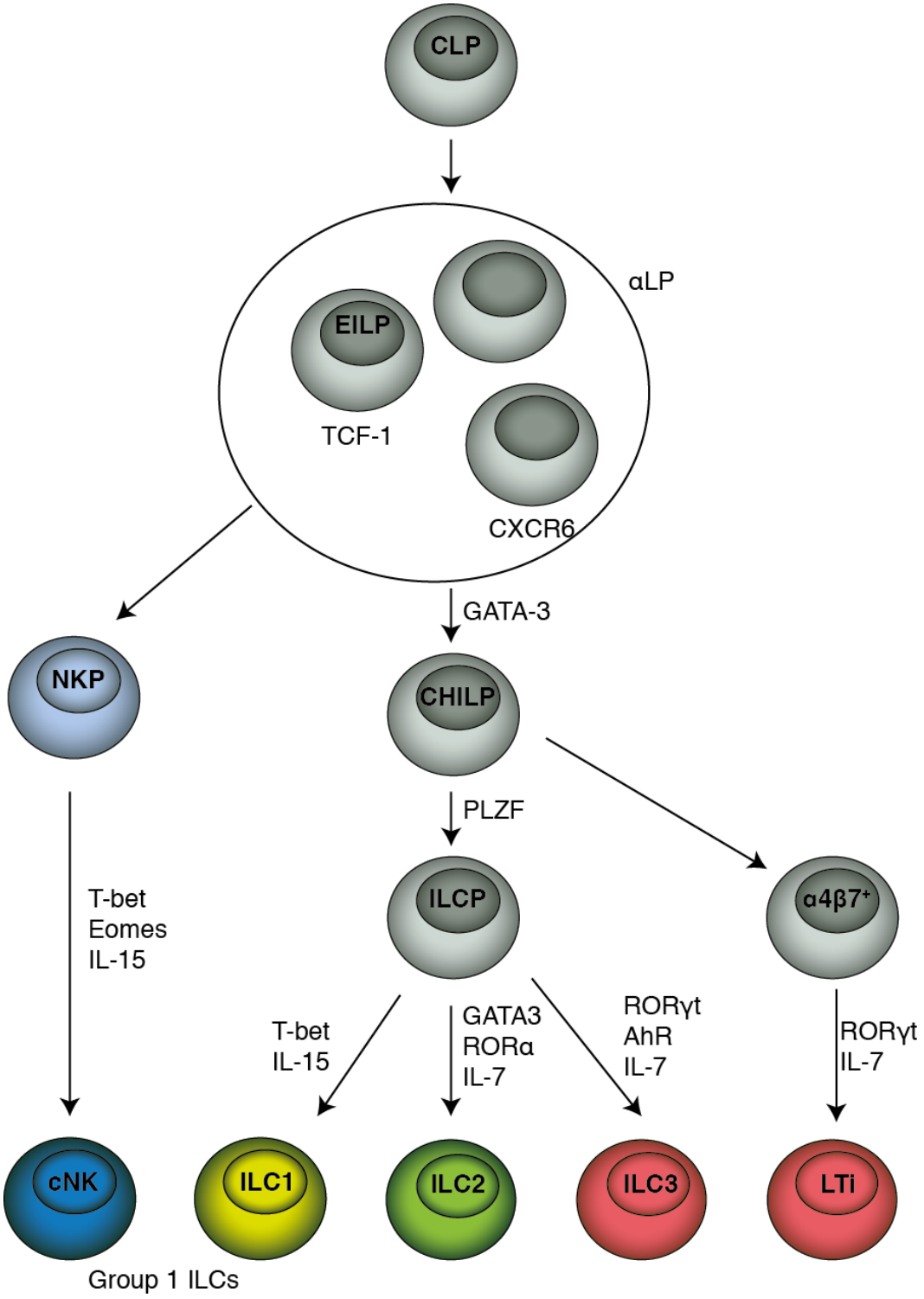

Figure B Model of murine ILC development
ILCs derive from a CLP. Precursors to all ILC lineages are found among α4β7+ lymphoid progenitors (αLPs). Downstream of these, cytotoxic and helper ILC development separates as only the latter are dependent on GATA3 and common helper-like ILC precursor (CHILP) was identified in BM. PLZF expression represses LTi potential and further lineage choices are based on the specific transcription factors for each subset. Figure is based on (Constantinides et al., 2015; Gronke et al., 2016; Klose et al., 2014; Possot et al., 2011; Yagi et al., 2014; Yang et al., 2015)

The majority of intestinal ILC3s at birth is positive for CCR6 (NKp46^{-} CD117^{hi}CD4$^{+/-}$) and resembles fetal LTi cells. Thereafter a CCR6^{-} population expands that contains an NKp46^{+}T-bet^{+} subset. To investigate their developmental relationship, Klose et al isolated each population from the small intestine of *Rorc*$^{Gfp/+}$ mice and transferred it into alymphoid animals. Whereas CCR6^{+} ILC3s remained negative for both markers, CCR6^{-} ILC3s up regulated T-bet, followed by NKp46. Notably, *Tbx21*$^{-/-}$ mice did not generate NKp46^{+} ILC3s (Klose et al., 2013). Helper (h)ILC1s were also absent (shown for LP), whereas their numbers remained normal in mice deficient in RORγt or Eomes (Klose et al., 2014). Hence, murine hILC1 development is dependent on the Th1-specific transcription factor T-bet, which is also required for the differentiation of NKp46^{+} ILC3s.

A BM progenitor with no B/T/DC potential but the ability to generate NK has also been reported. Its phenotype overlaps with the CHILP but for α4β7 expression, which or its capacity to generate other ILC subsets were not investigated (Fathman et al., 2011). Commitment towards the NK cell lineage is marked by acquisition of CD122 (IL-2/15Rβ) (Rosmaraki et al., 2001), which is essential for IL-15 signal transduction. The NK precursor (NKP) is itself independent of IL-15 and negative for NK-specific markers such as NK1.1 (Vosshenrich et al., 2005). Maturation to cNK cells is associated with acquisition of CD49b and variable expression Ly49 receptors as well as an increase in transcripts for perforin (encoded by *Prf1*). Eomes is critical for this step as *Eomes*$^{flox/flox}$*Vav-Cre*$^{+}$ mice have a drastic reduction in this population. Moreover, deletion of Eomes from mature NK cells results in reversion of this phenotype to NK1.1^{+}CD49b^{-}, indicating the latter constitutes a developmental intermediate (also shown *in vitro*) (Gordon et al., 2012). This NK1.1^{+}CD49b^{-} subset constitutively expresses the tumor necrosis factor (TNF)–related apoptosis-inducing ligand (TRAIL, encoded by *TNFSF10*), is present in the fetus and after birth persists predominantly in the liver (Gordon et al., 2012; Takeda et al., 2005) and its differentiation from the NKP and/or maintenance is dependent on T-bet (Gordon et al., 2012; Klose et al., 2014). Even though cNK cells can develop in absence of T-bet, with its close homologue Eomes being able to partially

substitute for its function (Daussy et al., 2014; Pikovskaya et al., 2016), compensatory mechanisms might account for this. With the identification of precursors that give rise to T-bet$^+$Eomes$^-$ but not Eomes$^+$ NK1.1$^+$ cells however (Constantinides et al., 2015; Klose et al., 2014; Yagi et al., 2014), it has been argued that these populations represent two distinct lineages, with the former being the so-called hILC1s. To establish whether a linear developmental relationship exists, several groups have performed adoptive transfer experiments of the hILC1 population under steady state conditions. When purified as Eomes$^-$ using *Eomes*$^{Gfp/+}$ reporter mice, the recovered cells kept their original phenotype (Daussy et al., 2014), whereas when purified as TRAIL$^+$(DX5$^-$) they showed tissue-specific differentiation with induction of CD49b and Eomes favored in spleen and BM, but restricted in liver (Gordon et al., 2012; Takeda et al., 2005). Daussy et al argued that differences arise from a minor Eomes$^+$ fraction within the TRAIL$^+$ population, but they also observed that BM microenvironment suppressed T-bet expression in spleen and liver-derived cells (Daussy et al., 2014). Curiously, ectopic expression of Eomes in T-bet$^+$ cells results in acquisition of CD49b and Ly49 receptors among hILC1s (Pikovskaya et al., 2016). Even though microenvironment dictates specific programs and cNK cells transition through an NK1.1$^+$CD49b$^-$ intermediate, this does not preclude cells with similar phenotype to originate from distinct progenitors. Thus, in mice NK cell development diverges from that of helper ILCs.

2. Cytokine requirements

Generation and homeostasis of NK cells requires IL-15. It binds a receptor composed of the subunits CD122 and CD132 (also know as common gamma chain, γ_c), both shared with IL-2 and required for signal transduction, and a third specific component IL15Rα, which increases the affinity of the complex for its ligand by 100-fold. IL-15 acts via a mechanism called trans-presentation, whereby cells bearing IL15Rα, expressed by hematopoietic and parenchymal cells, bind IL-15 and trans-present it to the responding cell. It has been demonstrated that the same cell must express both proteins, which form a complex before reaching the plasma membrane that is later shed from the

surface of presenting cells, reflecting the finding that all circulating IL-15 detected in mouse as well as human serum is coupled to IL15Rα. Mice deficient in IL-15 or its receptor components lack mature NK cells (among other populations) (Huntington, 2014). However, this defect was reversed in *IL15*$^{-/-}$ mice by exogenous administration of the cytokine (Di santo, 2006) as NKPs develop normally in the absence of γ_c cytokines (Vosshenrich et al., 2005). Recently, Ohs et al demonstrated that NK development can bypass γ_c signaling when exposed to the proinflammatory cytokine IL-12, e.g. during viral infection. The generated cells are however distinct from cNK cells; they display low surface levels of NK1.1 and NKp46 and exhibit a more immature profile as revealed by transcriptome analysis but are CD122$^+$CD49b$^+$Eomes$^+$ and exert tumor control (Ohs et al., 2016).

Single or combined deficiencies in IL-2, -4 and -7 (on a Rag$^{-/-}$ background) have been shown to have no impact on NK development or function (Vosshenrich et al., 2005). IL-7 however is required for ILC3 development and/or homeostasis. This dependence was revealed by analysis of intestinal ILC populations from mice deficient in IL-7, CD127 or CRLF2 (together with CD127 forms the thymic stromal lymphopoietin (TSLP) receptor). NKp46$^-$ ILC3s were virtually absent in CD127$^{-/-}$ mice, whereas only a partial (but significant) reduction was observed in the others, suggesting redundancy in IL-7 and TSLP roles (Vonarbourg et al., 2010). In contrast, NKp46$^+$ ILC3s were almost undetectable in mice lacking IL-7 or its receptor, with the few remaining being RORγt$^-$ (Satoh-Takayama et al., 2010). Furthermore, when adult mice were treated with α-CD127 blocking antibody (Ab) NKp46$^+$ ILC3 numbers as well as RORγt expression among the residual cells were diminished. Taken together, this demonstrated the role of IL-7 in their maintenance (Vonarbourg et al., 2010).

Although expression of CD127 is used to distinguish hILC1 from cNK cells, their numbers in knock-out (KO) mice are weakly affected (if at all), indicating that IL-7 is dispensable for their development. Like cNK cells though, they are dependent on IL-15 (et al., 2014a). Notably, ex-ILC3s are also greatly reduced in the absence of IL-15 (Klose et al., 2014), whereas their precursors NKp46$^+$ ILC3s are normally represented in *IL15*$^{-/-}$ mice (Satoh-Takayama et al., 2008) and local

IL-15 overexpression using transgenic (Tg) mice does not influence their numbers or RORγt expression (Satoh-Takayama et al., 2010).

Hence, IL-15 is required for the development of ILC1 populations, whereas ILC3s are dependent on IL-7 receptor signaling. Interestingly, cytotoxic unconventional NK cells can arise in the absence of IL-15 under inflammatory conditions (Ohs et al., 2016).

B. In humans

1. Development

Development of human ILCs is less well characterized with more available data on differentiation of NK cells, being the longest recognized member of the family. NK cell precursors have been detected exclusively among $CD34^{+/dim}CD45RA^{+}$ hematopoietic progenitor cells (HPCs), which represent the first stage in the NK cell differentiation model described by Freud et al. This model consists of four developmental intermediates that are naturally occurring in lymphoid tissues such as tonsils and LNs and are defined based on sequential acquisition of CD117 and CD94 and restriction in the T/DC potential (none generate B cells). These are stage 1 ($CD34^{+}CD117^{-}CD94^{-}$), stage 2 ($CD34^{+}CD117^{+}CD94^{-}$), stage 3 ($CD34^{-}CD117^{+}CD94^{-}$), and stage 4 ($CD34^{-}CD117^{+/-}CD94^{+}$) cells. Freshly isolated stage 3 cells show no perforin expression, cytotoxicity or IFNγ production and were regarded as immature NK cells, whereas stage 4 represent $CD56^{bright}$ mature NK cells (Freud et al., 2006).

With the description of ILC3s, it is now clear that stage 3 comprises a mixture of two populations or potentially (some) ILC3s give rise to NK cells. The latter hypothesis has been supported by the recent identification of a tonsillar $CD94^{+}NKp80^{-}$ population that has ILC3-associated characteristics. These so-called stage 4a cells have a surface phenotype intermediate between ILC3s and NK cells but are functionally more similar to ILC3s and do not yet express T-bet or Eomes, nevertheless *in vitro* and *in vivo* in the presence of IL-15 both stage 3 and 4a give rise to mature NK cells (Freud et al., 2016). Thus, despite strong evidence in mice that cNK development diverges from that of other ILCs, it

remains unclear how closely this reflects the human situation. In addition, lineage tracing studies have shown that cNK are RORγt-fm negative(Klose et al., 2014), yet Scoville et al observed expression of *RORC2* (which encodes RORγt) in stage 2 cells, with higher protein levels within an IL-1R1-expressing subset. This precursor ($Lin^{-}CD34^{+}CD45RA^{+}CD117^{+}IL\text{-}1R1^{+}$) is restricted towards the ILC lineage and gives rise to all subsets (Scoville et al., 2016). In concert with these findings low but consistent RORγt expression is detected in human PB (mRNA) and tonsillar $CD56^{bright}$ NK cells (Scoville et al., 2016) as well as in ILC2s (Mjösberg et al., 2011). These results however are not in agreement with data from Montaldo et al., which demonstrated that tonsil stage 2 cells are lineage-specified progenitors to ILC3s. In that study CD117 was defined as a surrogate marker for RORγt expression, the latter confined to $CD34^{+}$ progenitors derived from tonsils and intestinal lamina propria but not umbilical cord blood (UCB), BM or thymus. Tonsil $CD34^{dim}CD117^{+}$ cells had a transcriptome profile closer to ILC3s than NK cells, which by itself does not preclude NK cells being downstream of ILC3s in development, but they differentiated selectively towards ILC3s, with the few NK cells arguably derived from $ROR\gamma t^{-}$ cells within these precursors (around 10%) (Montaldo et al., 2014). These discrepancies between the two studies probably pertain to differences in culture conditions, as also $CD34^{+/bright}$ cells seemed to generate preferentially these two ILC populations with no report on any other lineage and the authors noted that SCF and aryl hydrocarbon receptor (AHR) ligands present in media favor ILC3 differentiation (Montaldo et al., 2014). It is worth mentioning though that (with some variations between studies) only a small fraction of the stage 2 (and 3) progeny are $CD94^{+}$ cells (Freud et al., 2006; 2016; Scoville et al., 2016). Thus, although distinct cultures result in different outcomes and *in vitro* conditions seem to be inefficient in driving NK differentiation and full maturation, it is also possible if not likely that $CD34^{dim}CD117^{+}$ stage 2 cells are not the only pathway of NK cell development. Supporting this notion, Moroso et al detected stage 2 and 3 cells in adult liver which displayed no transcripts for *RORC*, *IL22* or *IFNγ* but gave rise to functional NK cells (Moroso et al., 2011). Moreover, $RORC^{-/-}$ patients seem to have normal blood NK counts but absence of PB ILC3s as well as palpable axillary and cervical LNs (Okada et al., 2015).

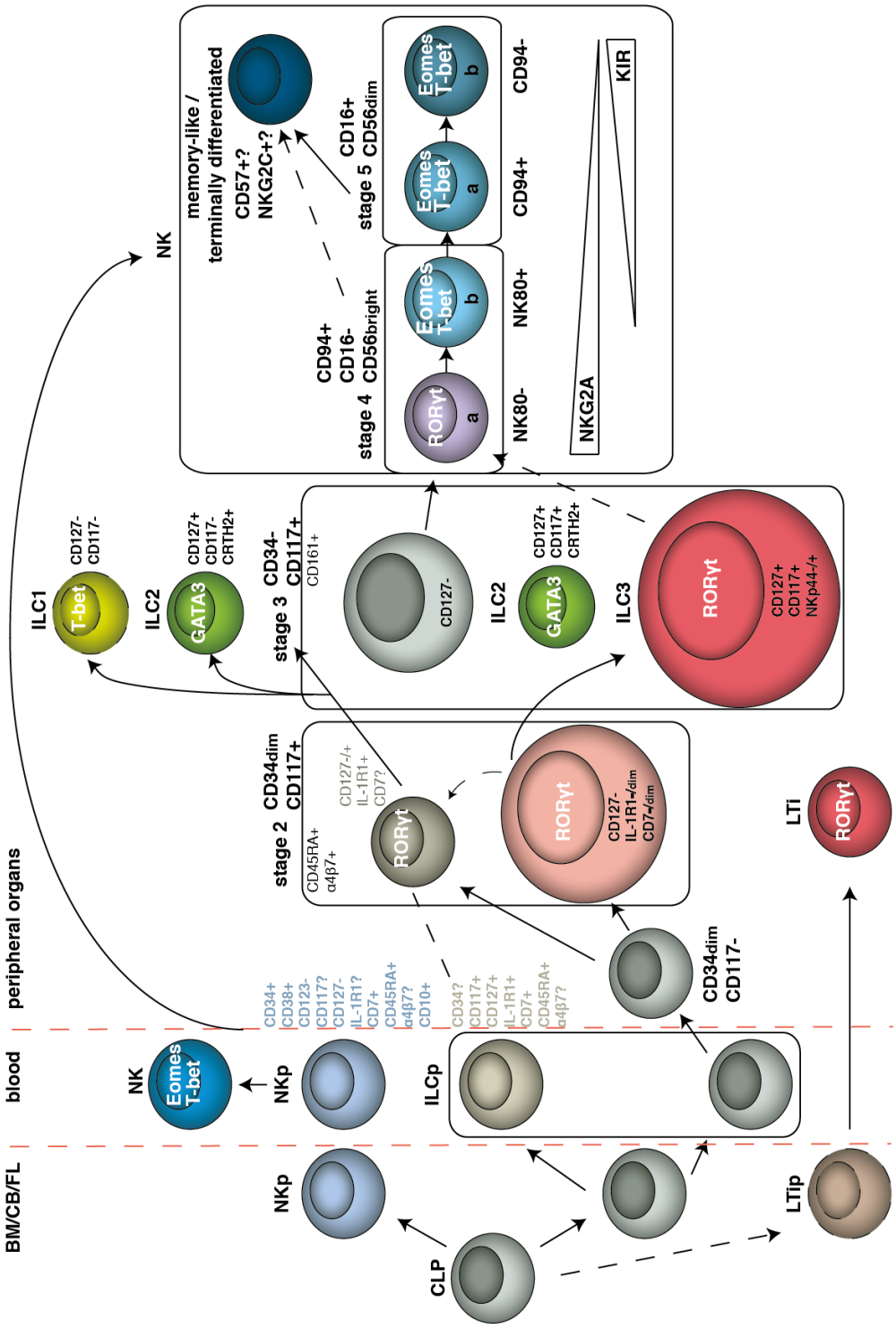

Figure C Model of human ILC development
Downstream of the CLP, an NKp, present in BM/CB and fetal tissues has been identified (Renoux et al., 2015). ILCps that gives rise to all subsets, including NK cells have been isolated from PB (Lim et al., 2017) and tonsils (Scoville et al., 2016). ILC3-specified progenitor has been purified from tonsils but is also present in intestinal lamina propria. Putative populations have dashed membrane. Unknown developmental steps are colored in grey. Dashed arrows represent origin of estimated precursor. Sizes in stage 2 and 3 cells indicate the frequency of the respective populations. Figure is based on (Collins et al., 2017; Lim et al., 2017; Montaldo et al., 2014; 2015; Renoux et al., 2015; Scoville et al., 2016; Yu et al., 2013)

Of note, the enrichment of ILC3/NK precursors in peripheral tissues, such as tonsils and intestinal lamina propria, compared to BM and PB (Freud et al., 2005; Montaldo et al., 2014) indicates ILC development outside the BM. Interestingly, NK precursors isolated from explanted liver grafts were found to be of recipient origin, indicating recruitment from the bloodstream (Moroso et al., 2011).

In fetal tissues as well as UCB and BM, progenitors with similar phenotype to stage 2 cells but positive for CD7 and CD10 (stage 2: $CD7^{-}CD10^{-/+}$) have been identified that are restricted to the NK cell lineage. When compared to upstream lymphoid-primed or committed progenitors, $Lin^{-}CD34^{+}CD38^{+}CD123^{-}CD45RA^{+}CD7^{+}CD10^{+}CD127^{-}$ NKPs express more transcripts for NK-related genes such as *EOMES*, *Prf1*, and *IL2RB* (encodes CD122). Of note, the NKP in mice is characterized by CD122 surface expression, which in human is below the detection limit. The NKP commitment was demonstrated also *in vivo* where the authors were able to detect NK cells but no other populations 11 weeks after reconstitution of newborn NOD/SCIDγc^{null} (NSG) mice with only 600 UCB-derived NKPs and without addition of human cytokines. NK development in this setting is quite surprising as it relies on mouse IL-15 that has poor reactivity on human cells and fails to induce their proliferation (Eisenman et al., 2002; Huntington et al., 2009) but, more importantly, the NOD background has an abnormal *IL15* expression with a subsequent NK cell defect (correctable by IL-15/IL-15Rα complexes injection) (Suwanai et al., 2010). NKPs, tonsil stage 2 $IL\text{-}1R1^{+}$ and stage 3 cells *in vivo* generate $CD16^{+}$ NK cells (Freud et al., 2016). *In vitro* CD16 as well as KIR expression can be induced on $CD56^{bright}$ NK cells from PB with IL-2 or IL-15 stimulation (Romagnani et al., 2007). Moreover, $CD56^{bright}$ NK cells transferred into immunodeficient mice give rise to $CD56^{dim}CD16^{+}$ NK cells (Chan et al., 2007; Huntington et al., 2009), with the latter also found to have shorter telomeres (Chan et al., 2007; Romagnani et al., 2007). These data, together with the identification of a PB $CD94^{hi}CD56^{dim}$ population with an intermediate phenotype and functionality between $CD56^{bright}$ and $CD94^{dim}CD56^{dim}CD16^{+}$ NK cells (Yu et al., 2010), supports a linear differentiation model between the two subsets, a notion challenged by a recent report in macaques (Wu et al., 2014). Finally, CD57 expression on $CD56^{dim}$ NK cells is

associated with lower proliferative capacity and responsiveness to cytokines but increased cytotoxicity, consequently CD57$^+$ NK cells are designated terminally differentiated (Lopez-Vergès et al., 2010).

Thus, a fraction of human NK cells might also arise from a RORγt$^+$ progenitor, as do ILC3s.

2. Cytokine requirements

In accordance to mouse data, IL-15 has been shown to maintain NK cell survival, induce their proliferation and differentiation. *In vitro*, IL-15 is sufficient for differentiation of CD34$^+$ BM cells towards cytotoxic NK cells (3 weeks culture), even though alone it does not promote their proliferation (Mrózek et al., 1996). In humanized mice (discussed below), supplementation of IL-15/IL-15Rα complexes induced robust NK cell proliferation as well as differentiation towards a CD56^{lo}CD16$^+$KIR$^+$ phenotype. Moreover, adoptively transferred CD56^{hi}CD16$^-$ KIRs$^-$ or CD56^{lo}CD16$^+$KIRs$^-$ NK cells from fetal spleen into immunodeficient *Rag2*$^{-/-}$*Il2rg*$^{-/-}$ mice acquired CD16 and KIRs with IL-15/IL-15Rα for 7 days, thus confirming the role of IL-15 in NK differentiation (Huntington et al., 2009). IL-2 shows some redundancy with IL-15 as observed in a humanized mouse model with transgenic expression of human IL-2. These mice had a predominant effect in the NK compartment, with both expansion and differentiation (Katano et al., 2015). Nevertheless, no change in NK cell numbers or activity was observed in an *IL2RA*^{null} (CD25) patient (Goudy et al., 2013), whereas they were absent in a patient with a deficiency in CD122 (IL-2/IL-15Rβ) (not mapped to *IL2RB*) (Orange, 2006), suggesting that IL-2 is not required for NK cell development. Finally, patients with defective *IL7R* expression have functional NK cells (Puel et al., 1998). Thus, IL-15, but not IL-2 or IL-7 is required for human NK cell development. Patients with severe combined immunodeficiency (SCID), resulting from *IL2RG* or *JAK3* mutations, lack not only NK cells but also other ILC subsets (Vély et al., 2016a) and have no LNs (Facchetti et al., 1998), suggesting that as in mice (Satoh-Takayama et al., 2010; Vonarbourg et al., 2010), human ILC3s rely on IL-7 for their development.

IV. ILC subsets and their characteristics

A. Group 1 ILCs

1. NK cells

The prototypic member of this family are NK cells, which were first discovered in mice for their intrinsic ability to lyse tumor cell lines. They were later recognized not only as important players in cancer immunosurveillance but also in infection. NK cells survey the host for "stressed", infected or transformed cells through expression of diverse set of receptors and exert their cytolytic activity through the release of cytotoxic granules containing perforin and granzymes (Gzms) or through death receptor-induced apoptosis, mediated by molecules such as TRAIL or FasL. They are also potent producers of pro-inflammatory cytokines, most notably IFNγ, and chemokines and thus are also able to modulate the immune response. Finally, NK cells rely on the T-box transcription factors Eomes and/or T-bet for their differentiation, maintenance and/or functionality. In mice, mature NK cells are $Eomes^+$ (Vivier et al., 2016). Thus, NK cells are the innate counterpart of cytotoxic $CD8^+$ T cells.

a. Receptors involved in target cell recognition

NK cell diversity is generated by the variable expression of germ line-encoded activating and inhibitory receptors. In humans, these include killer immunoglobulin-like receptors (KIRs), natural-killer group 2 (NKG2) receptors, and natural cytotoxicity receptors (NCRs), among others. The KIR family comprises activating and inhibitory receptors, which recognize epitopes of the highly polymorphic human leukocyte antigen (HLA) class I ligands HLA-A, HLA-B and HLA-C. The inhibitory KIRs are involved in a process termed NK cell education or licensing, whereby the presence of both receptor and cognate ligand is necessary for the functional competence of the cell. If self-HLA class I ligands are absent, NK cells remain hyporesponsive, which ensures self-tolerance. The murine functional analogues of KIRs are the Ly49 receptors. C-

type lectin NKG2 family members form heterodimers with CD94 and recognize HLA-E (Qa1^{b} in mice), which binds peptides from the leader sequence of class I molecules. Thus, NKG2 receptors act complementary to KIRs by allowing NK cells to indirectly monitor HLA expression. If the latter is obstructed as a result of infection or transformation, the cell will be targeted for elimination owing to the lack of inhibition, an interaction known as "missing self" recognition. The inhibitory NKG2A and activating NKG2C and NKG2D receptors are present both in mice and humans. Of note, NKG2D constitutes an exception from the family as it is expressed as a homodimer and binds the stress- or virus-induced ligands MHC class I chain-related protein A (MICA), MICB and UL-16 binding proteins (ULBPs) (in mice RAE1, H60 and MULT1). NCRs are activating receptors that belong to the immunoglobulin superfamily and are grouped together based on functionality. They comprise NKp46 (NCR1; CD335) (the only one found in mice), NKp44 (NCR2; CD336) and NKp30 (NCR3; CD337). NCRs are described to bind viral, bacterial, parasite as well as cellular ligands among which are viral hemagglutinins, the human cytomegalovirus (HCMV) tegument protein pp65 and heparan sulfates whose expression pattern varies on tumor cells. Besides these, the low-affinity IgG receptor CD16 (FcγRIII) is also a potent activator of NK cells, through which they mediate antibody-dependent cellular cytotoxicity (ADCC) (Björkström et al., 2016; Kruse et al., 2014; Pegram et al., 2011). Importantly, whereas inhibitory receptor expression (although poorly understood) is determined primarily by genetics and is strictly regulated, expression of activating and co-stimulatory receptors like DNAX Accessory Molecule-1 (DNAM-1, CD226) is largely affected by environmental factors (Horowitz et al., 2013).

b. NK subsets across tissues

Human NK cells are defined as CD3^{-}NKp46^{+}(CD94$^{+/dim}$) and are divided according to CD56 and CD16 differential expression into CD56^{bright}CD16^{-} and CD56^{dim}CD16^{+} cells. Whereas the former is enriched in tonsils and LNs and has primarily immunoregulatory functions, the latter is the predominant subset in PB and spleen and has potent cytotoxic activity. CD56^{dim}CD16^{+} cells can express

in addition KIRs and CD57, a marker of NK terminal differentiation/antigen exposure (Björkström et al., 2016). Importantly, activation influences CD56 and CD16 expression, therefore this designation is relevant mostly for analysis of PB from healthy subjects. For example, in HIV-infected patients an unconventional $CD56^{-}CD16^{+/dim}$ NK population expands that has low lytic activity (Spits et al., 2016). Whereas PB $CD56^{bright}$ cells are $Eomes^{+}$ but exhibit a variable T-bet expression, $CD56^{dim}$ cells are $Eomes^{lo}T\text{-}bet^{hi}$ (Knox et al., 2014).

In mice NK cells do not express CD56 but are positive for NK1.1 (not expressed by all mouse strains) and the integrin α2 (CD49b), recognized by the DX5 antibody (Di santo, 2006).

Apart from blood and secondary lymphoid tissues (SLTs), NK cells are found in peripheral organs with the highest prevalence in liver, lung and uterus. To what extent these represent circulating NK cells transiently recruited to tissues or resident NK cells was not clear until the characterization of molecules governing cell trafficking or retention within organs and subsequent work. For example, NK cells, particularly the $CD56^{dim}$ subset, preferentially express sphingosine 1-phosphate (S1P) receptor 5, which allows them to egress from tissues along an increasing S1P gradient. On the other hand, CD69 was found to inhibit S1P-1, respectively, CD69 is rarely expressed in blood, but is found on the majority of NK cells within tissues such as liver and skin. Similar observations are made for CD49a (α1 integrin), which in a complex with β1 binds collagen, and CD103 (αE integrin), which interacts with β7 and bind E-cadherin, expressed on epithelial cells. Based on these markers tissue-resident populations can been distinguished (Björkström et al., 2016).

Stegmann et al identified a $CD69^{hi}CXCR6^{+}T\text{-}bet^{lo}Eomes^{hi}$ subset residing in liver with variable frequencies (5-88% of total NK cells). CXCR6 expression at steady state provides a mechanism for tissue retention in addition to CD69, as its ligand CXCL16 is highly expressed by liver sinusoidal cells. $CXCR6^{+}$ NK cells show lower expression of cytotoxic molecules and pro-inflammatory cytokines upon stimulation than their $CXCR6^{-}$ counterparts, however TRAIL induction (in diseased liver) was demonstrated to be largely restricted to the former. Of note, whereas in mice liver-resident $CD49a^{+}CD49b^{-}$ NK/ILC1 cells constitutively express high levels of TRAIL, in healthy human livers its expression is negligible.

Moreover, in mice these cells are T-bet^{+}Eomes^{-} and in humans they have the converse TF profile with CXCR6 but not CD49a segregating the two (Stegmann et al., 2016). Marquardt et al characterized another intrahepatic CD49a^{+}CD56^{bright}T-bet^{+}Eomes^{-} NK subset that is positive for KIRs (>80%, oligoclonal pattern) and NKG2C but negative for CD16 and CD57. CD49a^{+} NK cells express granzymes but only low levels of perforin and compared to CD49^{-} cells have lower degranulation capacity but are more potent cytokine producers. Interestingly, they were able to maintain their phenotype in long-term culture (3 weeks with IL-15 or NKG2C), suggesting CD49a^{+} NK cells represent a stable subset, distinct from cNK cells. Of note, the subset represented on average 2.3% of total CD3^{-}CD56^{+} lymphocytes and was present in 12 out 29 livers examined (virtually absent in fetal livers), suggesting environmental, infectious or genetic factors might be driving the accumulation of this population (Marquardt et al., 2015). Overall, tissue-resident NK cells seem to have distinct properties compared to cNK cells but also differ from their mouse NK/ILC1 counterparts.

Fuchs et al identified a CD103^{+} ILC population within tonsil that has NK-associated features, i.e. expression of CD94, T-bet, Eomes, and NKp44 (>75%). These cells were denoted as intraepithelial (ie) ILC1s, even though they have bi-modal expression of perforin and granzymes and show cytolytic activity (in comparison to ILC3s but not reported for cNKs). Interestingly, they bear markers of exposure to TGFβ, which can maintain CD103 expression on cultured cells (9 days with IL-15). In contrast, only few blood NK cells up-regulated CD103 under the same conditions or with addition of supernatant from intestinal epithelial cell lines. These observations prompted the notion that ieILC1 and cNK cells might have alternative developmental pathway (Fuchs et al., 2013). Nevertheless, in an unbiased manner, using t-Distributed Stochastic Neighbor Embedding (t-SNE) analysis, Simoni et al showed that ieILC1s cluster with NK cells, indicating a close similarity between the two. ieILC1s are also positive for other tissue-related markers such as CD49a, CD69, CXCR6 (at steady state) and CD160, the latter shown to interact with herpes virus entry mediator (HVEM) on epithelia to promote host defense (Simoni et al., 2017). ieILC1s have been detected within the mucosal epithelium (only weakly in LP) in small intestine and colon (Fuchs et al., 2013), where their NKp44 expression is lower compared

to tonsil and is highly variable across individuals, demonstrating that NKp44 is neither sufficient nor required to define this subset (Simoni et al., 2017). Therefore, ieILC1 bear striking similarities to NK cells.

c. NK cell activation

The dynamic balance of incorporated activating and inhibitory signals regulates cell activation. NK cells however respond not only to cell surface-bound ligands but also other alert molecules such as Toll-like receptor (TLR) ligands and strongly to cytokines such as type I interferons (IFN), interleukin-12 (IL-12), IL-15 and IL-18 (Vivier et al., 2008). $CD56^{bright}CD16^{-}$ NK cells, especially from SLTs, are more responsive to DC stimulation than $CD16^{+}$ NK cells. They do so by IFNγ production and proliferation, whereas the former is induced by IL-12, the latter is triggered by IL-15 (Ferlazzo et al., 2004). Combination of those cytokines has a synergistic effect with respect to IFNγ production and this is true also for $CD103^{+}$ILC1s. IL-12 and IL-18 also show synergistic effect in NK cells but not in $CD103^{+}$ILC1s (Fuchs et al., 2013). Thus, similar cytokines elicit cytokine production of NK cells and ILC1s.

2. Helper (h) ILC1s cells

hILC1s are defined as $CD127(IL\text{-}7R\alpha)^{+}T\text{-}bet^{+}(ROR\gamma t^{-}$ for mice) cells that produce high amounts of IFNγ in response to IL-12 and IL-18 and are distinguished from NK cells by their lack of Eomes expression and cytotoxic abilities (Bernink et al., 2013).

The concept of an IFNγ-producing ILC population distinct from NK cells originated from mouse studies, which showed that (1) $CD127^{+}$ ILCs development is completely abrogated in the absence of GATA3 which is not the case for NK cells (Yagi et al., 2014) and (2) hepatic or intestinal $Eomes^{-}NKp46^{+}NK1.1^{+}$ cells do not convert into $Eomes^{+}$ cells (Daussy et al., 2014; Klose et al., 2014). It is noteworthy that the latter was shown under physiologic conditions and not for spleen-derived cells, which is important because isolated cells have skewed tropism and the tissue-specific environment modulates cell phenotype. In line

with this, lineage-tracing studies have demonstrated that even at steady state intestinal NKp46^{+} ILC3s, recovered from recipient colon or spleen, up regulate T-bet at the expense of RORγt and acquire the ability to produce IFNγ (Klose et al., 2013; Vonarbourg et al., 2010). These cells termed ex-ILC3s represent a fraction of hILC1s, which are recognized as a separate lineage only through the use of *Rorc(gt)*-Cre^{Tg} x *Rosa26R*$^{Yfp/+}$ (RORγt-fm) mice. The further generation of a double-reporter strain with *Eomes*$^{Gfp/+}$ allowed transcriptome comparison between cNK cells and hILC1s, distinct from ILC3s. Intestinal cNK cells highly express *Ly49*, cytotoxic granule effectors such as *Prf1* and *GzmK*, and molecules required for homing to (*Ccr7*), entry (*Sell*, encoding CD62L) and egress (*S1pr5*) from lymphoid organs, indicating they recirculate, whereas hILC1s had a tissue-resident phenotype (*Cxcr6*, *Itga1*, encoding CD49a) (Klose et al., 2014). Moreover, although originally described as non-cytotoxic, hepatic hILC1s have higher expression of genes encoding GzmC and TRAIL, with the latter constitutively expressed on the protein level (Daussy et al., 2014).

In humans, an IFNγ-producing Lin^{-}CD127^{+}CRTH2^{-}CD117^{-}NKp44^{-} subset has been described in tonsils that lacks CD94, CD56, perforin and GzmB but expressed T-bet (bi-modal population). After long-term expansion (4-6 weeks) with feeders and IL-2, hILC1 cells maintained their phenotype. Furthermore, in accordance with high transcripts for *IL12RB2*, activation (4 days) with IL-12 plus IL-2 and/or IL-18 triggered IFNγ secretion (Bernink et al., 2013). Strikingly, RNAseq analysis of tonsil ILCs revealed no differential expression of *Tbx21* or *IL12RB2* in putative hILC1s, which however expressed transcripts encoding TCR variable regions and other T cell-associated molecules such as CD3 chains, CD4, and CD5. The authors argued that as cytoplasmic CD3 is induced in NK cells upon Notch signaling, similar mechanisms might account for their hILC1 findings (Bjorklund et al., 2016). However, TCR gene rearrangement analysis has to be performed to ensure there is no T cell contamination because upon activation, TCR-CD3 complexes are down regulated, bringing these T cells closer to the Lin^{-} gate. In RORγt-fm mice, Burkhard et al detected CD5 expression in the ILC3 gate after exclusion of CD3 and TCRβ, which was absent when mice were crossed to *RAG1*$^{-/-}$ mice, indicating these are T cells. CD5 is up regulated upon TCR engagement, thus its addition to the lineage is recommended to avoid T cell

contamination. (Burkhard et al., 2014) Indeed, Vely et al showed that most putative hILC1s express CD5 (Vély et al., 2016a). Moreover, mass cytometry with t-SNE analysis revealed no cluster corresponding to hILC1s and when tonsil Lin^- $CD94^-CD127^+CRTH2^-CD117^-NKp44^-$ cells were back gated, they fell into mostly T cell but also DC, ILC3 and HPC clusters. Thus, human $CD127^+$ hILC1s remain controversial (Simoni et al., 2017).

B. Group 2 ILCs

ILC2s are GATA-3^+ cells that express CD127, CD117 (tyrosine-protein kinase Kit (c-Kit)), and CD294 (prostaglandin D2 receptor 2 (CRTH2)). They produce in response to helminth infection or activation by IL-25, IL-33 and TSLP, Th2 cell signature cytokines such as IL-5 and IL-13 that drive eosinophilic inflammation as well as amphiregulin, important for tissue repair (Hazenberg and Spits, 2014).

C. Group 3 ILCs

ILC3s rely on RORγt for their development and function and are defined as $CD127^+CD117^+CD294^-$. In addition, they express IL-23R and IL-1R and in response to a combination of the respective cytokines mainly secrete IL-22, which promotes epithelial tissue integrity, but also GM-CSF and IL-2. They also produce a number of TNF family members such as lymphotoxin (LT) α1β2 and TNF that mediates lymphoid tissue formation. In addition, fetal LTi cells but not adult ILC3s produce the inflammation-related cytokine IL-17 (Killig et al., 2014).

ILC3s are subdivided according to NCR expression, specifically NKp44 in humans and NKp46 in mice. Unlike human, under physiologic conditions murine $NKp46^+$ ILC3s can produce not only IL-22 but also IFNγ and require T-bet for their differentiation. Furthermore, whereas the chemokine receptor CCR6 is uniformly expressed by human ILC3s (Killig et al., 2014), it dissects their mouse counterparts into $CCR6^+$ cells to which IL-17 expression is confined and $CCR6^-$ cells, which gradually acquire T-bet and consequently NKp46 at the expense of IL-22 and LT expression (Klose et al., 2013). In humans, IL-22 secretion is largely

restricted to the NKp44$^+$ subset (Hoorweg et al., 2012). Interestingly, triggering of NKp44 rather induces TNF and IL-2 production and pro-inflammatory gene pattern expression. Cytokine and NKp44 engagement have a synergistic effect (Glatzer et al., 2013).

Mass cytometry profiling of tonsil ILC3s revealed a high degree of heterogeneity in this subset and while NKp44 clearly divided them, expression of other NCRs was scattered within the cluster. CD56 showed a gradient expression that neither overlapped with NKp44 or any other examined marker nor was mutually exclusive (Simoni et al., 2017).

Finally, ILC3s are enriched in tonsils, adenoids and the intestine and uniformly express CD69, but not CD49a, CD103 or CCR7 (Simoni et al., 2017).

V. Role of ILC1s and ILC3s at steady state and disease

A. Role of NK cells

In patients and mouse models, NK cell immunodeficiencies that affect their numbers or function have been associated with high susceptibility to virus infections, especially by herpes viruses, as well as increased incidence of cancer. This indicates their importance in virus control and tumor immunosurveillance (Morvan and Lanier, 2016; Orange, 2006; Vivier et al., 2008). Truly NK-specific deficiencies are rare but such patients manifest with Epstein–Barr virus (EBV)-associated malignancies (Eidenschenk et al., 2006; Gineau et al., 2012; Shaw et al., 2012). NK cells have also been shown to mediate a graft-versus-leukemia (GvL) effect in patients receiving haplo-identical hematopoietic (stem) cell (HSCT) transplantation, where KIR-HLA interactions are mismatched (Vivier et al., 2016). Furthermore, an 11-year follow-up study correlated high NK cell cytotoxic activity with reduced cancer risk (Vivier et al., 2008). Malignant cells might down-regulate MHC class I or up-regulate ligands for activating NK receptors which changes the balance of incorporated signals and renders them susceptible for lysis. For example, *Klrk1* (encoding NKG2D)-deficient mice develop spontaneous tumors and there have been several reports of tumors that shed NKG2D ligands as decoys (Morvan and Lanier, 2016). *In vivo* NK cell anti-

tumor activity has been demonstrated by targeting this subset with depleting antibodies. Notably, both NK1.1 and asialo-GM1 are also expressed on T cell subsets and therefore interpretation has to be cautious (Vivier et al., 2008). Likewise, many NK deficiencies, characterized primarily by herpes virus-related complications, also include absence of NKT cells (Orange, 2006). Nonetheless, they seem to result from abnormal innate recognition such as through 2B4 and subsequently SAP, and patients with SAP mutations present with severe EBV infection (Fischer, 2007; Parolini et al., 2000). NK cells have been demonstrated *in vivo* to exert control over lytic EBV infection (Chijioke et al., 2013) during which ligands for NKG2D and DNAM-1 are elevated (Pappworth et al., 2007). Unlike EBV (Landtwing et al., 2016), CMV infection skews the total NK repertoire and drives clonal-like expansion of memory-like NKG2C^{+} cells, implicating NK cells in CMV control (Béziat et al., 2012; Foley et al., 2012; Hendricks et al., 2014). Of note, CMV reactivation is also associated with reduced risk of leukemia relapse after allogeneic H(S)CT (Vivier et al., 2016). Hence, NK cells play important role in the immune control of viral infections, especially with herpes viruses, and cancer.

Importantly, SCID patients with *IL2RG* or *JAK3* mutations, remained ILC-deficient after non-myeloablative HSCT. Neither circulating nor tissue-infiltrating (CD3^{-}NKp46^{+} in intestinal and skin tissue sections) ILCs were detected without complete donor chimerism. Strikingly, these patients did not show an apparent increased susceptibility to infection or tumor development long after reconstitution (7-39 years), which shows the redundancy of ILC function when T cells are present (Vély et al., 2016a). Of note, in mice an emergency NK-cell lymphopoiesis from NKPs into NK1.1^{lo}NK46^{lo} occurs under inflammatory conditions, induced by IL-12 (Ohs et al., 2016). Thus, one can envision a similar situation in humans.

B. Role of hILC1s

hILC1s seem to have dual roles in infectious and inflammatory diseases. In mice during infection with the intracellular parasite *Toxoplasma gondii* hILC1s represent the majority of IFNγ- and TNF-producing ILCs and are able to attract

inflammatory monocytes and control the parasite replication upon transfer in *Rag2*$^{-/-}$*Il2rg*$^{-/-}$ mice (Klose et al., 2014). Similarly, in *Salmonella* infection hILC1 are the main innate source of IFNγ, however this has negative impact on the disease as depletion of ILCs (α-Thy-1 Ab) improves clinical signs of colitis, also observed in *Ifngr1*$^{-/-}$mice (Klose et al., 2013). Moreover, α-CD40 stimulation in *Rag*$^{-/-}$ mice induces colitis, which is mediated by IFNγ^{+} hILC1 (including ex-ILC3 and ieILC1s) (Fuchs et al., 2013; Vonarbourg et al., 2010) as well as GM-CSF^{+} ILC3s (Pearson et al., 2016). Unfortunately, most studies with focus on ILCs either disregard the adaptive compartment or use *Rag*$^{-/-}$ mice; therefore, the relevance of these findings for protective immune responses in immune competent hosts remains unclear.

In humans, putative hILC1s have been implicated in the pathogenesis of inflammatory conditions such as inflammatory bowel disease (IBD). Bernink et al reported an increase in the frequency of hILC1s at the cost of other ILCs in CD intestine (Bernink et al., 2013; 2015). Patients with chronic obstructive pulmonary disease (COPD) have also significantly increased hILC1s at the cost of ILC2s that correlate with diminished lung function, disease severity and susceptibility to exacerbations. Moreover, inflammatory triggers associated with exacerbation of COPD such as respiratory tract infection with virus (influenza A), trigger loss of ILC2 with a concomitant increase in hILC1s (Silver et al., 2016).

Simoni et al found ieILC1 to constitute a major fraction of the non-cNK ILCs in pathological omentum adipose tissues (omentum AT) from obese patients, lung tumors, and colorectal tumors, where these cells show low NKp44 expression and express low levels of cytotoxic granule effectors (Simoni et al., 2017). Fuchs et al also demonstrated higher frequency of ieILC1s within intraepithelial lymphocytes in Crohn's disease (CD) compared to non-IBD controls (Fuchs et al., 2013). However, both studies did not correlate these populations with disease severity and their role remains unclear.

C. Role of ILC3s

In the mouse fetus, LTi cells are essential to initiate secondary lymphoid organ development. Through LTβ or TNF receptor triggering they induce the

expression of adhesion molecules and chemokines such as vascular cell adhesion molecule-1 (VCAM-1), intercellular adhesion molecule 1 (ICAM-1) and CXCL13 in stromal cells, thus recruiting other lymphocytes (Killig et al., 2014). In humans, peripheral LNs are present already at gestational week 6, mesenteric LNs from about week 14 and subsequently the first signs of PPs are detected. Accordingly, *RORC*-expressing Lin$^-$CD45^{int}CD127^{hi} cells with LTi characteristics were described in first-trimester mesentery and second-trimester LNs, which in contrast to murine LTi cells lacked CD4 expression (Cupedo et al., 2008). NKp44$^+$ ILC3 were then found to colonize fetal intestine during late first trimester and later represent the majority of ILC3s there (Bernink et al., 2015; Hoorweg et al., 2012), indicating differentiation independent of microflora.

Apart from lymphoid tissue formation, ILC3s play a role in the maintenance of epithelial tissue integrity and function. The IL-22 receptor is exclusively expressed on epithelial cells and its stimulation promotes proliferation and regeneration as well as production of antimicrobial peptides such as β defensins, mucus-associated molecules and IL-10. In mice, ILC3s play a role in intestinal homeostasis by restricting the commensal-specific T cell pool through MHC class II presentation or by containing commensal dissemination. They also protect against pathogens such as *Citrobacter rodentium*, a murine analog for enteropathogenic and enterohemorrhagic *Escherichia coli* (Killig et al., 2014). Notably, most studies examined their function in the context of T and B cell deficiency, thus their importance when adaptive immunity is present has not been extensively investigated. For example, in the *C. rodentium* model their absence in T cell-sufficient mice has little impact on control of infection (Song et al., 2015). Moreover, patients that exhibit a selective ILC deficiency are not more susceptible to disease (Vély et al., 2016a).

Importantly, one of the initial descriptions of ILC3s was in a bacteria-driven innate colitis model. In this study, *Rag*$^{-/-}$*Rorc*$^{-/-}$ mice developed only mild intestinal inflammation, which demonstrated a role in driving pathology (Buonocore et al., 2010). Reinforcing this data, neutralization of IL-17, GM-CSF or IFNγ, produced by CCR6$^+$, CCR6$^-$NKp46$^-$ ILC3 and ILC1 cells, respectively, ameliorated pathology, whereas blockade of IL-22 had no effect (Buonocore et al., 2010; Pearson et al., 2016). One of the main ILC3 activators, IL-23, has been

associated with autoimmune and chronic inflammatory disorders such as IBD and psoriasis. In IBD, intestinal $CD3^-$ cells show increased transcripts for *IL22* and *IL17A/F*. Moreover, $CD127^+CD56^-$ ILCs accumulate in the intestines of CD but not ulcerative colitis patients and are the main (if not only) source of IL-17 (Geremia et al., 2011). Surprisingly, in a clinical trial treatment of CD patients with α-IL-17A Ab worsened the disease. Both cytokines are also involved in the pathogenesis of psoriasis and NCR^+ ILC3 cells are increased in affected skin, suggesting they might contribute to the pathology {PhD:2016ip}.

ILC3s have been found also in colorectal and lung tumors (Simoni et al., 2017). In colorectal cancer (CRC), IL-22 expression is significantly higher in tumor tissue compared to adjacent healthy sections. The majority of IL-22-producing cells are T cells, but a fraction is within the Lin^- gate. In a mouse model of colitis-associated CRC, ILC depletion as well as blocking of IL-22 ameliorated the disease (Hazenberg and Spits, 2014). In non-small cell lung cancer (NSCLC), NCR^+ ILC3s accumulate at the edge of tumor-associated tertiary lymphoid structures (TLSs), which are predictive of favorable prognosis. In co-culture experiments with NSCLC cell lines expressing NCR ligands, tumor-infiltrating NCR^+ ILC3s (both *ex vivo* and expanded) produced TNF and IL-8, which were reduced in the presence of α-NKp44 Ab (only weakly affected by blocking of NKp30). Moreover, they induced adhesion molecule expression on human endothelial cells, but did not modify their migration, suggesting no angiogenic effects (Carrega et al., 2015). In mice, IL-12-driven suppression of B16 melanoma is mediated by $NKp46^+$ ILC3s, but the exact mechanism remains enigmatic. Transferred $NKp46^+$RORγt-fm^+CD3^- cells could suppress tumor growth, but so does injection of αNK1.1 Ab, which depletes ILC1 but not $NKp46^+$ ILC3 ($NK1.1^{dim}$). Curiously, tumors are still repressed in mice deficient in IL-22, IL-17A, IFNγ or its receptor, perforin and LTβR (Eisenring et al., 2010). Thus, ILC3s seem to restrict or support tumors dependent on the type of malignancy.

VI. Plasticity of hILCs

A. In mice

ILC identity is highly modulated by the microenvironment. The abundance of ILC3s in the intestine has prompted investigation into the effect of the microbiota on this subset. It has been demonstrated that its eradication leads to RORγt down-regulation in NKp46^{+} ILC3s, although their numbers remain unchanged (Vonarbourg et al., 2010). Moreover, signals from the microbiota were shown to regulate T-bet expression in intestinal ILC3s, which is reflected in the selective reduction of the T-bet^{+} subset in germ-free mice or mice deficient in TLR signaling. Similar effects were observed in absence of IL-23 (Klose et al., 2013). Spleen, colon and peripheral LNs have been shown to be permissive for RORγt loss in the NKp46^{+} ILC3 subset, demonstrated both through adoptive transfer experiments of RORγt-reporter positive ILC3s and via lineage tracing studies employing *Rorc(gt)*-Cre^{Tg} x *Rosa26R*$^{Yfp/+}$ (RORγt-fate map (fm)) mice (Klose et al., 2013; Vonarbourg et al., 2010). These NKp46^{+}RORγt^{-} cells, termed ex-ILC3s, express T-bet but not Eomes and are unaffected in Eomes-deficient mice (Klose et al., 2014). Therefore, tissue microenvironment has a profound impact on murine ILC3 profile, which might display an ILC1 phenotype even under homeostatic conditions.

B. In humans

ILC2 cells are activated by IL-25, IL-33 and thymic stromal lymphopoietin (TSLP), produced by epithelial cells. Interestingly, circulating ILC2s have low transcripts for the corresponding receptors with no surface expression and are thus naïve in their effector functions (Lim et al., 2016; Ohne et al., 2016). Upon culture (5-7 d) with IL-2, (-7, -25) and IL-33, ILC2s quickly adopt their signature profile; this however is not stable and can be modified by addition of PBMCs as feeders or IL-12. Already a short-term stimulation (> 48 h) increases *IL12RB1* and *IL12RB2* expression and cultures from patients with biallelic mutations in the former fail to generate plastic ILC2s. IL-12 up-regulates T-bet and,

consequently, augments IFNγ expression, which is mostly detected in IL-13-producing cells (Lim et al., 2016; Silver et al., 2016).

As ILC2 cells express IL-1R1, IL-1β stimulation has also been investigated. In short-term cultures (6-7 d), IL-1β in combination with IL-2 induces proliferation and cytokine production similar or even greater to that elicited by IL-33 (Bal et al., 2016; Ohne et al., 2016). Of note, neither leads to expansion without IL-2, which by itself promotes only survival. Moreover, transcriptome analysis revealed that, relative to freshly isolated ILC2s, IL-1β-primed cells have increased expression of *IL1RL1* and *IL17RB*, thus improving their responsiveness to IL-33, which also explains the observed synergistic effect of the two cytokines. Strikingly, IL-1β boosts also transcription of ILC1-related genes such as *TBX21*, *EOMES*, *IL12RB1* and *IL12RB2* and in combination with IL-12 shifts their program to ILC1s (Bal et al., 2016; Ohne et al., 2016). Hence, human ILCs are also strongly influenced by the microenvironment, with IL-12 exposure able switch ILC2 functionality towards IFNγ production.

Tonsil stage 3 cells, defined as $Lin^{-}CD117^{+}CD94^{-}$, comprise ILC3s and NK precursors. More than 70% of those are $IL\text{-}1R1^{hi}$ and *IL22* as well as *AHR* (but not *RORC*) expression is confined to this subset. As stage 3 cells give rise to NK cells under IL-15 containing conditions, Hughes et al investigated the impact of IL-1β addition on NK cell differentiation. Whereas this selectively expanded the $IL\text{-}1R1^{hi}$ subset, it significantly diminished progression to mature NK cells (Hughes et al., 2010). Moreover, the addition of IL-1β in combination with an AHR agonist promoted the ILC3 phenotype. In contrast, AHR pharmacological blockade or gene silencing induced NK cell maturation (Hughes et al., 2014). Thus, ILC3 profile is maintained in the presence of IL-1β, whereas IL-15 alone drives NK cell differentiation. Although *in vitro* only about 20% of stage 3 cells acquire CD94, *in vivo* IL-15 treatment generates only NK cells (Freud et al., 2016). The drawback of these studies is however not refining the sort to delineate which population(s) within the $Lin^{-}CD117^{+}$ cells can give rise to NK cells. Even though the phenotype and function of stage 3 cells overlap with that of ILC3s and they might comprise the same cell type, it is possible that a minor NK precursor fraction within the former population exists. Crellin et al identified a small $CD127^{-}$ population within tonsil $Lin^{-}CD161^{+}CD117^{+}$ cells that

preferentially generates NK cells, concluding that CD127 delineates ILC3s from NK precursors (Crellin et al., 2010). However, CD94 was not included in the lineage mix and others have demonstrated that tonsil NK cells are mostly positive for CD161 and some show low levels of CD117 expression (Freud et al., 2006; 2016; Simoni et al., 2017), therefore it is likely that the starting population already contained NK cells. In the same study, LTi-like cells (sorted as $Lin^{-}CD127^{+}CD56^{-}$) were cultured in the presence of feeders plus IL-2 and despite maintaining some IL-22 and TNFα production as well as high *RORC* expression, they deviated towards IFNγ production, expressed low levels of perforin and GzmB and showed moderate cytolytic activity. This might either be attributed again to $CD94^{+}$ cells present in the sorted population, although the data suggests no rapidly dividing contaminating $CD56^{+}$ cells, or indeed acquisition of a cytotoxic program, previously associated solely with NK cells (CD94 or Eomes expression was not checked). LTi-like clones gave similar results but, despite comparable levels of cytotoxic proteins to bulk cultures, displayed no target killing (shown for 3 out of 20 clones) (Crellin et al., 2010). Also tonsil ILC3s, sorted as $Lin^{-}CD56^{+}NKp44^{+}CCR6^{+}CD103^{-}$ cells, exposed to IL-2 exhibit increased IFNγ production and responsiveness to IL-12 as well as CD94 up-regulation (Cella and Colonna, 2010).

Using more strict purification procedures ($Lin(including\ CD94)^{-}CD127^{+}CD117^{+}$), Bernink et al reported that ILC3s derived from fetal gut or tonsil tissues partly lose their expression of CD117 (and NKp44) when cultured for 8 days with IL-2 and IL-12, as opposed to IL-2, IL-23 and IL-1β, thus acquiring a group 1 ILC phenotype. Furthermore, tonsil $NKp44^{+}$ ILC3 cultures had significantly lower *RORC* but higher *TBX21* and *IFNG* transcripts as compared to freshly isolated cells (Bernink et al., 2013). This was observed also on a protein level. Although cytolytic activity was not assessed, Eomes was not up-regulated (Bernink et al., 2015), suggesting that either previous results were impacted by NK (precursor) contamination and ILC3s cannot convert to cNK cells or that IL-12 is not required for this differentiation, as demonstrated by Freud et al (Freud et al., 2016).

Collectively, these data demonstrates that the cytokine milieu strongly modulates ILC3 phenotype. They can divert to a type 1 effector program when

exposed to IL-2 or in combination with IL-12, but whether they can acquire cytotoxic properties is not entirely clear.

VII. Mice reconstituted with human immune system components (humanized mice)

The need for a small animal model better suited for translation of biomedical research into clinical applications has resulted in the development of humanized mice, defined here as immunodeficient mice repopulated with human hematopoietic cells and for some studies additionally transplanted with human tissues. They have become useful tools to study human immune system development and function, especially in a disease setting. For example, their importance in the research of the pathogenesis and immune control of human-tropic viruses such as human immunodeficiency virus (HIV) and EBV is undeniable. Moreover, they emerge as valuable models for preclinical evaluation of vaccine candidates and therapeutics (Gujer et al., 2015; Theocharides et al., 2016; Poluektova et al., 2015).

The discovery of mice with a *Prkdc*^{scid} (*scid*) mutation led the development of suitable hosts for xenotransplantation. These lack T and B cells, but due to their leakiness and radiosensitivity, mice with targeted *Rag2* mutations were thus generated. Still, crossing the *scid* mutation onto the non-obese diabetic (NOD) background further improved human cell engraftment. One of the reasons for that is the reduced phagocytosis by murine macrophages due to a sufficient interaction of the NOD signal regulatory protein α (SIRPα) with human CD47 to trigger an inhibitory signal. The last constraint to avoid transplant rejection was NK-cell activity, which was abrogated by incorporation of an IL-2 receptor common gamma chain (γ_c) (*Il2rg*) mutation. Of note, formation of SLTs such as LNs and PPs is compromised due to the common γ_c deficiency. The NOD-*scid* *Il2rg*^{null} (NSG) strain supports high human reconstitution after CD34$^+$ HPC injection and is our choice of recipient. In addition to lack of rejection, engrafted cells need a niche, which is usually achieved by sub-lethal total body irradiation (Theocharides et al., 2016; Poluektova et al., 2015).

Notably, humanized mice only partially recapitulate the human immune system development. Among other shortcomings, reconstitution of NK cells is low and incomplete (Poluektova et al., 2015). Although having a less differentiated phenotype, NK cells were demonstrated to achieve functional competence after *in vitro* stimulation with IL-15 or *in vivo* treatment with TLR3-agonist polyinosinic:polycytidylic acid (polyIC) (Strowig et al., 2010). The suboptimal human cell differentiation and maintenance in part reflects the lack of cross-reactivity or biological activity of mouse cytokines, chemokines, or survival factors. There are numerous efforts to overcome these limitations, for example administration or transgenic expression of human cytokines (Theocharides et al., 2016). Nonetheless, humanized mice reproduce many features of the human immune response. For example, HIV-1-driven reduction of ILC3s has been reported in humanized mice, which is reversed by antiretroviral therapy (ART). Depletion is mediated by pDC-produced type I IFNs that up-regulate CD95 (Fas) on activated ILC3s (Zhang et al., 2015). This data was later confirmed for HIV-1 patients, where transcriptome analysis also revealed up-regulation of genes associated with cell death (Kløverpris et al., 2016). Immune responses against EBV can also be modeled *in vivo* only in humanized mice, for which it was shown that NK cells exert control over lytic EBV infection and their depletion enhances features of the symptomatic infection, termed infectious mononucleosis (IM) (Chijioke et al., 2013). This was later corroborated by a longitudinal analysis of NK subsets in pediatric IM patients (Azzi et al., 2014).

VIII. EBV

EBV is a human-specific γ-herpesvirus that is transmitted via saliva exchange and establishes a life-long infection in more than 90% of the adult population. It has tropism primarily for B lymphocytes but also resides in epithelial cells. Upon entry into B cells, it initiates a latency program (III) by expressing six Epstein-Barr nuclear antigens (EBNAs), two latent membrane proteins (LMPs), two EBV encoded RNAs (EBERs) and about 40 microRNAs. These induce B cell proliferation, with a concurrent EBV replication, and a subsequent differentiation into resting memory B cells, in which the virus

persists with a restricted gene expression. Occasionally and likely upon BCR activation, EBV enters the lytic cycle, induced by expression of BZLF1 (ZEBRA) and BRLF1 (Rta). This leads to production of infectious viral particles that infect epithelial cells and shed into the saliva, completing the life cycle (Gujer et al., 2015; Münz, 2015a; 2015b).

EBV is usually acquired before the age of 5 years when infection is believed to occur mostly asymptomatically, whereas above 70% of individuals develop IM, often when primary infection occurs later in life (Balfour et al., 2013). IM is characterized by high EBV titer and a massive expansion of cytotoxic $CD8^+$ T cells, which are essential for containment of the disease. Patients with loss of T cell immunosurveillance, for example in AIDS or after transplant, are at risk for developing EBV-associated tumors. Such malignancies include Burkitt's and Hodgkin's lymphomas, nasopharyngeal carcinoma and EBV Post-Transplant Lymphoproliferative Disease (EBV-PTLD) (Gujer et al., 2015; Münz, 2015a; 2015b). NK cell-mediated control has also been reported for IM, in particular of lytic EBV infection (Azzi et al., 2014; Chijioke et al., 2013). Moreover, as previously discussed, patients with NK deficiencies have high susceptibility to EBV and associated tumors (Eidenschenk et al., 2006; Gineau et al., 2012; Orange, 2006; Parolini et al., 2000; Shaw et al., 2012). Thus, EBV is a powerful infectious model to study human NK responses.

Aim of the study

Human ILC2 and ILC3 cells possess functional plasticity and under IL-12 containing conditions convert into T-bet- and IFNγ-expressing cells (Bal et al., 2016; Bernink et al., 2013; 2015; Lim et al., 2016; Ohne et al., 2016; Silver et al., 2016). Since in mice ex-ILC3s acquire a helper and not cytotoxic ILC1 program (Klose et al., 2014), this possibility has not been conclusively explored in humans with some controversial reports. Even though initial studies of ILC3 cells showed $CD94^+$ expression or some cytolytic activity in *in vitro* expanded cells (Cella and Colonna, 2010; Crellin et al., 2010), these failed to exclude CD94 during purification and thus failed to exclude classical NK cells. On the other hand, $CD94^-CD117^+$ cells, which include ILC3s ($CD127^+$ in addition), are sorted as a precursor population in NK developmental studies and give rise to NK cells under IL-15-containing conditions (Freud et al., 2006; 2016).

Thus, to explore in detail whether human ILC3s can acquire also a cytotoxic program, which might be potentially harnessed in the context of viral infection or cancer at mucosal sites, we purified $NKp44^+$ and NCR^- ILC3s from tonsils and humanized mouse tissues and analyzed their functionality under inflammatory conditions *in vitro* and *in vivo*.

Results

I. ILC3s in tonsils and humanized mouse tissues

Human ILC3s at steady state are most abundant in mucosal tissues, in particular in tonsils and the intestine (Bernink et al., 2015; Simoni et al., 2017). For our studies, we used ILC3s from pediatric tonsils and in order to be able to later investigate the relevance of our *in vitro* findings *in vivo*, we compared them to ILC3s isolated from tissues of our in-house humanized mouse model (huNSG), specifically spleen and small intestine. Prior to flow cytometric sorting (FACS), tonsil and spleen mononuclear cells were depleted of T cells, B cells and monocytes/macrophages, which were also removed by FACS. We further excluded human hematopoietic progenitor cells (HPCs), myeloid cells, $CD16^+$ NK cells as well as ILC2s ($CD294^+$) and sorted ILC3s as viable human hematopoietic ($CD45^+$) cells that express CD127 and CD117. We purified $NKp44^+$ and NCR^- (defined as $NKp44^-NKp46^-$) ILC3 subsets as well as NK cells to be used as controls (Figure 1A).

NK cells and ILC3s were similarly represented in human tonsils (24 ± 10% and 18 ± 10% of ILCs of interest, respectively) and at even increased but equal proportions in huNSG small intestine (SI), in contrast, NK cells were 2-fold higher and on average represented 54% of ILCs in huNSG spleen. These two populations together constituted three-quarters of ILCs both in spleen and SI, however $NKp44^+$ ILC3s were a minor fraction of ILC3s in spleen, unlike in SI (Figure 1B). Importantly, spleen and SI differed not only in ILC subset distribution, but also in frequency of ILCs among overall human $CD45^+$ cells (Figure 1C). Whereas each ILC3 subset represented 6-9% of $CD45^+$ cells in SI, their percentage in spleen was below 0.2. This was similar to their yield, indicating the high level of human reconstitution in spleen and the efficiency of the sort. ILC3s recovered from tonsil were 7-fold less than in spleen, in line with a previous report (Magri et al., 2014). Surprisingly, NK cells had lower yield than expected (Figure 1D).

Figure 1

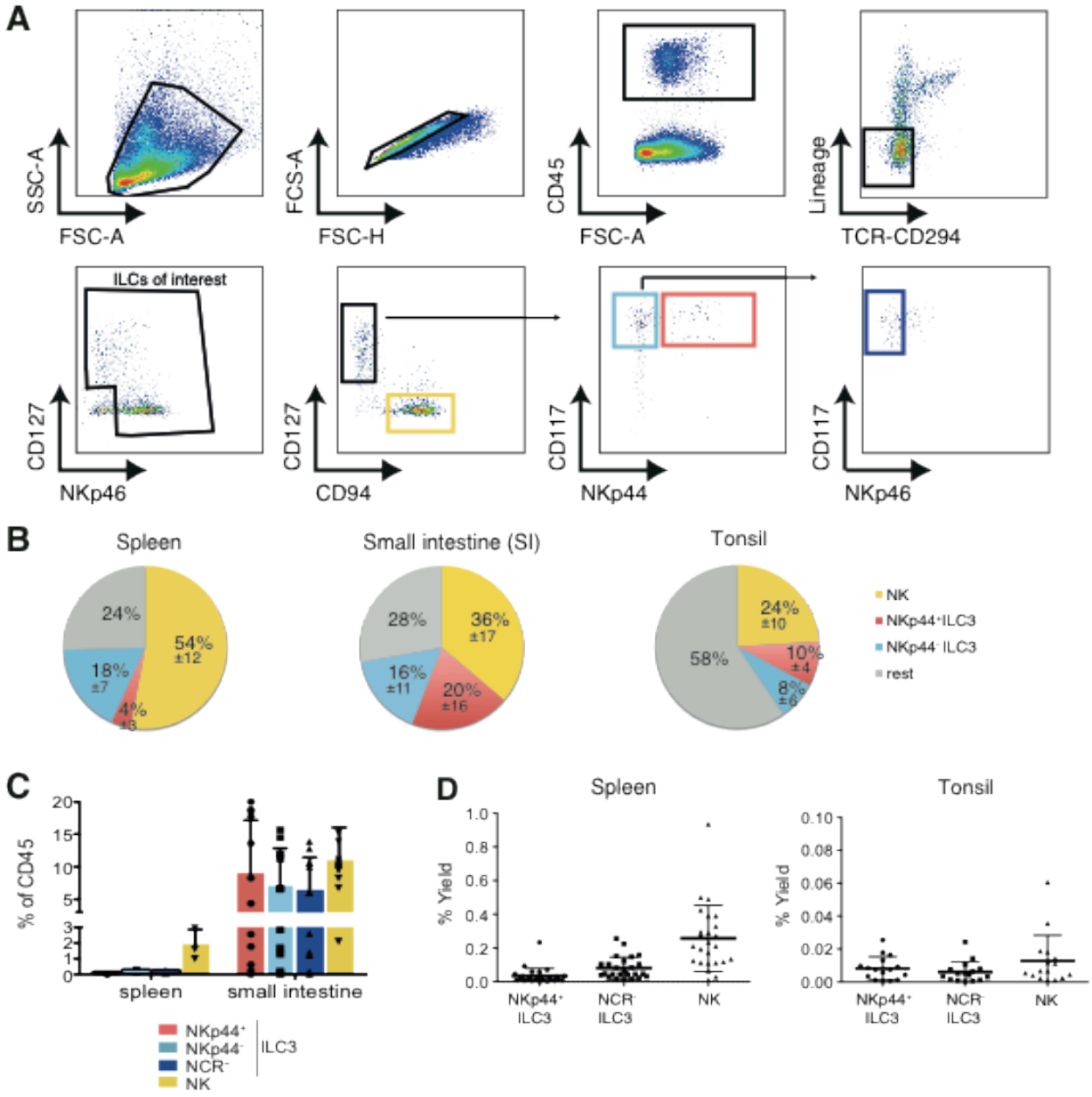

Figure 1 ILC3 cells in tonsils and humanized mouse tissues
(A) Gating strategy for isolation of ILCs of interest, defined as viable CD45$^+$ Lin$^-$ (CD3$^-$ CD19$^-$CD14$^-$**CD16**$^-$FcεRIα$^-$CD34$^-$TCRα/β$^-$TCRγ/δ$^-$**CD294**$^-$) CD127$^+$ and/or NKp46$^+$; NK cells (yellow) are further sorted as CD94$^+$CD127$^-$, NKp44$^+$ ILC3s (red) as CD94$^-$ CD127$^+$CD117$^+$NKp44$^+$ and NCR$^-$ ILC3s (dark blue) are identified as CD94$^-$ CD127$^+$CD117$^+$NKp44$^-$NKp46$^-$. Transcription factor staining of purified populations is shown in the Appendix Figure 13. Gating shown for a representative spleen MACS-depleted sample. (B) Mean frequency (± *SD*) of the indicated populations among ILCs of interest within pediatric tonsils (N=16); spleen (N=20, 2-15 mice per HFL donor) and small intestine (SI) (N=9, 4-15 mice per HFL donor) of huNSG mice. For samples details refer to Tables 1 and 2. (C) Frequency of the indicated populations within spleen (N=3, 1-8 mice per donor) and SI (as above) from human CD45$^+$ cells. (D) Yield from tonsils and spleen, calculated as percentage of sorted cells from total isolated mononuclear cells.

Of note, NKp46 expression on ILC3s was variable, which is consistent with published results (Simoni et al., 2017), and also significantly lower in comparison to that on NK cells (data not shown); therefore, this marker was not included in the subset distribution assessment (Figure 1B).

Thus, both NCR positive and negative ILC3s could be recovered from tonsils of children, spleen and small intestine of humanized mice.

II. ILC3s up-regulate NK cell markers in response to IL-12 and/or IL-15

To investigate whether ILC3s can acquire NK properties under inflammatory conditions, we expanded tonsil NKp44^{+} ILC3s with IL-2 and IL-7 to gain sufficient numbers for stimulation of re-sorted CD117^{+}CD94^{-} cells with all possible combinations of IL-2, -12, -15, and -18 (Figure 2A). After 1 week (data not shown) and 2 weeks, we observed acquisition of CD94, an NK-associated marker, in all conditions. CD94^{+} cells had down-regulated expression of the ILC3 master regulator RORγt when compared to CD117^{+}CD94^{-} cells, which still constituted the majority of the culture (Figure 2B). These results indicated that cells that acquired CD94 shifted away from their ILC3 profile. Moreover, we detected a slight increase in T-bet levels, which was previously demonstrated for freshly isolated tonsil and intestinal ILC3s after combined stimulation with IL-2 and IL-12 for 4 days (Bernink et al., 2013; 2015). IL-12 was described to promote T-bet expression and IFNγ production also in human ILC2 cells (Bal et al., 2016; Lim et al., 2016; Ohne et al., 2016; Silver et al., 2016) and consistent with this data, conditions containing IL-12 most efficiently induced CD94 expression (Figure 2C). Importantly, in contrast to these studies and mouse data (Klose et al., 2014), we found up-regulation of Eomes, which is known to be expressed solely in cytotoxic lymphocytes.

Figure 2

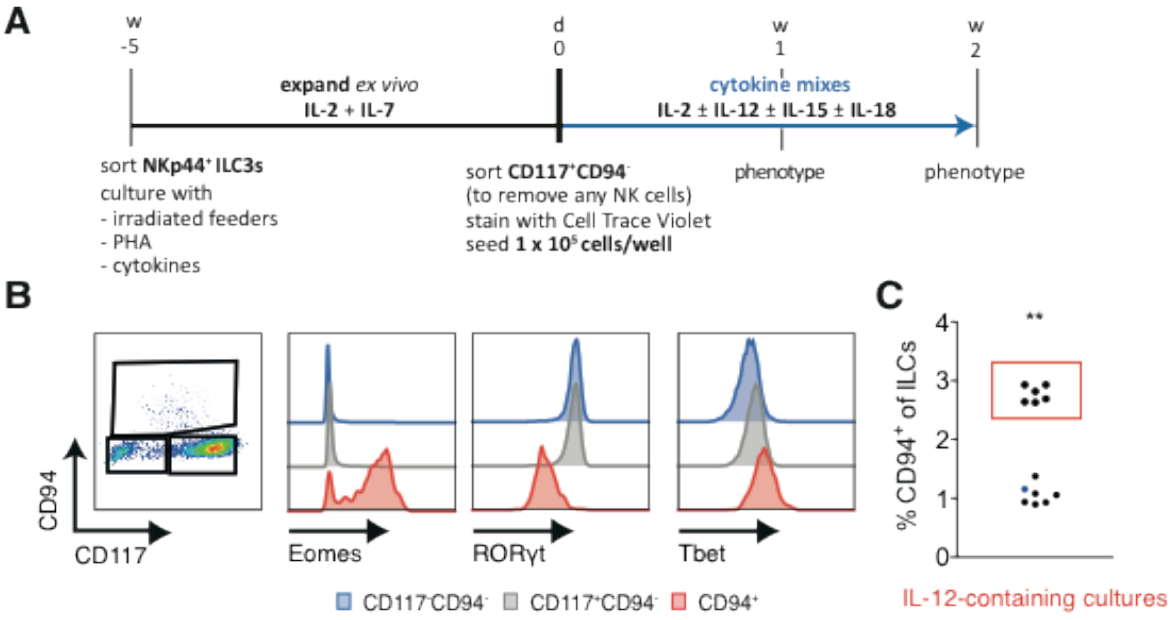

Figure 2 IL-12 induces expression of NK cell markers in IL-2 and IL-7 expanded tonsil-derived NKp44+ ILC3s

(A) Experimental outline. All possible combinations of the indicated cytokines (15 conditions) and IL-2 and IL-7 culture as a reference population (B) Representative flow cytometric analysis of stimulated NKp44+ ILC3s. (C) Percentage of CD94-expressing cells among the different conditions, IL-2 and IL-7 control is shown in blue. Cells stimulated with IL-12 and -18 alone or in combination did not survive for 2 weeks. Data obtained from 1 donor. ns $P > 0.05$, * $P < 0.05$, ** $P < 0.01$ using paired *t* test.

We next sought to confirm this plasticity with respect to NK-specific marker expression by stimulating freshly isolated tonsil NKp44+ ILC3s for 2 weeks under different conditions. Culture with IL-7 alone was previously shown to be sufficient only for survival of cells with ILC3 characteristics (sorted as CD56+NKp44+CCR6+CD103-) and the addition of IL-2, which promoted proliferation, changed their profile, even though *RORC* expression was maintained (Cella and Colonna, 2010). Indeed, unlike IL-7 alone, exposure to both IL-2 and IL-7 up-regulated Eomes but not T-bet (Figure 3). Of note, this condition was used as a control culture in later experiments. IL-12 induced low T-bet expression, which was not observed in any of the other conditions. More importantly, IL-12 promoted expression of both Eomes and CD94, but not as much as stimulation with IL-15. A combination of both had a strong synergistic effect (Figure 3). Therefore, we focused on this condition for further *in vitro* investigation, the experimental outline for which is shown in Figure 4A.

Figure 3

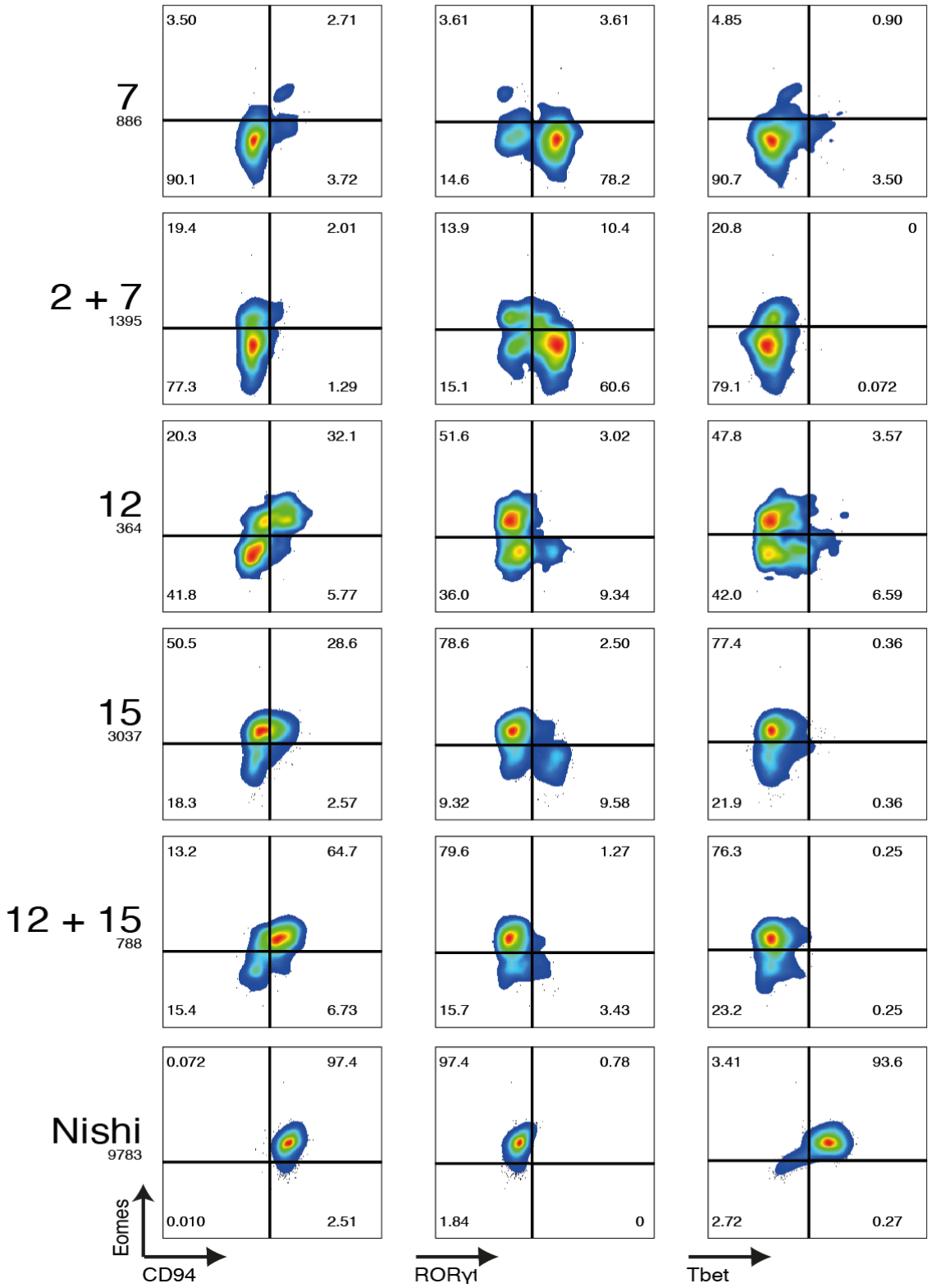

Figure 3 Plasticity of NKp44⁺ ILC3s
Tonsillar NKp44⁺ ILC3s were cultured on irradiated feeders with the indicated cytokines for 2 weeks and expression of CD94 as well as ILC3 and NK transcription factors was determined by flow cytometry. The human NK cell line Nishi was used as a positive control. Data obtained from 1 donor.

ILC3s cultured for 3 weeks (4 weeks for SI) with IL-2 plus IL-7 or IL-12 plus IL-15 expanded similarly (Figure 4B).

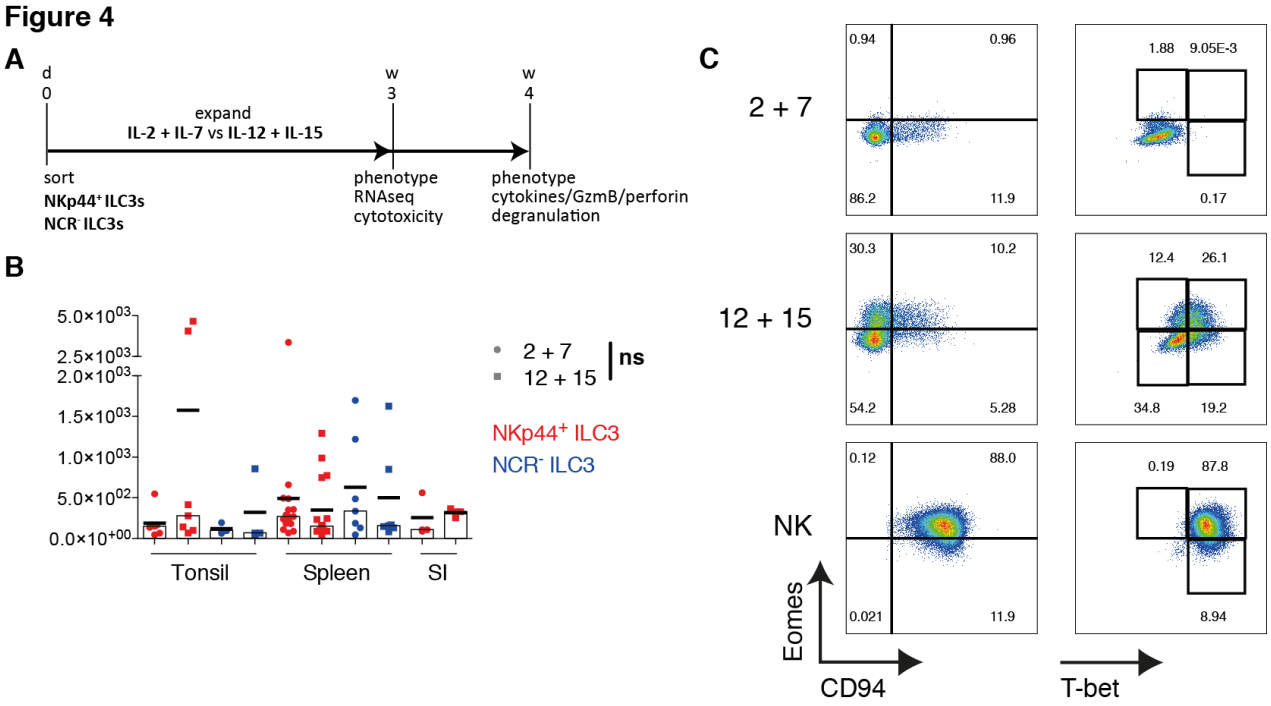

Figure 4 IL-12 and IL-15 promote expression of phenotypic NK cell markers on ILC3s

(A) Experimental outline. (B) Fold expansion of NKp44+ and NCR- ILC3s from pediatric tonsils and spleen after 3 weeks and from SI after 4 weeks. (C) Flow cytometric analysis of tonsillar NKp44+ ILC3s and NK cells expanded for 3 weeks, each column gated on viable ILCs. Numbers indicate percent cells in each quadrant or gate. (D-F) Quantification of the indicated subsets in cultures of (D and E) NKp44+ and (F) NCR- ILC3s in the indicated tissues. For tonsil N=6 and 3 in D and F, respectively, and the same donors are color-coded. For spleen N=14 (10 HFL donors) in D and N=6 (6 HFL donors, 3-8 mice each) in F. For SI (assessed after 4 weeks) N=3 (3 HFL donors, 4-5 mice each) in E. Red lines show mean and box-and-whiskers plot extend min to max with grey line representing median value. ns $P > 0.05$, * $P < 0.05$, ** $P < 0.01$ using paired *t* test. (G) Eomes vs T-bet expression in IL-12 plus IL-15 condition. Subsets were further analyzed for RORγt expression, (H) which was quantified for total Eomes+ cells in the indicated populations for tonsil- and spleen-derived ILC3 cultures. ns $P > 0.05$, * $P < 0.05$, ** $P < 0.01$ using unpaired *t* test (H) Single-cell sorted ILC3s were cultured onto irradiated Cell Trace Violet-stained feeders with IL-2 plus IL-7 or IL-12 plus IL-15. Clonal cultures were analyzed by flow cytometry after 21 days. C, F and H Gating shown for tonsillar NKp44+ ILC3s. IL-15-expanded bulk NK cells were used as a positive control. Figure continues on the next pages.

Figure 4

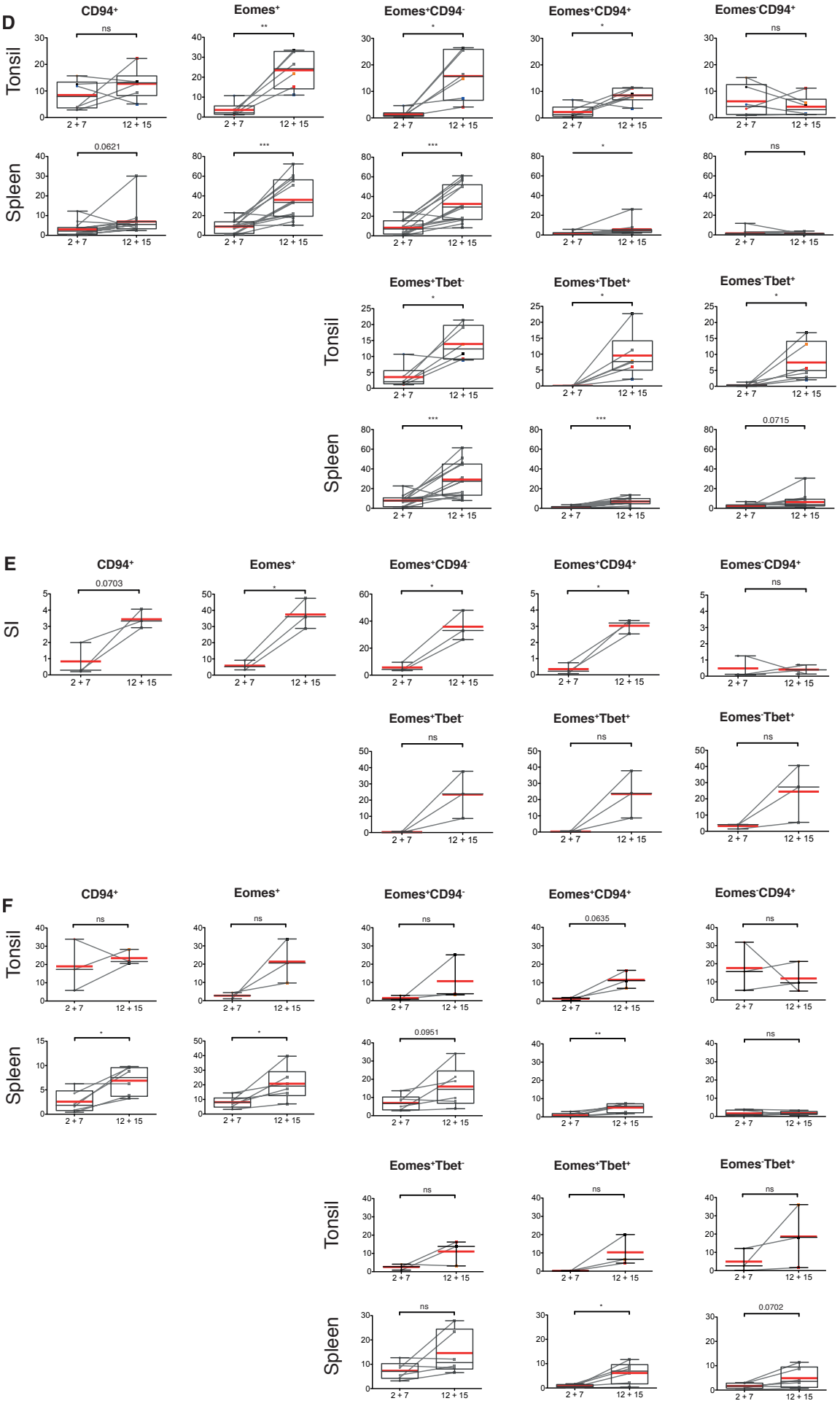
D
CD94+
Eomes+
Eomes+CD94-
Eomes+CD94+
Eomes-CD94+
Tonsil
Spleen
Eomes+Tbet-
Eomes+Tbet+
Eomes-Tbet+
E
SI
F
2 + 7
12 + 15

Figure 4

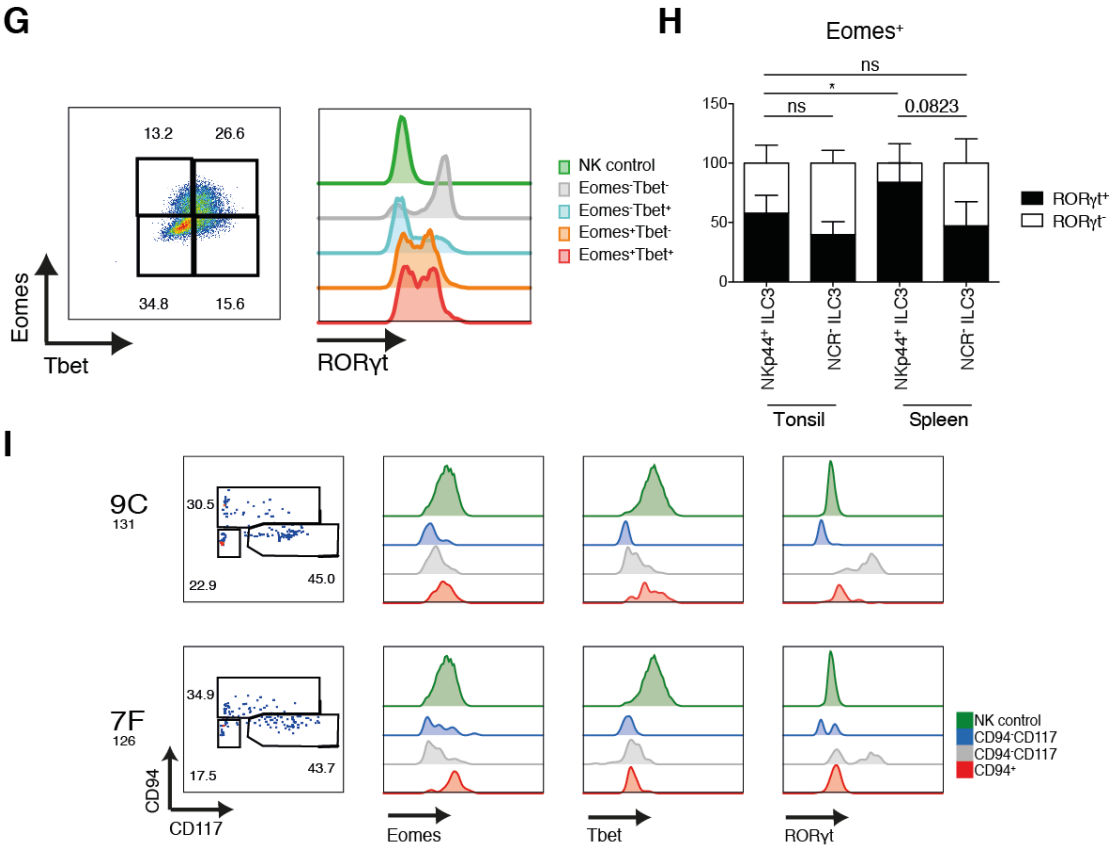

IL-12 and IL-15 significantly up-regulated Eomes in NKp44$^+$ ILC3s compared to controls, with average frequency of about 20% in tonsils and 35-40% in tissues derived from huNSG mice (Figure 4C, D and E). However, only a minor fraction of Eomes$^+$ cells co-expressed CD94 and, thus, resembled mature NK cells. Curiously, in tonsil-derived cultures we observed a CD94$^+$ population that was negative for both Eomes and T-bet (not shown) and was as frequent as CD94$^+$Eomes$^+$ cells in IL-2 and IL-7 conditions but lower in the IL-12 and IL-15 ones. T-bet was detected only upon IL-12 and IL-15 stimulation and was also expressed without Eomes, as previously described for IL-2 and IL-12 stimulation of tonsillar ILC3s (Bernink et al., 2015). Eomes$^-$T-bet$^+$ cells were found at a similar frequency to Eomes$^+$T-bet$^+$ ones, but the former were less abundant compared to the total Eomes-expressing cells (Figure 4D and E).

These phenotypic changes however could not be recapitulated for tonsillar NCR$^-$ ILC3s (Figure 4F). Compared to their NKp44$^+$ counterparts, splenic NCR$^-$ ILC3 stimulated with IL-12 plus IL-15 had lower expansion of Eomes$^+$ cells, which nonetheless were significantly higher than in controls. Notably,

Eomes$^+$CD94$^+$ and Eomes$^+$Tbet$^+$ (also Eomes$^-$Tbet$^+$) cells were found at a similar frequency (calculation not shown) (Figure 4F).

Surprisingly, Eomes$^+$ cells, derived from IL-12 and IL-15 stimulated ILC3s, irrespective of T-bet presence, had a bi-modal expression of RORγt (Figure 4G). This was in contrast to the 2-week cultures, at which time point this transcription factor was almost entirely down-regulated (Figure 3). In fact, 40-65% of Eomes-expressing cells were positive for RORγt in tonsil-derived cells. In spleen, this number reached 80% on average for NKp44$^+$ cultures, whereas Eomes$^+$RORγt$^+$ cells were slightly less frequent in NCR$^-$ ones and comparable to tonsil (Figure 4H). Therefore, a significant fraction of the Eomes-expressing cells arising in the culture differed from classical NK cells in RORγt and only partial T-bet expression. These differences suggested that the observed Eomes$^+$ cells were indeed derived from ILC3s and not a NK contamination from the sort.

To further address this issue, we cultured single-cell sorted tonsil NKp44$^+$ ILC3s onto Cell Trace Violet-stained feeders. In line with data from bulk cultures, we found few wells with a mixture of cells that acquired expression of CD94 and Eomes, but down-regulated RORγt, and cells that retained their ILC3 CD117$^+$RORγt$^+$ phenotype (Figure 4H).

Collectively, IL-12 plus IL-15 stimulation led to up-regulation of Eomes, T-bet and to a lesser extent CD94, although differentiated cells only partially lost their ILC3 phenotype.

III. Transcriptional profile of NKp44$^+$ ILC3s upon IL-12 and IL-15 culture is reminiscent of early differentiated NK cells

To investigate the extent in which culture conditions transcriptionally change ILC3s and how close exposure to IL-12 and -15 brings their profile to that of NK cells, we performed RNA sequencing (RNAseq) of the two investigated culture conditions (IL-2 plus IL-7 and IL-12 plus IL-15) and included untreated cells as a reference population. We used NKp44$^+$ ILC3s as they exhibited a significant increase in Eomes expression upon IL-12 and IL-15 exposure compared to IL-2 and IL-7 treated cells and this was higher than in NCR$^-$ cells.

In a principal component analysis (PCA) of the RNAseq data, samples formed individual clusters dependent on their tissue origin and cytokine exposure with the exception of those cultured with IL-12 and IL-15. These surprisingly co-segregated, whereas the rest of tonsil and spleen samples separated along PC2 (Figure 5A). Hierarchical clustering of the samples showed closer relationship between treatments than across tissues and also that freshly isolated cells were more closely related to the cells stimulated with IL-2 and IL-7 (Figure 5B).

Freshly sorted NKp44^{+} ILC3s expressed genes encoding IL-1R1, IL-23R, TRANCE, BAFF, APRIL (variable) and CCL20 (Figure 5C), which were reported to be selectively transcribed in ILC3s among innate lymphocytes (Bjorklund et al., 2016). *IL17A* expression was not detected, as previously reported for adult ILC3s (Hoorweg et al., 2012), whereas *IL17F* transcripts were present in only a few tonsil samples. Splenic ILC3s showed higher amount of *LTA*, *LTB*, and *TNF* transcripts relative to tonsillar cells. Instead abundant expression of *IL22* was found within tonsil- but not spleen-derived ILC3s. These findings were consistent with a study, which in addition demonstrated that upon cytokine stimulation both populations secreted IL-22 at a similar level (Magri et al., 2014). Furthermore, we observed variable expression of *IL2* and *CSF2* (encoding GM-CSF), even without *ex vivo* stimulation. Low but homogenous *RORC* expression was found in spleen samples, whereas tonsil ones exhibited a more diverse pattern. They however expressed transcripts encoding other transcription factors associated with ILC3s such as *TOX2* and *AHR* as well as for some that are shared with other ILCs such as *GATA3* and *RORA* (Bjorklund et al., 2016) (Figure 5C). Taken together, ILC3s isolated from huNSG spleens were similar to those derived from human tissues, demonstrating that this model can be a valuable tool to study human ILC development and functionality *in vivo*.

Figure 5

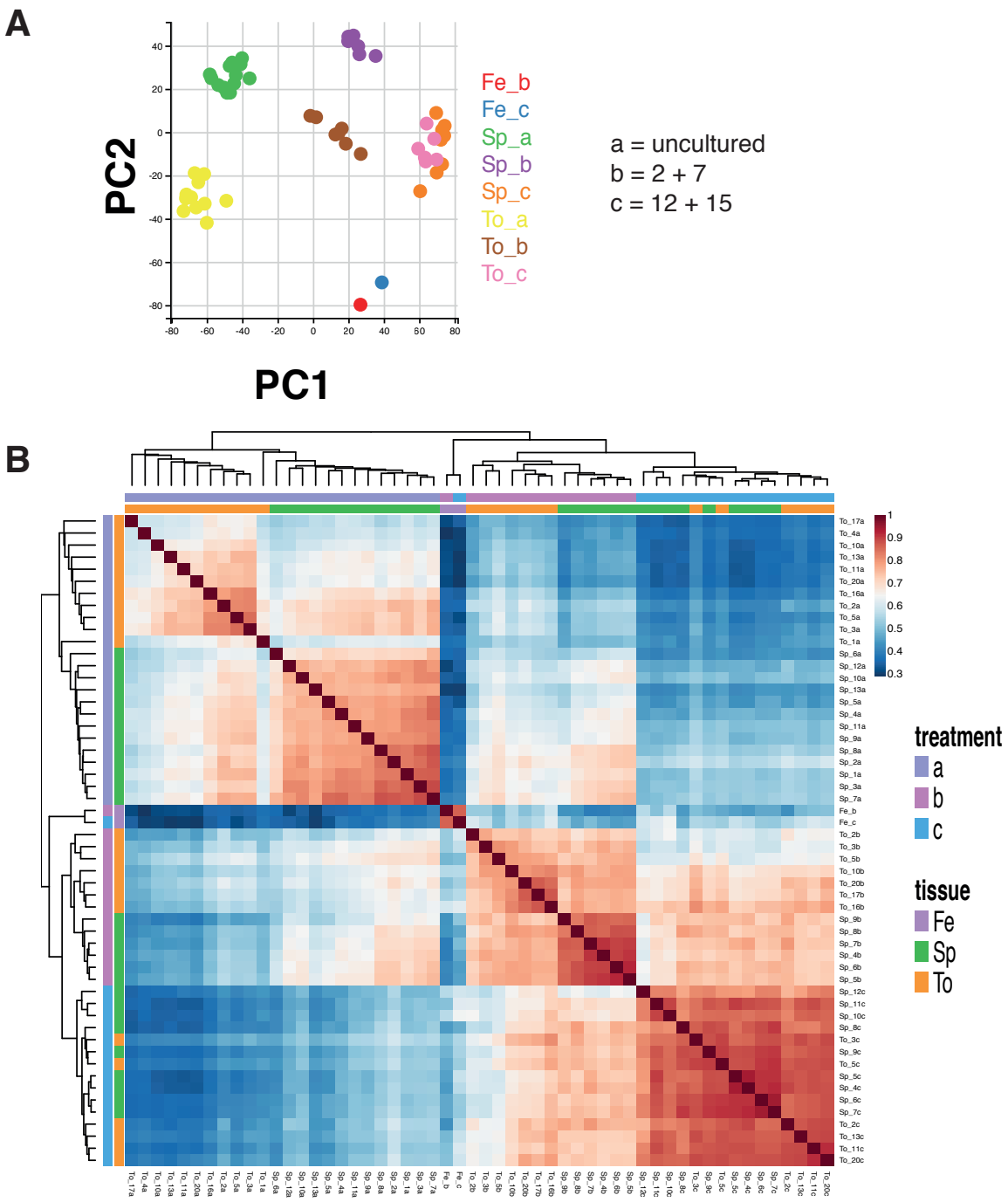

Figure 5 Transcriptional profile of NKp44⁺ ILC3s upon IL-12 and IL-15 culture is reminiscent of early differentiated NK cells

(A) PCA analysis with samples plotted using the first two principal components. (B) Hierarchical clustering of all samples. (C) (next page) Heat maps of selected genes, grouped in the indicated categories, showing differential expression across treatment conditions and tissues. Condition a represents uncultured cells, condition b and c indicate cells expanded for 3 weeks with IL-2 and IL-7 or IL-12 and IL-15, respectively. Fe is feeders, Sp is spleen, and To is tonsil. Samples used for RNA sequencing and incorporated into analysis are shown in Tables 1 and 2.

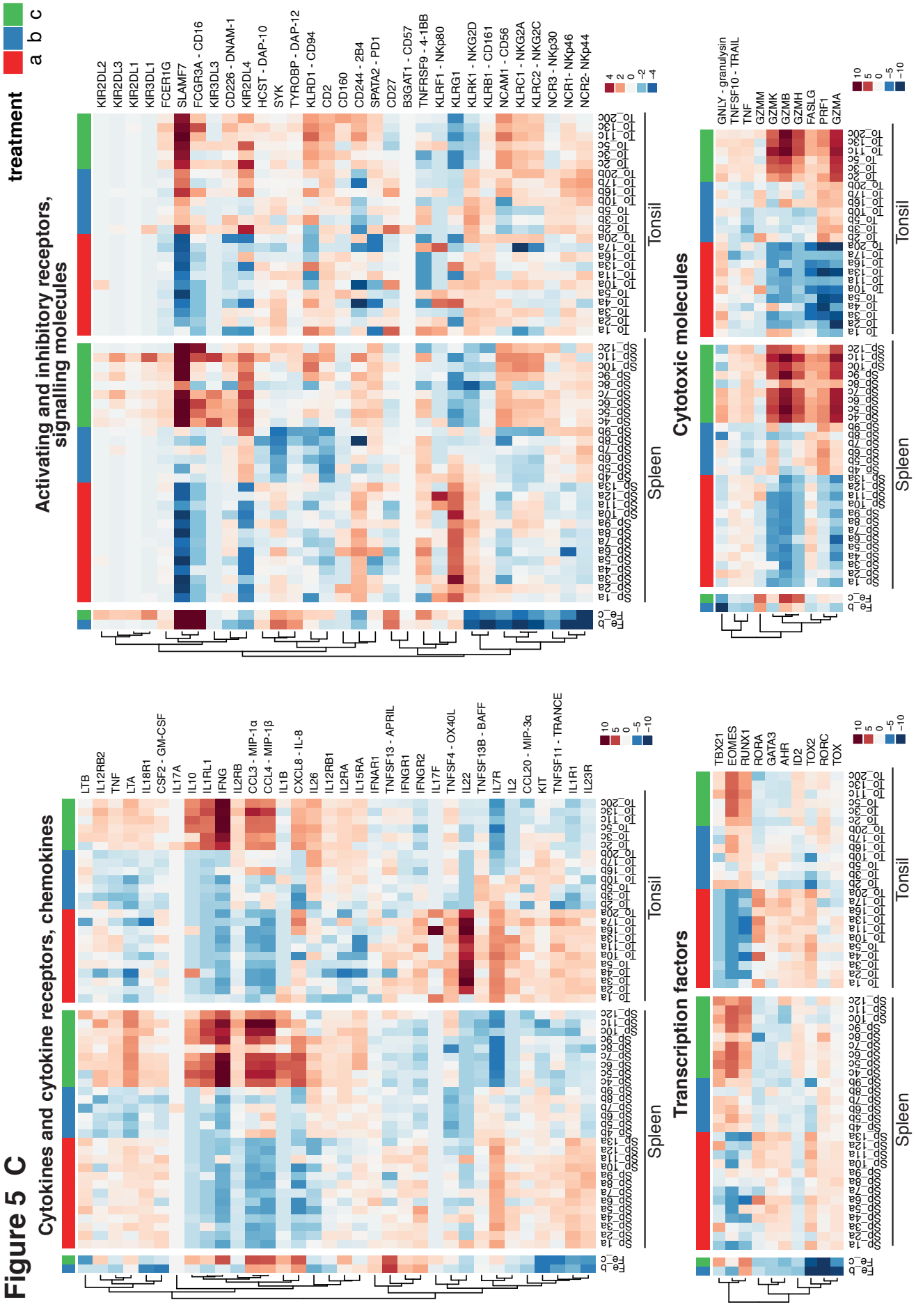
Figure 5 C
Cytokines and cytokine receptors, chemokines
Activating and inhibitory receptors, signalling molecules
Transcription factors
Cytotoxic molecules
treatment
a b c
Spleen
Tonsil

We next assessed changes in NKp44$^+$ ILC3 transcriptome induced by treatment with IL-2 and IL-7. Although *KIT* and *RORC* expression was retained, expanded cells down-regulated *IL7R*, *IL1R1, IL23R* and *IL22* (for tonsils). Concurrently, they up-regulated *EOMES*, *TBX21* (variable in tonsils), *PRF1* (perforin) and transcripts encoding granzymes, in particular *GZMA* in tonsils and *GZMK* in spleen (Figure 5C), indicating they shifted away from an ILC3 transcriptional program.

Upon IL-12 and IL-15 culture NKp44$^+$ ILC3s up-regulated genes that encode NK-related markers such as CD56, CD94, NKG2A, NKG2C, DNAM-1 and CD2. Surprisingly, transcripts for NKG2D were lower compared to the other conditions. *FCGR3A* (encoding CD16) expression was also increased, however it was diverse across samples and tissues and detected only in a few Eomes$^+$ cells on the protein level (Appendix, Figure 14). *KIR3DL3* expression partially overlapped with that of *FCGR3A* in spleen and less so in tonsils, whereas other inhibitory KIRs had lower and more scattered expression pattern in spleen and were absent in tonsils. We found higher expression of *KIR2DL4*, which encodes an activating receptor for HLA-G that induces a pro-inflammatory rather than a cytotoxic response in NK cells upon triggering (Rajagopalan and Long, 2012; Vély et al., 2016b). Overall, IL-12 and IL-15 stimulated ILC3 seemed to acquire a profile reminiscent of early differentiated NK cells (Béziat et al., 2010; Björkström et al., 2010). Moreover, they showed enrichment of genes encoding IFNγ, MIP-1α, MIP-1β, and IL-8 (in spleen) as well as subunits of the IL-2/12/15/18 receptors, thus IL-12 and IL-15 primed ILC3s towards a type 1 inflammatory response. Of note, in line with the maintained RORγt expression, they also displayed transcripts for *LTA* and *LTB*. Interestingly, splenic NKp44$^+$ ILC3s showed some *TNFSF10* (TRAIL) expression without stimulation, which was not influenced by IL-12 and IL-15 and was even down-regulated after IL-2 and IL-7 culture. Conversely, *TNFSF10* transcripts were elevated in tonsillar cells upon IL-12 and IL-15 stimulation. IL-12 and IL-15 increased *EOMES*, *FASLG*, and granzyme expression also compared to IL-2 and IL-7 treated cells, whereas *PRF1* levels were similar between the two culture conditions. (Figure 5C). Hence, depending on the cytokine milieu ILC3s can acquire a cytotoxic transcriptional profile.

This data supported our findings that ILC3s stimulated with IL-12 and IL-15 shared features with NK cells and we next analyzed their functionality.

IV. Stimulation with IL-12 and IL-15 induces a functional program of NK cells in ILC3s

A. Acquisition of an ILC1 cytokine profile upon IL-12 and IL-15 stimulation

The transcriptome analysis revealed a shift in NKp44$^+$ ILC3s cultured with IL-12 and IL-15 towards an ILC1/NK cytokine profile; therefore we assessed the IFNγ and TNFα expression in response to stimulation with a prototypic NK cell target, erythroleukemic K562 cells, as well as with PMAi (Figure 6A-C). In IL-12 and IL-15 cultures, IFNγ expression was almost undetectable unless cells were exposed to PMAi, which suggested that signals triggered by K562 cells were insufficient to induce a proper IFNγ production (Figure 6B and C). IFNγ expression was completely absent in IL-2 and -7 treated cells even upon PMAi stimulation (Figure 6B and C), which is in contrast to published data from tonsils (Cella and Colonna, 2010). On the other hand, expanded cells were potent TNFα producers but that potential was reduced upon treatment with IL-12 and -15. In this condition however K562 cells evoked a better response and TNFα expression was found in both CD117$^+$ and CD117$^-$ cells (Figure 6A and C). We further tested expression of IL-22, as another study reported its induction upon stimulation of spleen ILC3s even though mRNA levels were low (Magri et al., 2014). PMAi however did not drive IL-22 expression (Figure 6D and E). Previous studies on tonsil ILC3s are inconclusive with respect to IL-22 induction by PMAi alone (Cella and Colonna, 2010; Cella et al., 2008) but cytokines combinations including IL-23 or IL-1 were demonstrated to promote it (Glatzer et al., 2013; Magri et al., 2014). Therefore, PMAi alone might not be sufficient or spleen-derived NKp44$^+$ ILC3s (under these conditions) do not produce IL-22.

Thus, also on the protein level, IL-12 and-15 induced a cytokine profile associated with NK cells.

Figure 6

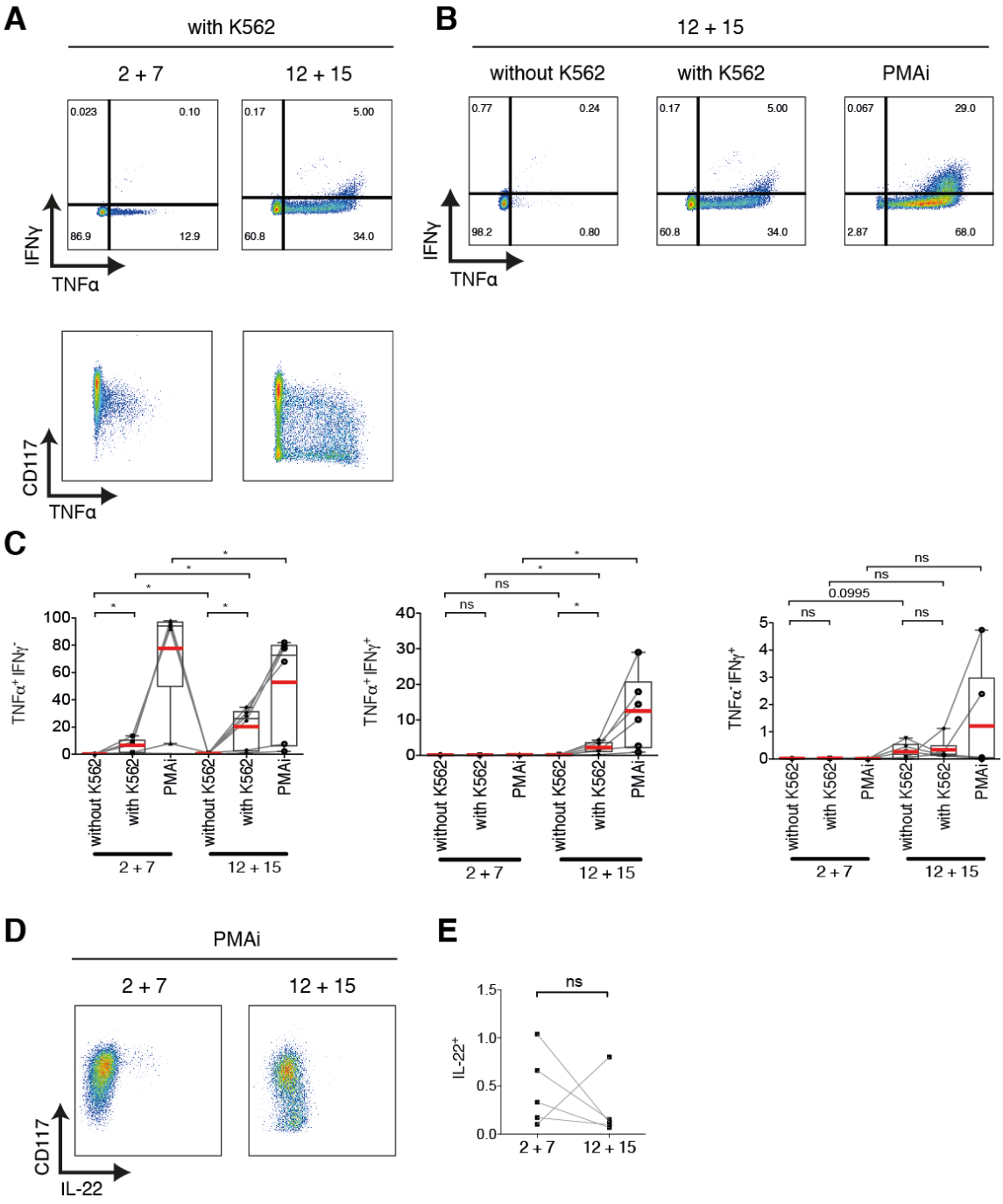

Figure 6 Acquisition of an ILC1 cytokine profile in spleen-derived NKp44⁺ ILC3s upon IL-12 and IL-15 stimulation

(A) Flow cytometric analysis of spleen-derived NKp44⁺ ILC3 after 4-week culture. Intracellular staining for IFNγ and TNFα and expression of TNFα in CD117⁺ and CD117⁻ cells after K562 target cell and PMAi stimulation for 4 hr. (B) Expression of the indicated cytokines in differentially stimulated IL-12 and IL-15 cultured cells. (C) Quantification of IFNγ and TNFα in the indicated conditions. N=6 (3 HFL donors, 4 mice each) (D) Flow cytometry and (E) quantification of IL-22 expression after PMAi stimulation for 4 hrs. N=5 (2 HFL donors, 4 mice each). Red lines show mean and box-and-whiskers plot extend min to max with grey line representing median value. ns $P > 0.05$, * $P < 0.05$, ** $P < 0.01$ using paired t test.

B. Up-regulation of cytotoxic molecules and degranulation in response to classical NK cell targets upon IL-12 and IL-15 exposure

Having observed on the mRNA level an induction in cytotoxic mediators in NKp44^{+} ILC3s cultured with IL-12 and IL-15, we set out to investigate their granzyme B (GzmB) and perforin protein expression. Perforin was hardly detectable in both culture conditions but was slightly increased in IL-12 and IL-15 treated cells (Figure 7A and B). Upon K562 interaction its expression declined, indicative of a rapid cytotoxic granule release as protein transport was inhibited after 45 min of incubation.

Consistent with its abundant expression on the mRNA level, GzmB was significantly higher upon stimulation with IL-12 plus IL-15. Moreover, cells that down-regulated CD117, which is associated with NK differentiation (Freud et al., 2016), were the primary producers. Unlike perforin however, GzmB levels remained unchanged during K562 co-culture (Figure 7A and B), which might indicate that it was faster recovered. Alternative explanation could be that the majority was not released. Of note, GzmB expression was previously demonstrated in non-cytotoxic plasmacytoid DCs (Fuchs, 2005).

Next, we checked degranulation as a surrogate for cytotoxicity towards K562 cells in a 4-hour assay and to our surprise it was unchanged in the conditions tested (circa 13%) (data not shown). Therefore, we evaluated degranulation among the various subsets (Figure 7C and D). CD117^{-} cells were significantly increased in IL-12 and IL-15 cultures and Eomes^{+} cells represented the majority of those. Once cells expressed this transcription factor, they showed high degranulation capacity (30-40% on average) and more so when CD117 was down-regulated. The Eomes^{-} subsets had similar levels of degranulation, which was even less when cultured with IL-12 and IL-15 (Figure 7D).

Altogether, Eomes up-regulation correlated with degranulation ability across all culture conditions.

Figure 7

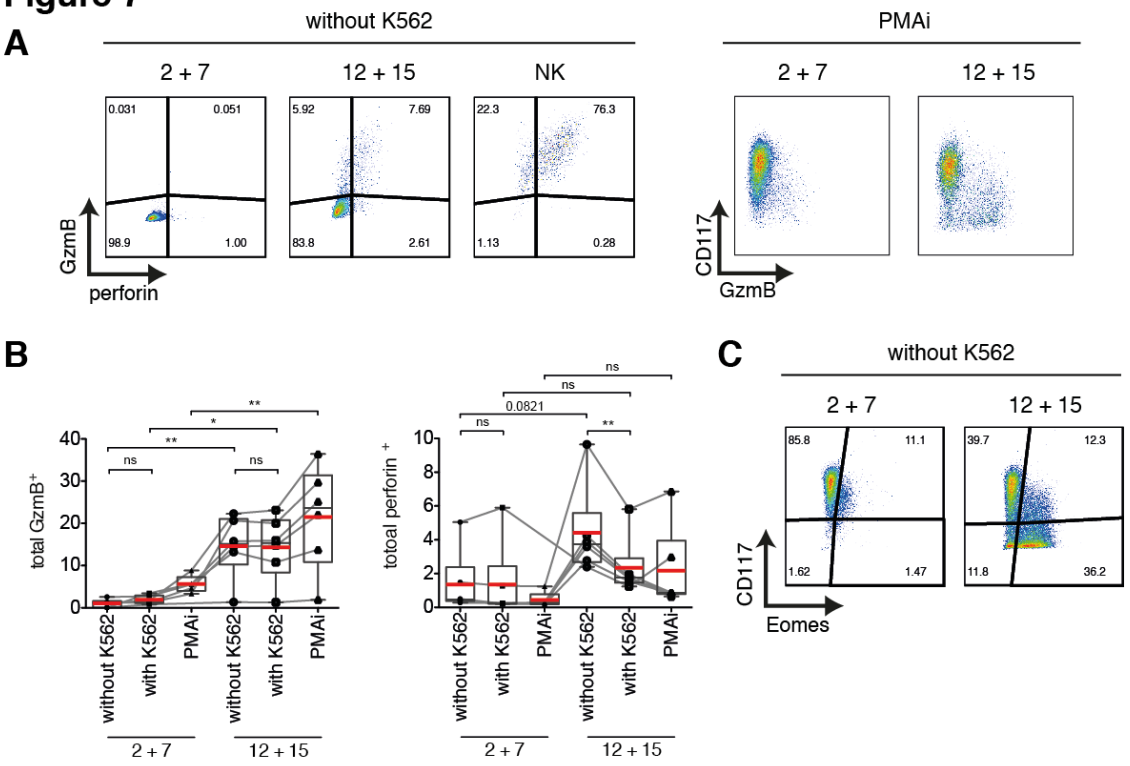

Figure 7 Up-regulation of cytotoxic machinery in spleen-derived NKp44⁺ ILC3s upon IL-12 and IL-15 exposure and degranulation in response to classical NK cell targets K562

(A) Flow cytometric analysis and (B) quantification of total GzmB and perforin in spleen-derived NKp44+ ILC3 4-week cultures after stimulation with K562 cells, PMAi or without treatment (4 hr), GzmB versus CD117 expression is shown for PMAi exposed cells. Expanded NK cells were used as a positive control. (C) CD117 and Eomes expression 4-week cultures. Numbers indicate percent cells in each quadrant. (D) Differences in the subsets shown in (C) and degranulation upon K562 co-culture for 4 hr. Δ%CD107a refers to the difference in degranulation with and without K562 stimulation. For quantifications N=6, obtained from 3 HFL donors (4 mice each). Same samples used in (B), (D) and Figure 6. Red lines show mean and box-and-whiskers plot extend min to max with grey line representing median value. ns $P > 0.05$, * $P < 0.05$, ** $P < 0.01$ using paired t test. Figure continues on the next page.

Figure 7

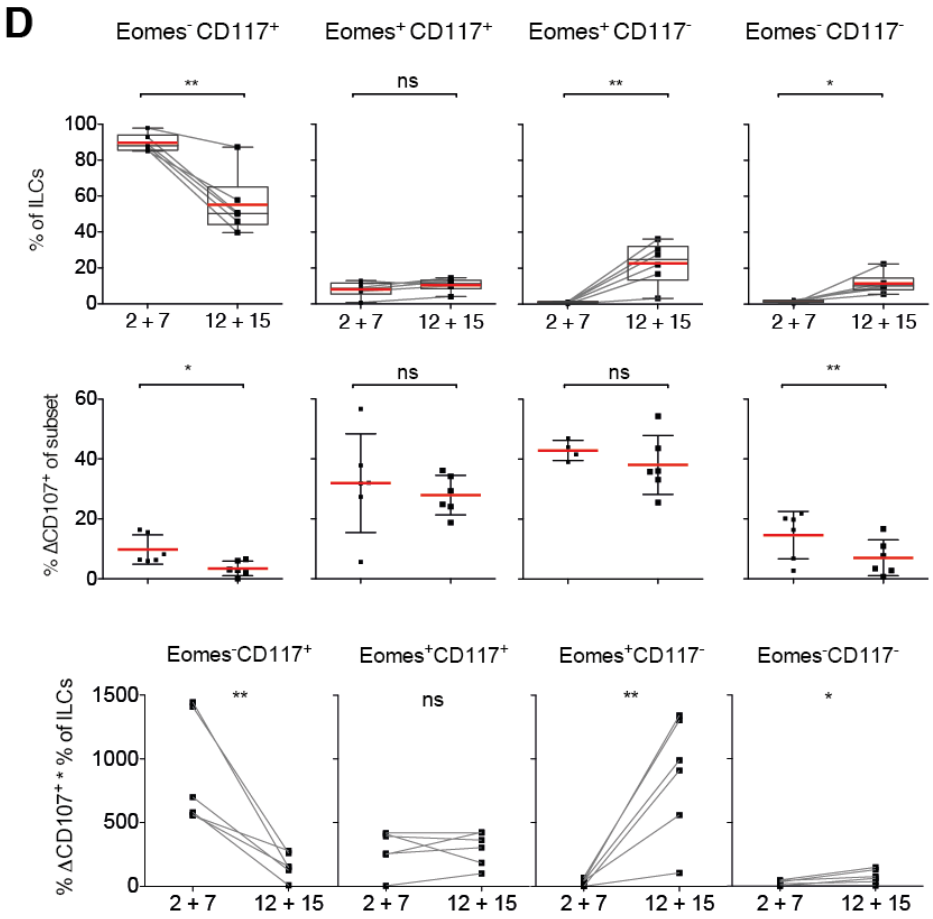

C. Cytotoxicity of IL-12 and IL-15 cultured ILC3s towards classical NK cell targets and correlation with NK-related markers

To further demonstrate cytolytic activity, we co-incubated expanded ILC3s with K562 cells and measured target-cell death via lactate dehydrogenase (LDH) release from damaged cells or by flow cytometry of Cell Trace Violet (CTV)-stained K562 cells. Consistent with the degranulation results, by flow cytometry we detected low NKp44⁺ ILC3 mediated cell lysis in tonsil (one donor) and SI (three donors) with no difference between culture conditions (data not shown). As IL-12 and IL-15 treated cells expressed cytotoxic effectors (on both mRNA and protein levels), we set out to investigate whether longer co-culture would increase the level of killing, also because they might employ other mechanisms, such as TRAIL-induced cell death that requires longer time periods. After an 18-hour incubation, IL-12 and -15 cultures of tonsillar NKp44⁺ but not

NCR$^-$ ILC3s had 4-fold higher cytotoxicity compared to the IL-2 and IL-7 control condition, which still did not reach that of cNK cells. It is noteworthy that CD94$^+$ cells were not separated for the co-culture and thus the effectors are a heterogeneous population of ILCs. Although we observed the same trend in the flow cytometry assay, the cytotoxicity was higher at a lower effector to target ratio (E:T), which might be explained by differences in assay sensitivity. In contrast, splenic NKp44$^+$ ILC3s showed no difference between the culture conditions, whereas NCR$^-$ ILC3s had a 3-fold increase in cytolytic activity, which was still lower than in cNK cells. This however was not reflected in the flow cytometry assay (Figure 8A).

Next, we measured the cytolytic activity of spleen NCR$^-$ ILC3s following 4 and 18 hours of co-culture at different E:T ratios (Figure 8B). With an increasing E:T ratio, cytotoxicity improved for both conditions (calculation not shown). We indeed did not observe differences between conditions after 4 hours, but target-cell lysis was increased after 18 hours co-incubation at higher E:T ratios. Of note, one more donor for the 10:1 E:T ratio at the 18-hour time point was included in Figure 8A (marked in green). Importantly, the differences between IL-12 and IL-15 expanded cells and cultured NK cells became smaller with increasing E:T ratios and were no more significantly different at the 20:1 ratio. NK cytotoxicity itself was enhanced by increase in effectors (in 4- but not 18-hour assay) but largely remained constant over time (Figure 8B).

We then sought to determine which subset is responsible for the increase in cytotoxicity. For tonsil NKp44$^+$ ILC3s, this correlated best with Eomes$^+$CD94$^+$ cells and both Eomes and T-bet expression. The less frequent Eomes$^-$T-bet$^+$ cells also correlated with cytolytic activity (Figure 8C). Similar results were observed for spleen NCR$^-$ ILC3s with Eomes$^+$T-bet$^+$ cells showing the highest correlation (Figure 8D). Collectively, our data demonstrated that ILC3s cultured with IL-12 and IL-15 not only up-regulated markers associated with NK cells but also acquired a cytotoxic program, which might however rely more on other cytolytic mechanisms than the perforin/granzyme mediated lysis of classical NK cells.

Figure 8 A

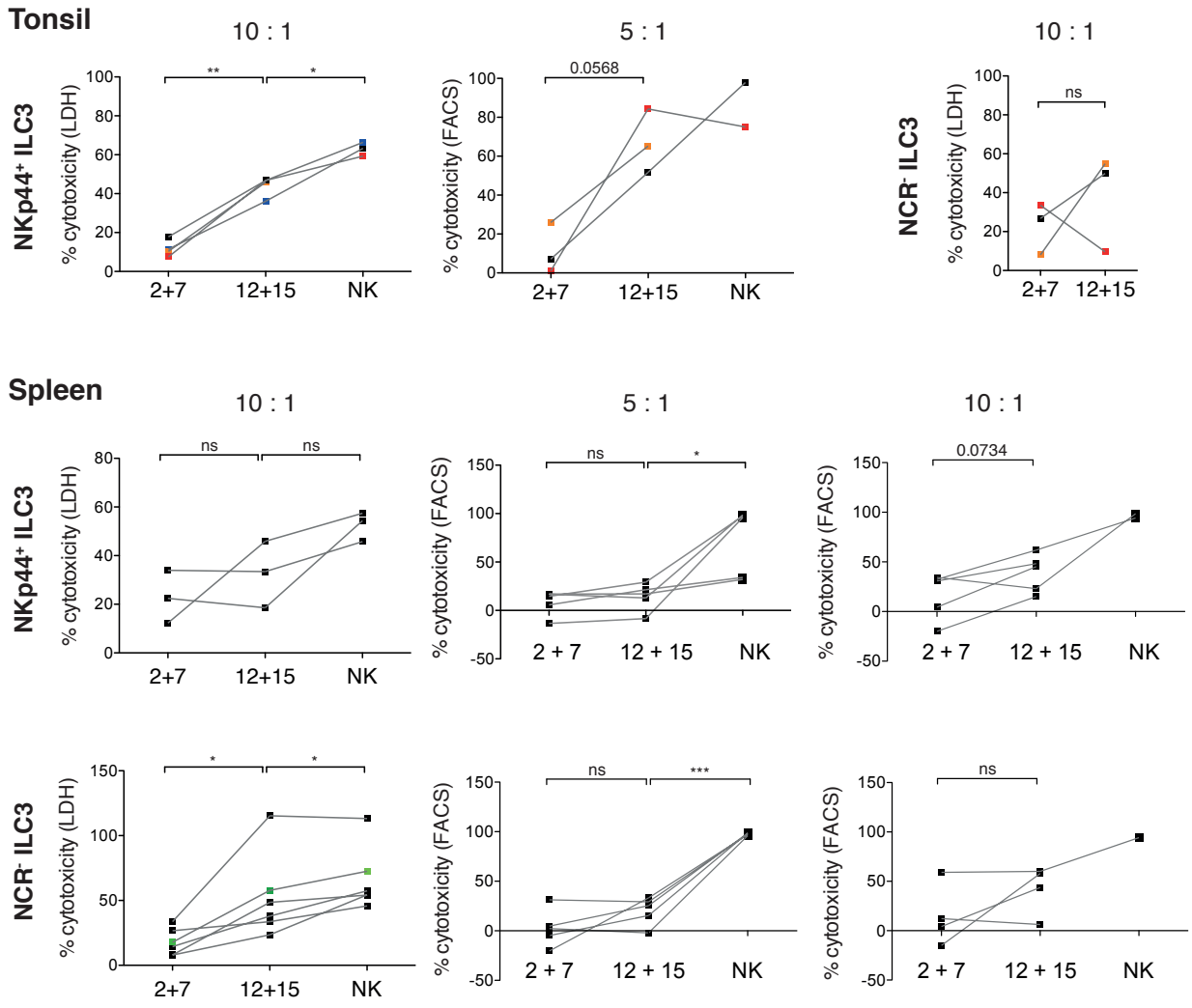

Figure 8 Cytotoxicity of IL-12 and IL-15 cultured ILC3s towards classical NK cell targets K562 and correlation with differentiated ILC3s

(A) ILC3 subsets expanded for 3 weeks under the indicated conditions were co-incubated with K562 for 18 hours. Cytotoxicity measured by LDH assay or flow cytometry with CTV-stained targets. Numbers indicate E:T ratios. For tonsil NKp44+ ILC3 N=4 and 3 in LDH and flow cytometry assays, respectively. For tonsil NCR- ILC3 cultures N=3. Same donors are color-coded as in Figure 4 (D) and (F). For splenic NKp44+ ILC3 in LDH assay N=3, in flow cytometry assay N=6 for 5:1 and N=5 for 10:1 E:T ratios. For spleen NCR- ILC3 in LDH assay N=6, in flow cytometric assay N=5 for 5:1 and N=4 for 10:1 E:T ratios. Same samples were used in (B) with the exception of one donor, colored in green (B) Splenic NCR- ILC3s (week 3) were co-cultured with K562 target cells for 4 and 18 hr. Cytotoxicity was measured using LDH assay and quantified for the indicated E:T ratios and time points. N=5, 20:1 4 hr time point measurement is obtained from 3 donors. Sample details are shown in Tables 1 and 2. Expanded NK cells were used as a positive control. (C) and (D) Correlation plots of Eomes-, T-bet-, and CD94-expressing cells in tonsillar NKp44+ (C) and splenic NCR- (D) ILC3 cultures with LDH cytotoxicity. ns $P > 0.05$, * $P < 0.05$, ** $P < 0.01$ using paired t test. r indicates Spearman's rank correlation coefficient. Figure continues on next pages.

Figure 8

B

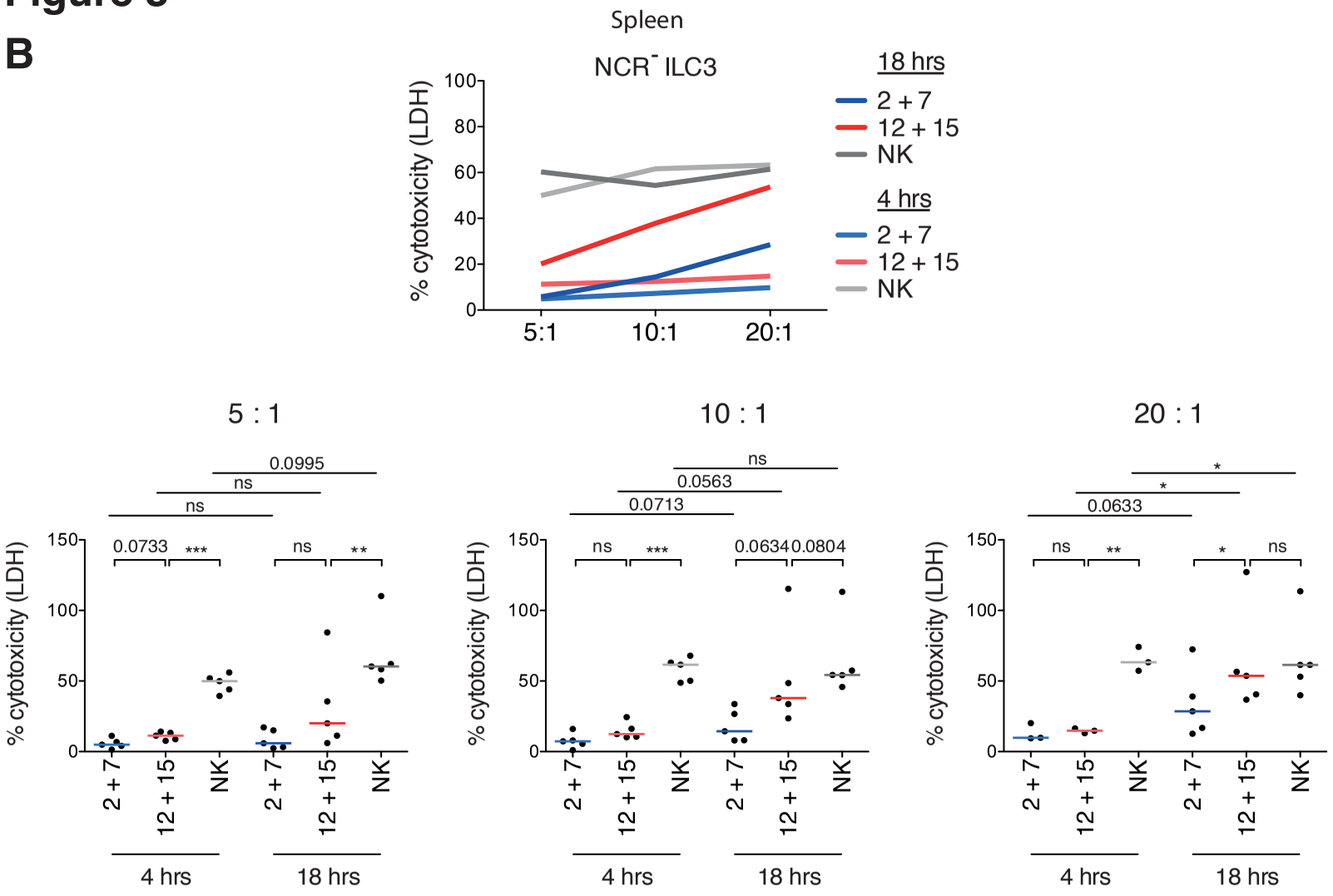
Spleen
NCR⁻ ILC3
% cytotoxicity (LDH)
100
80
60
40
20
0
5:1
10:1
20:1
18 hrs
2 + 7
12 + 15
NK
4 hrs
2 + 7
12 + 15
NK
5 : 1
10 : 1
20 : 1
0.0995
ns
ns
0.0733
***
ns
**
0.0563
0.0713
0.0634
0.0804
0.0633
*
*
*
150
100
50
0
2 + 7
12 + 15
NK
4 hrs
18 hrs

Figure 8

C

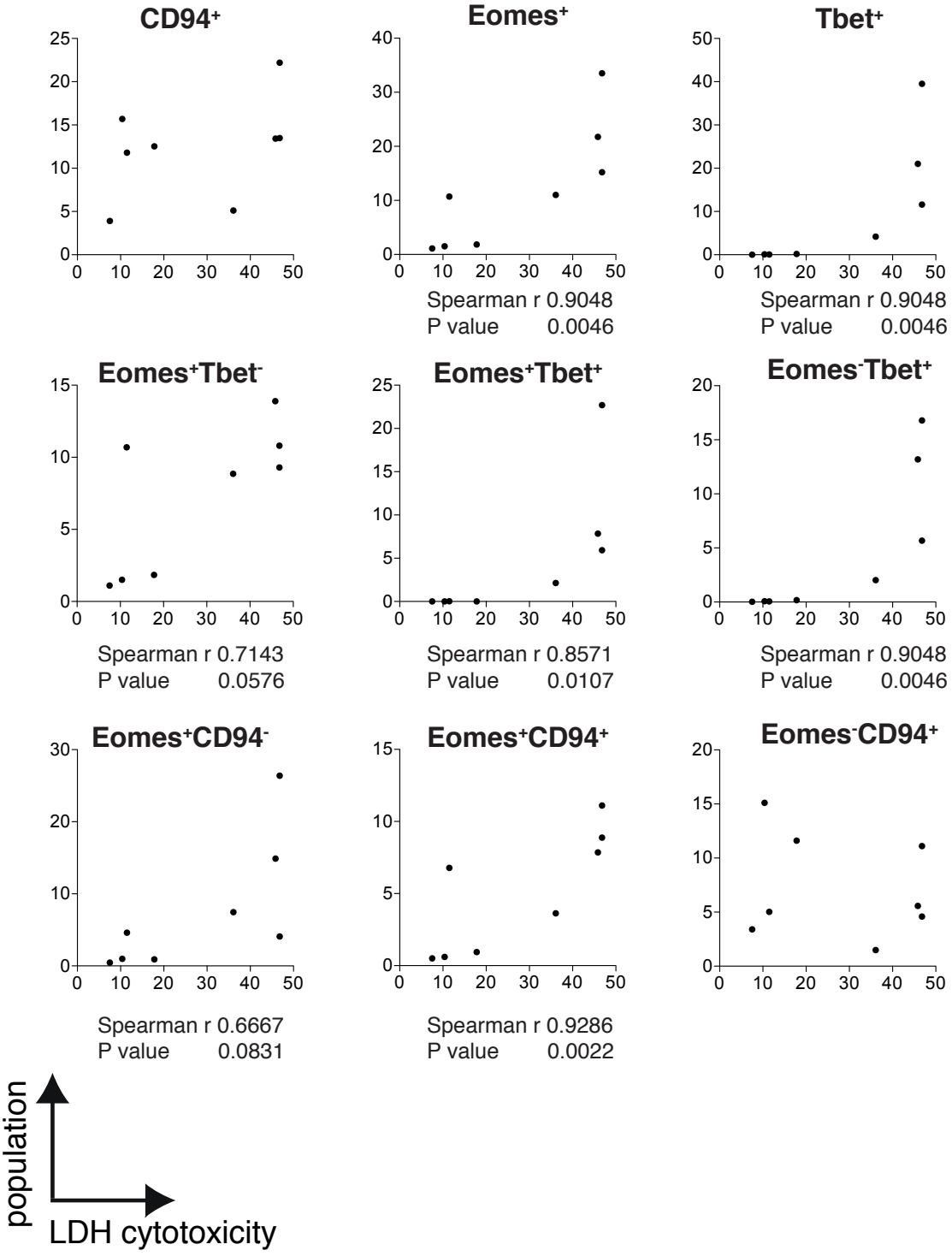
CD94+
Eomes+
Tbet+
Spearman r 0.9048
P value 0.0046
Spearman r 0.9048
P value 0.0046
Eomes+Tbet-
Eomes+Tbet+
Eomes-Tbet+
Spearman r 0.7143
P value 0.0576
Spearman r 0.8571
P value 0.0107
Spearman r 0.9048
P value 0.0046
Eomes+CD94-
Eomes+CD94+
Eomes-CD94+
Spearman r 0.6667
P value 0.0831
Spearman r 0.9286
P value 0.0022
population
LDH cytotoxicity

Figure 8

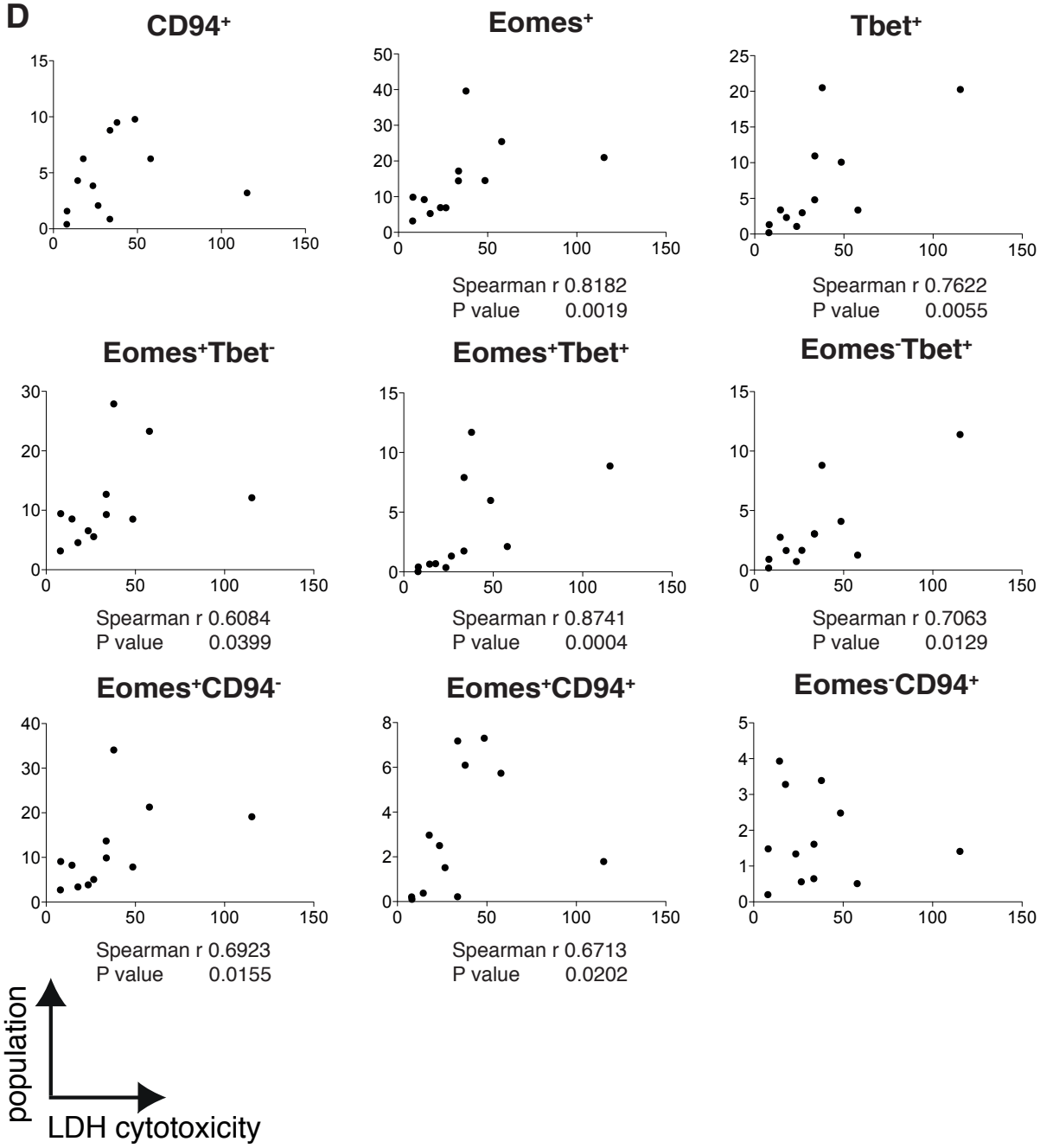
D
CD94+
Eomes+
Tbet+
Spearman r 0.8182
P value 0.0019
Spearman r 0.7622
P value 0.0055
Eomes+Tbet-
Eomes+Tbet+
Eomes-Tbet+
Spearman r 0.6084
P value 0.0399
Spearman r 0.8741
P value 0.0004
Spearman r 0.7063
P value 0.0129
Eomes+CD94-
Eomes+CD94+
Eomes-CD94+
Spearman r 0.6923
P value 0.0155
Spearman r 0.6713
P value 0.0202
population
LDH cytotoxicity

V. NKp44$^+$ ILC3s might differentiate into CD94-expressing cells *in vivo*

To determine whether our *in vitro* data can be recapitulated *in vivo*, we took advantage of the humanized mouse (huNSG) model. To that end, freshly sorted spleen ILC3s were labeled with a cell tracker dye and i.v. injected into autologous reconstituted recipient mice. Differentiation was analyzed at steady state and under inflammatory conditions such as EBV infection and poly-ICLC treatment. In this EBV infection model, NK cells (defined as CD3$^-$NKp46$^+$ cells) peaked at 4 weeks post infection (Chijioke et al., 2013) and, consequently, we chose this time point for the adoptive transfer of ILC3s. In comparison to other adjuvants tested in huNSG mice, poly-ICLC was described to elicit the highest serum levels of IL-12, which was detected between 8-14 hours after injection (Meixlsperger et al., 2013). Therefore, we transferred ILC3s 14 hours after treatment. HuNSG mice were euthanized 4 days after transfer, which was previously described to be enough for *in vivo* ILC1 to ILC3 differentiation (Bernink et al., 2015), and presence of Cell Trace Violet (CTV)$^+$ cells in various tissues was analyzed. Most cells homed back to the spleen (Figure 9) with no CTV$^+$ cells present in blood, lung or LNs and only few detected in the liver (data not shown). Under homeostatic conditions, ILC3s remained unchanged. At 4 weeks post EBV infection, some NKp44$^+$ but not NCR$^-$ ILC3s acquired CD94 expression at a frequency similar to that found *in vitro* (refer to Figure 4D), whereas in poly-ICLC treated mice the number of cells was too low to draw reliable conclusions (Figure 9). We injected ILC3s in 1-2 recipient mice to be able to detect enough CTV$^+$ cells for analysis. Importantly, for each adoptive transfer experiment, 9-15 highly reconstituted donor mice were pooled to purify ILC3s. Thus, it was not feasible to increase the number of injected cells and also to find a time point at which proliferation does not occur but acquisition of NK-related markers is detected. Overall, our *in vivo* data was inconclusive, but we did observe a tendency towards conversion to an NK-like phenotype.

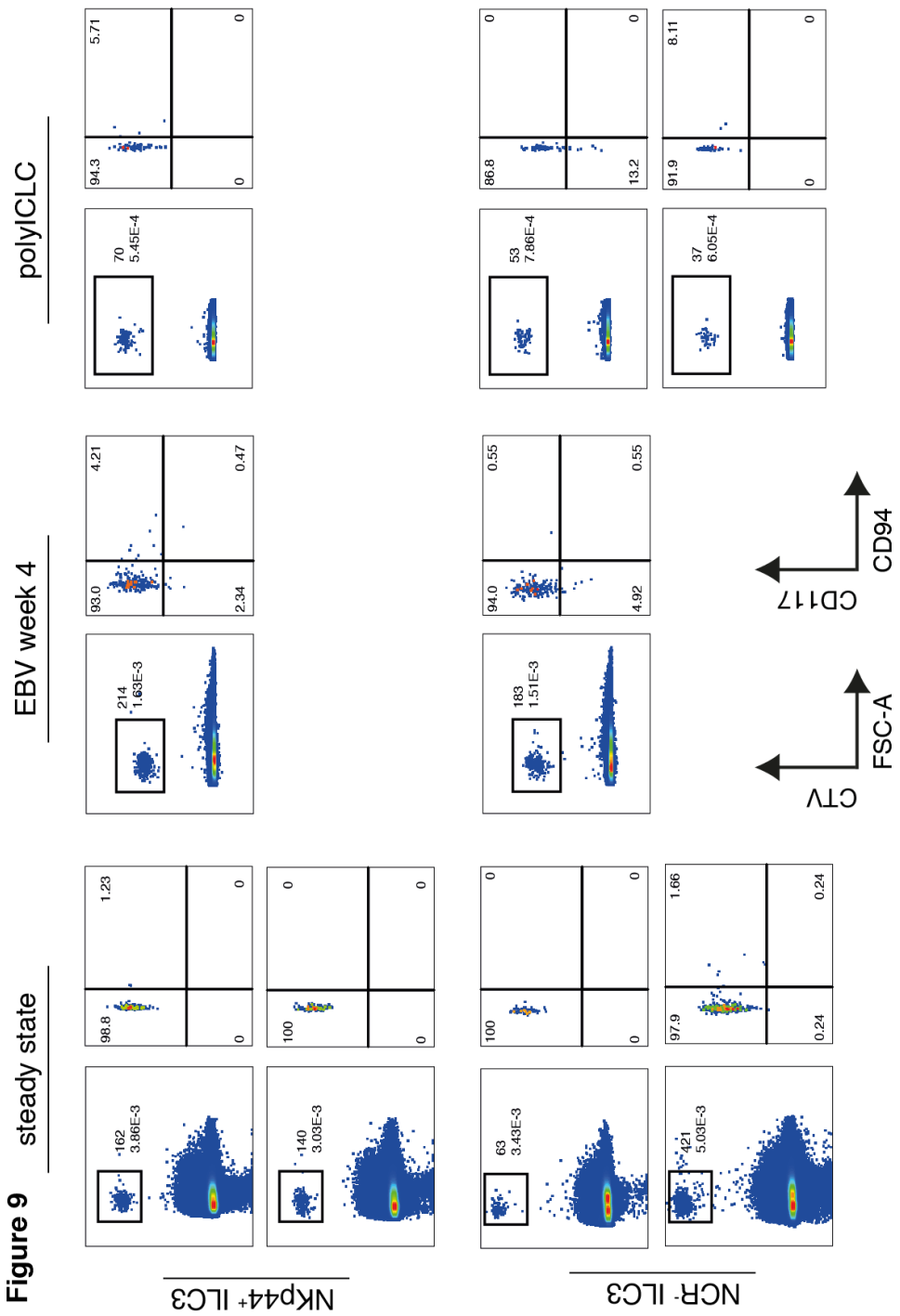

Figure 9 NKp44⁺ ILC3s might differentiate into CD94-expressing cells *in vivo*
HuNSG mice were inoculated i.v. with untreated autologous CTV-stained ILC3s at steady state, at 4 weeks post EBV infection (1 x 10^5 RIU) or 14 hrs after polyICLC treatment (2 shots, 24 hrs apart, cells injected after 1st dose). Mice were euthanized 4 days later and different organs were analyzed for presence of cell tracker-positive cells (top value indicates number of detected cells and bottom ones represent frequency from viable cells. Flow cytometry shown for spleen. One experiment per treatment. ILC3s were obtained from one HFL donor with 9-15 pooled mice.

VI. NKp44$^+$ ILC3s seem not to affect EBV disease progression *in vivo*

The striking similarities between ILC3s cultured under inflammatory conditions and NK cells prompted us to study their role in a disease setting. As NK cells play an important role in the control of herpes viruses and were demonstrated to prevent lytic EBV infection in humanized mice (Chijioke et al., 2013), we again used the same infection model to analyze the *in vivo* potential of ILC3s to take over NK–associated functions. As NK depletion without concomitant loss of transferred cells was not feasible and in order to gain sufficient numbers to draw any conclusions, we expanded ILC3s with IL-2 and IL-7 for 5 weeks and purified CD117$^+$CD94$^-$ cells before transfer. Because some NKp44$^+$ ILC3s converted to CD94$^+$ cells when placed under EBV-driven inflammatory conditions, we focused on this population in our further investigation. Concurrently with ILC3 transfer (1 x 10^6/mouse), huNSG mice were infected with EBV.

In our first autologous experiment, in comparison to the control EBV group, animals that received expanded ILC3s showed no weight loss, associated with EBV disease progression, a tendency for lower EBV titers and lower tumor burden but no change in absolute numbers, determined at time of sacrifice (Figure 10A). To investigate whether cells are still present 5 weeks post infection and to analyze their phenotype, we applied two strategies – transfer of ILC3s purified from HLA-A2 positive reconstitutions into humanized mice reconstituted from HLA-A2 negative donors (Figure 9B) or of GFP-transduced autologous ILC3s (11.6% GFP$^+$) (Figure 9C). In neither case we found the transferred cells when mice were euthanized (across different organs, data not shown), indicating they did not survive in that environment for this prolonged time period. Moreover, we could not recapitulate the results from the initial experiment, although not repeated with the exact same settings, suggesting (expanded) NKp44$^+$ ILC3s do not play a role in EBV disease progression under the conditions tested.

Figure 10

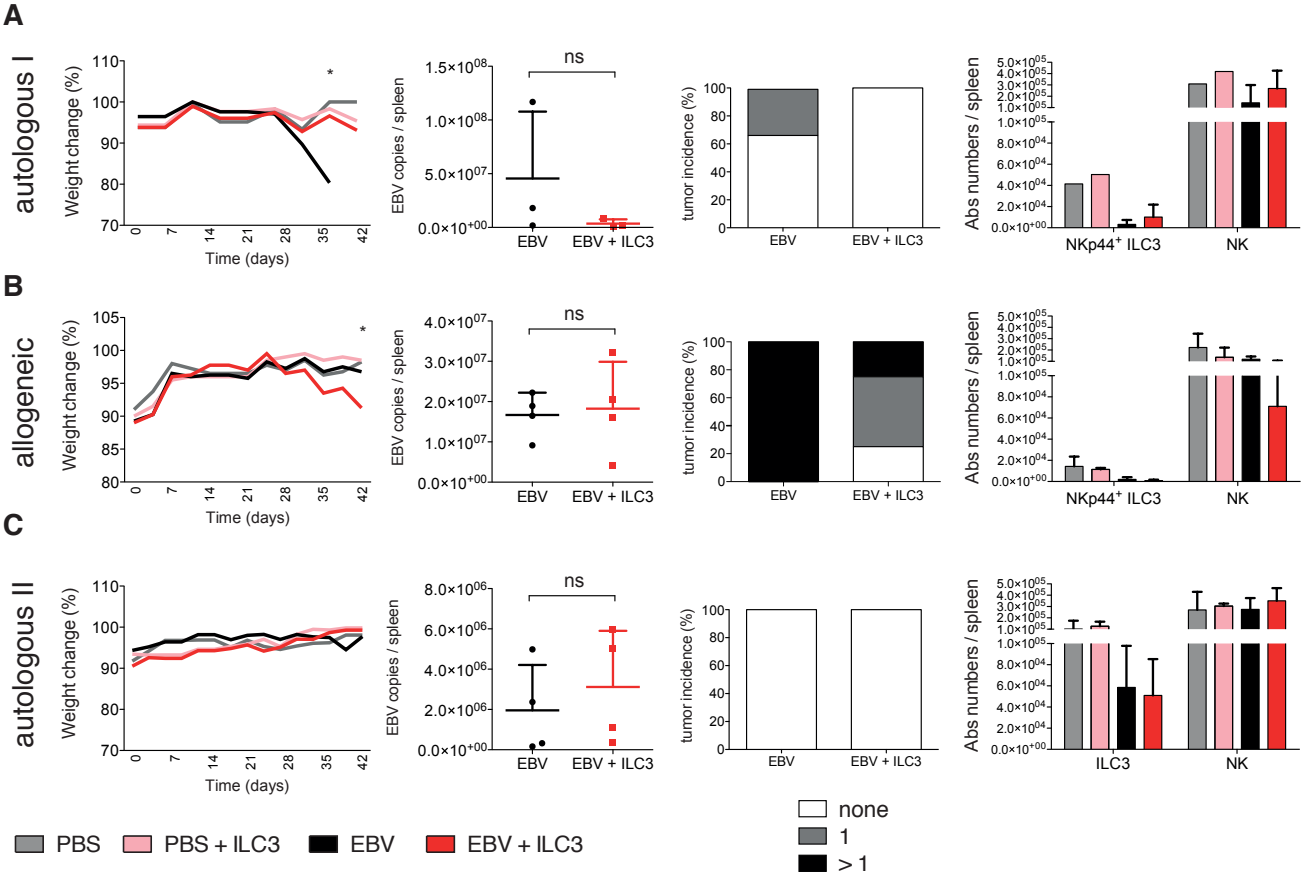

Figure 10 NKp44⁺ ILC3s seem not to affect EBV disease progression *in vivo*
HuNSG mice were injected i.v. with IL-2 and IL-7 expanded (A) autologous (B) allogeneic or (C) GFP-transduced autologous NKp44⁺ ILC3s (11.6% GFP⁺). Cells were sorted from 5 mice, cultured for 5 weeks and re-sorted for viable CD117⁺CD94⁻ cells before inoculation. 1 x 10^6 ILC3s were injected per mouse into 1-4 mice per PBS group and 3-5 per EBV group. EBV (1 x 10^5 RIU) was injected i.p. at the same time point as ILC3s. Far-left, weight changes in the course of a 40-42-day EBV experiment. Left, EBV copies per spleen. Right, Tumor burden. Far right, Absolute numbers of the indicated populations in spleens. ns $P > 0.05$, * $P < 0.05$, ** $P < 0.01$ using Mann-Whitney test.

Discussion

Although still under debate (Montaldo et al., 2014), previous studies have demonstrated NK cell development from a RORγt$^+$ progenitor in humans (Freud et al., 2016; Scoville et al., 2016). Whether ILC3s can be a direct precursor of NK cells however has not been established as differentiation towards NK cells could be attributed to a distinct NK precursor within the few CD127$^-$ among stage 3 cells.

In this study, we demonstrated that ILC3s from lymphoid and non-lymphoid tissues can adopt NK-related features and that this transition is enhanced by exposure to IL-12. In such inflammatory settings, ILC3s gave rise to NK cells, defined as Eomes$^+$CD94$^+$, but also CD94$^-$ cells with mutually exclusive expression of Eomes and T-bet. Together with the emergence of cells with the unconventional Eomes$^+$RORγt$^+$ phenotype, found in stage 4a immature NK cells (Freud et al., 2016), this suggests that culture conditions are not sufficient to drive complete differentiation. Notably, these populations constituted only small fractions of the expanded cells and the majority stably remained negative for NK markers, which indicates that only a fraction of ILC3s has the potential to be diverted to an NK profile.

Stimulation with IL-12 and IL-15 conditioned ILC3s for enhanced responsiveness to the type 1 response-polarizing cytokines IL-2, - 12, -15 and -18 (the last only in tonsil) and induced a program reminiscent of early-differentiated NK cells (Béziat et al., 2010; Björkström et al., 2010), as revealed by transcriptional analysis. Relative to freshly isolated ILC3s, IL-12 and IL-15 expanded cells up-regulated NK signature markers such as CD56, NKG2A, NKG2C and CD16. Furthermore, we observed an increase in genes associated with NK cell immunoregulatory functions such as *IFNG*, *TNF*, *CCL3* (MIP-1α) and *CCL4* (MIP-1β) but also with their cytotoxic functions like granzymes, perforin, and FasL.

We showed *in vitro* that IL-12 and IL-15 induced expression of IFNγ in ILC3s but limited their capacity for TNFα production upon PMAi stimulation.

Upon co-culture with K562 cells, however, IL-12 and IL-15 expanded ILC3s showed higher TNFα response, which suggests increased target cell recognition.

Previous reports demonstrated such modulation of the cytokine profile by IL-12 for tonsil and intestinal NKp44$^+$ ILC3 (Bernink et al., 2013; 2015), here we showed that spleen ILC3s react in the same fashion, which also validates our huNSG mouse model for studying human ILC differentiation and immune response. However since ILC3s stimulated with IL-12 and IL-2 (4 d) in these previous studies did not up-regulate Eomes (Bernink et al., 2015), the cytotoxic potential of differentiated ILC3s was not investigated.

The current study addressed this and found that IL-12 and IL-15 promote acquisition of cytotoxic properties in ILC3s, which correlates with Eomes and T-bet expression. Although we observed tissue-specific differences, both tonsil and spleen-derived ILC3 subsets showed moderate cytolytic activity, which improved with longer target cell incubation at higher effector to target cell ratios. The slower killing kinetics compared to NK cells suggested that differentiated ILC3s might use other mechanisms to induce cytotoxicity. For example, compared to controls, IL-12 and IL-15 expanded cells displayed more transcripts encoding TRAIL, which is constitutively expressed by murine ILC1s (Daussy et al., 2014; Gordon et al., 2012; Takeda et al., 2005) and detected on *in vitro* differentiated human NK cells (Hughes et al., 2014). Since most granzymes showed much higher differential expression, alternatively, this might reflect the heterogeneity of the cultures or potentially the response intensity in differentiated ILC3s. This might be lower as a result of less efficient synapse formation, granule polarization, or differences in granule morphology and content (de Saint Basile et al., 2010; Mace et al., 2014).

Interestingly, expanded tonsillar but not splenic NKp44$^+$ ILC3s showed enhanced cytotoxicity relative to controls. To address this tissue-specific effect, we examined differential expression of the up-regulated genes after culture with IL-12 and IL-15. Since stimulatory NK cell receptors were reported to induce degranulation in a synergistic fashion, with the exception of CD16 (Bryceson et al., 2009; Long et al., 2013), we speculated that the differences in cytolysis are a result of a distinct receptor repertoire. Among the investigated activating receptors only *CD244* encoding 2B4 was up-regulated, albeit not significantly,

however K562 cells do no express its ligand CD48 (Endt et al., 2007). When we performed a Gene Set Enrichment Analysis (GSEA) (Appendix, Figure 15), top hits were rather associated with cell proliferation (Dimova and Dyson, 2005; O'Donnell et al., 2005; Pelengaris et al., 2002). Comparison with the immunological signatures database revealed an overlap with a gene set from a study reporting a role for TNF- receptor-associated factor 6 (TRAF6) in fatty acid metabolism and consequently in generation of memory CD8 T cell responses (Pearce et al., 2009). TRAF6 is involved in signal transduction of the TNF receptor (TNFR) and IL-1R/TLR superfamilies as well as of IL-17R (Cao et al., 1996; Lomaga et al., 1999; Naito et al., 1999; Wu et al., 2015). Since *IL17RB* and *IL1R1* were among the significantly up-regulated genes in tonsils, this hit likely relates to general differences in ILC3s across tissues rather than explaining the increased cytotoxic activity relative to controls of tonsil- but not spleen-derived differentiated NKp44^{+} ILC3s, which necessitates further investigation.

Splenic NKp44^{+} ILC3s acquired more NK cell markers and GzmB (also *TNFSF10, GzmA,* etc.) upon IL-12 and IL-15 stimulation, however these phenotypic features did not translate into higher cytotoxicity. This suggested that differentially expanded ILC3s might mount distinct cytotoxic responses, triggered or exerted in a different fashion. Expansion with IL-2 and IL-7 up-regulated genes associated with a type 1 immune response such as *EOMES*, *TBX21*, *STAT1*, *PRF1*, and *GZMA*, relative to their expression in freshly isolated ILC3s. We did not detect appreciable differences in perforin (mRNA and protein) between the conditions, which could explain the modest cytolytic activity seen upon stimulation with IL-2 and IL-7. Of note, *FASLG* expression was also similar but K562 cells are Fas-negative (Hodgson et al., 1999). In mice, expression of perforin and GzmB seems primarily regulated by Eomes (Cruz-Guilloty et al., 2009; Pearce et al., 2003; Pipkin et al., 2010), whereas Eomes^{-}T-bet^{+} ILCs were shown to express TRAIL (Gordon et al., 2012; Takeda et al., 2005). The lower *TNFSF10* expression and the absence (or low levels) of Eomes^{-}T-bet^{+} population in IL-2 and IL-7 expanded ILC3s suggest they exert perforin-mediated cytotoxicity, whereas both pathways are probably triggered in IL-12 and IL-15 cultures. Transcriptional analysis revealed small differences in the NCR family genes and significantly higher *KLRK1* (encoding NKG2D) expression in IL-2 and

IL-7 compared to IL-12 and IL-15 cultured cells; together these receptors could potentially induce degranulation (Long et al., 2013).

Collectively, this data demonstrated that ILC3s can be diverted to a cytotoxic program, most efficiently so in the presence of IL-12 and IL-15. Blocking perforin, granzymes and TRAIL could delineate the exact cytolytic mechanism(s) involved and different target cell lines should be used to explore the full potential of cytotoxic differentiated ILC3s.

These results substantiate previous observations that environmental signals strongly modulate the functional profile of ILC3 cells (Bernink et al., 2013; 2015) (less stringently sorted, tonsil-derived in these studies (Cella and Colonna, 2010; Crellin et al., 2010; Hughes et al., 2010; 2014)). For example, IL-2 in the presence of IL-7 promoted IFNγ production in ILC3s, whereas its substitution with IL-1β resulted in constitutive IL-22 expression and acute exposure to IL-12 did not affect their cytokine profile (Cella and Colonna, 2010). Moreover, addition of IL-1β to IL-15 containing cultures of stage 3 cells could inhibit differentiation towards NK cells and sustain IL-22 expression (Hughes et al., 2010). On the other hand, we showed that culture with IL-12 and IL-15 down-regulated *IL1R1* expression (together with that of *IL23R* and *IL7R*). Thus, an outstanding question is when both pro-inflammatory cytokines are present in the microenvironment, whether IL-12 is able to override IL-1β signals and switch ILC3 profile. It is also essential to address whether constant signals are necessary to sustain this adopted program if this plasticity is to be exploited therapeutically. Bernink et al demonstrated that murine ex-ILC3s ($ROR\gamma t^{-}fm^{+}$) revert back to their ILC3 profile when transferred into a different steady state environment. In the same study, the authors reported that human $CD127^{+}$ ILC1s can give rise to ILC3s (Bernink et al., 2015). However, in light of recent findings (Simoni et al., 2017) we are tempted to speculate that ILC1 cells, distinct from NK cells, do not exist in humans, although they are a separate lineage in mice (Klose et al., 2014). In our study, in addition to IFNγ production, expanded ILC3s also showed cytolytic activity, albeit that the response was slower and lower than that of NK cells. Moreover, we attempted to purify the described ILC1 population (Bernink et al., 2013; 2015) and tested them alongside our ILC3 cultures (Appendix, Figure 16). The majority of expanded cells were indeed T

cells (and showed no cytotoxicity against K562), similar to the findings of Simoni et al. The lack of ILC1 specific markers and the down-regulation of the TCR-CD3 complex after activation make this population prone to T cell contamination (Burkhard et al., 2014). Single-cell RNAseq revealed presence of transcripts for TCR variable regions (Bjorklund et al., 2016), whereas un-biased mass cytometry analysis could not distinguish this cell type and after back-gating they overlapped with T cells (mostly) and ILC3s among others (Simoni et al., 2017). Thus, reported differentiation towards IL-22-producing ILC3s could come from a contamination from the sort, especially since putative ILC1s produced IL-22 already in the presence of the type 1 response-polarizing cytokines IL-2 and IL-12 (Bernink et al., 2015). Thus, whether differentiated ILC3s can retain their immunomodulatory/cytotoxic profile in the absence of pro-inflammatory signals remains to be determined.

To explore whether such plasticity can be induced *in vivo*, we transferred freshly sorted ILC3s in the steady state or under inflammatory conditions, in the setting of EBV infection or after treatment with the adjuvant poly-ICLC. The results were inconclusive due to low number of the recovered tracer-labeled cells, which potentially could be improved, for example by IL-7/anti-IL-7 mAb complexes that were previously shown to induce T cell expansion (Boyman et al., 2008). Nevertheless, in accordance with our i*n vitro* findings, we observed a modest increase in CD94 expression of the adoptively transferred cells in the course of EBV infection.

Interestingly, helper $CD4^+$ T cell cells capable of cytotoxic activity expand during chronic viral infections such as HIV (Appay et al., 2002). These cytolytic $CD4^+$ T cells express Eomes (Hirschhorn-Cymerman et al., 2012; Raveney et al., 2015) and mediate cytotoxicity via perforin (Appay et al., 2002; Yasukawa et al., 2000) or FasL (Nikiforow et al., 2003; Paludan et al., 2002). Thus, both innate (as reported here) and adaptive helper lymphocytes can adopt cytotoxic properties during inflammation.

As such cytolytic $CD4^+$ T cell cells are also markedly increased upon acute EBV infection (Appay et al., 2002) and since early-differentiated NK cells restrict EBV through both IFNγ production and killing of lytically EBV-replicating B cells (Azzi et al., 2014; Chijioke et al., 2013; Lünemann et al., 2013; Strowig et al.,

2008), we explored the role of ILC3s in EBV infection and disease pathogenesis. HuNSG mice that received IL-2 and IL-7 expanded ILC3s before virus injection did not show any consistent differences with respect to viral load or tumor burden. Although we observed a trend towards protection in the initial experiment, we could not confirm this in the two subsequent ones, where we also sought to address the ILC3 fate. Notably, killing of transferred cells due to MHC class I-mismatch or an unexplained effect from the transduction might account for the results of the last two experiments. Also, the experimental set-up has likely been too long to detect the cells as with this protocol they undergo 5 weeks of expansion *in vitro* and we harvest the organs 6 weeks post infection. Nevertheless, the humanized mouse model is a powerful tool to study ILC3 functional plasticity, especially since in mice ILC3s cannot acquire an NK profile. Of note, murine ILC3 plasticity has been investigated predominantly under homeostatic conditions (Bernink et al., 2015; Klose et al., 2014; Vonarbourg et al., 2010) or intestinal inflammation (Klose et al., 2013; Vonarbourg et al., 2010), but not in virus infection or cancer, in which NK cells are important.

To our knowledge only two studies addressed ILC3 function in cancer. In human NSCLC, NCR^+ ILC3s might have a protective role via a contribution to the formation of tertiary lymphoid structures (Carrega et al., 2015). In mice, ILC3s inhibited B16 melanoma tumor growth in an IL-12-dependent manner. The exact mechanism however remained unresolved, with perforin shown to be dispensable for tumor rejection (Eisenring et al., 2010). According to our findings, ILC3s in that model might for example mediate antitumor activity through TRAIL-mediated cytotoxicity. The role of IL-12 in tumor suppression has been extensively demonstrated in various mouse tumor models and thus IL-12 therapy is currently tested in clinical trials. It, however, has inconsistent effects with respect to antitumor efficacy, which to some extent might be attributed to the mode of delivery as local administration showed better results. Moreover, patients may exhibit adverse reactions such as cytokine toxicity or induction of IL-10. Therefore, tumor-targeted administration in combination with additional anti-immunosuppressive therapies might be a promising approach in inducing innate and adaptive cytotoxicity to combat cancer (Tugues et al., 2014).

Thus, with this study, we provided evidence that ILC3s can adapt to an inflammatory tissue milieu not only, as previously believed, by acquisition of a helper but also a cytotoxic NK cell profile, a mechanism that likely evolved for protection against pathogens at mucosal sites. This cytotoxic potential, triggered most efficiently by IL-12 and IL-15, can be potentially harnessed in the treatment of chronic viral infections and cancer.

Materials and Methods

Tissue collection

Tonsils were collected from patients undergoing tonsillectomy at the University Children's Hospital of Zurich. A description of the samples used for ILC isolation and in which experiments they were included is provided in Table 1.

Human fetal liver tissues were procured from Advanced Bioscience Resources. Tissues were collected after patients provided informed consent in accordance with the Declaration of Helsinki. All studies involving human samples were reviewed and approved by the cantonal ethical committee of Zurich, Switzerland (protocol no. KEK-StV-Nr.19/08).

Humanized mice

NOD.Cg–*Prkdc*^{scid}*Il2rg*^{tm1Wjl}/SzJ (NOD-*scid* γ_c^{null} or NSG) and HLA-A2 transgenic NSG (A2-NSG) mice were purchased from the Jackson Laboratory and housed at the Institute of Experimental Immunology, University of Zurich, under specific pathogen-free conditions. All animal protocols were approved by the Cantonal Veterinary Office Zurich, Switzerland (protocol Nos. 148/2011 and 209/2014). Newborn NSG mice (1 to 5 days old) were irradiated with 1 Gy using X-ray or Cs-source and 5-7 hours later injected intrahepatically with on average 2×10^5 $CD34^+$ hematopoietic progenitor cells (HPCs) derived from human fetal liver (HFL) tissues. Reconstitution of human immune system components was analyzed in blood circa 12 weeks after engraftment (Figure 11) or 1 day prior EBV infection (Figure 12). A detailed description of cohorts used for ILC isolation and in which experiments they were included is provided in Table 2.

Table 1

					NKp44+ ILC3								NCR- ILC3				
sort	Tonsil ID	procured (YY/MM/DD)	Exp ID	Fig 1B	Fig 2	Fig 3	Fig 4B	Fig 4D	Fig 4I	Fig 5C	Fig 8A	Fig 8A	Fig 4B	Fig 4E	Fig 8A	MACS	feeders
23-Jul-15	T88		T88														
10-May-16	15.06.03	090818	1														
	22.12.01	091012	2														
	04.05.04	101130	3														
	T175	120614	4														
	160116	160116	5														
31-May-16	T17	101130	10														
	T58	110517	11														
	T71	110705	13														
8-Jun-16	TMC 4	101216	16														
	T154	120606	17														
	T179	120904	20														
14-Oct-16	T390	161005	T390														
	T391	161005	T391														
	T392	161011	T392														
19-Oct-16	T395	161017	T395														
10-Mar-17	T393	161011	T393														

a
b
c
LDH FACS 5:1

CD19
CD19/CD4/CD8/CD14

feeders
PBMC 40 Gy, 721.221 60 Gy X-ray
PBMC 20 Gy, 721.221 60 Gy Co-source
PBMC 20 Gy, 721.221 60 Gy X-ray

PBMC - 150 000 cells/well
721.221 - 15 000 cells/well

Table 1 Tonsil samples details

Table 2

					spleen	NKp44+ ILC3							NCR- ILC3				SI	NKp44+ ILC3 SI				
sort date	reconstitution	No of mice	HFL donor	age	Fig 1B	Fig 4B	Fig 4D	Fig 5	Fig 6	Fig 7	Fig 8A	Fig 8A	Fig 4B	Fig 4F	Fig 8A/B	Fig 8A	Fig 1B	Fig 4B	Fig 4E	Fig 11	feeders	experiment
24-Jun-14	A2-123	4	Nov-19-2013	3																		expansion for autologous I
14-Jul-15	A2-R155-158	15	May-06-2014	4.5																		expansion for allogeneic
23-Jul-15	R197-200	6	Jul-15-2014	3.5																		expansion for autologous II
17-Sep-15	A2-R162	15	Jan-14-2014	4				1													✗	short-term steady state
30-Oct-15	R197-200	2	Jul-15-2014	6.5																		
	R201-203	9	Nov-19-2014	5.5				2													✗	short-term EBV
3-Feb-16	A2-R172-173	5	Dec-16-2014	4																		
8-Feb-16	A2-R174-178	15	Apr-8-2014	3.5				3													✗	short-term polyICLC
15-Mar-16	A2-R172-173	4	Dec-16-2014	5.5				4														
		4		5.5				5														
		4		5.5				6														
		4		5.5				7														
30-Mar-16	R222-224	4	Jan-20-2015	3.25				8														
	A2-R181-182	4	Dec-15-2014	3.25				9														
20-May-16	R227	5	Jul-28-2015	3				10														
	A2-R184-186	4	Jan-27-2015	3.5				11														
	A2-R181-183	4	Dec-15-2014	5																		
3-Jun-16	R228-230	5	Jun-24-2015	3.5				12														
	A2-R187-190	5	Apr-29-2014	3.5				13														
6-Sep-16	R231	5	Apr-28-2015	5																		
	A2-R191	4	Feb-11-2015	5																		
	R235	5	Apr-11-2015	4																		
25-Nov-16	A2-208	4	Oct-12-2015	3																		
	A2-200-201	2	Mar-17-2015	5																		
	R243	5	Oct-28-2014	3																		
12-Jan-17	R237-242	8	Jan-20-2015	5.5																		
	A2-210	3	Jun-30-2015	4																		
10-Mar-17	A2-218	5	Aug-17-2015	2.5											- Fig 8B							
	R252	5	Aug-18-2015	3																		

a
b
c

LDH FACS 5:1

CD19
CD19/CD4/CD8/CD14

feeders

PBMC 40 Gy, 721.221 60 Gy X-ray
PBMC 20 Gy, 721.221 60 Gy Co-source
PBMC 20 Gy, 721.221 60 Gy X-ray

PBMC - 150 000 cells/well
721.221 - 15 000 cells/well

Table 2 Humanized mouse samples details

Figure 11

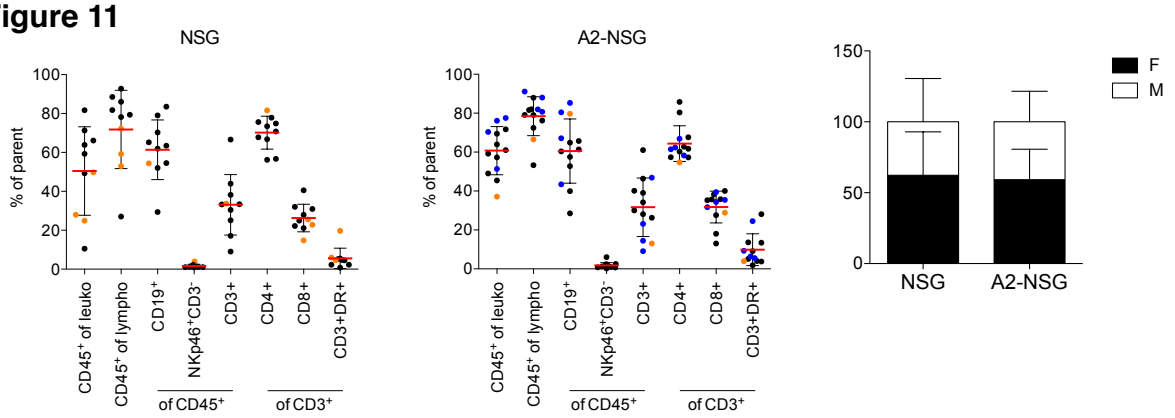

Figure 11 Reconstitution of human immune system components in huNSG and HLA-A2 huNSG used for ILC3 purification.
Sample details shown in Table 2

Figure 12

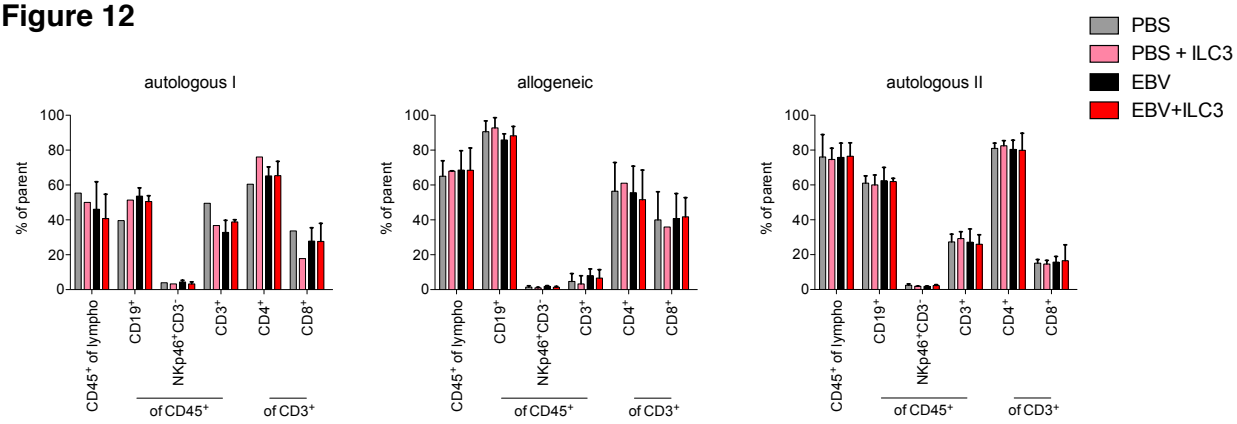

Figure 12 Reconstitution and group distribution of humanized mice used for adoptive transfer EBV experiments
Sample details shown in Table 2

Cell lines

K562, 721.221, Raji and Nishi were maintained in R10 (RMPI with 10% FCS (Bioswisstec/Gibco)) and antibiotics (penicillin (50 U/ml), streptomycin (50 µg/ml). Nishi culture was supplemented with 300 U/ml IL-2 (Peprotech) every 3 days and kept at 10% CO_2. HEK293/EBV-wild type (wt) cells that carry p2089 were kindly provided by Prof. Henri-Jacques Delecluse. Cells were seeded at 1-1.5 x10^6 cells/10 cm^2 in D10 (DMEM with 10% FCS) and antibiotics (gentamicin (20 µg/ml), hygromycin B (100 µg/ml)) and split at 70-80% confluency using 0.25% trypsin/EDTA. 293T cells were cultured in D10 supplemented with 25

µg/ml gentamicin. All culture reagents, unless otherwise indicated, were purchased from Life Technologies.

Cell isolation and purification

Human fetal liver tissues were minced and digested with 2 mg/ml collagenase D (Roche) and 20 µg/ml DNase I (Roche) in HBSS (with Ca^{2+} and Mg^{2+}, Gibco) for 25 min at RT. Reaction was stopped by addition of 10 mM EDTA (5 min at RT) and tissue was mashed through a 70 µm cell strainer before separation by density gradient centrifugation on Ficoll-Paque (GE Healthcare) (1000 g, 30 min, RT). $CD34^+$ HPCs were isolated by magnetic-activated cell sorting (MACS) via double positive selection using CD34 MicroBead kit (Miltenyi).

Tonsil tissues were mechanically dissociated, filtered through a 70 µm cell strainer and mononuclear cells were obtained via Ficoll-Paque fractionation (2100 rpm, 25 min, RT; used for all tissues except HFL).

Mice were euthanized using CO_2, organs were harvested and processed as follows:

Whole blood erythrocyte lysis was done using NH_4Cl solution for 5 min at RT.

Spleen and lymph nodes were processed the same way as tonsillar tissue.

Livers were digested with 0.4 mg/ml collagenase D and 20 µg/ml DNase I in PBS for 45 min at 37°C under agitation (stopped with 10 mM EDTA, 5 min at 37°C). Tissues were mechanically disrupted and filtered before leukocyte enrichment using Percoll (GE Healthcare) centrifugation (1450 g, 30 min, 4°C) (lower ring).

Lungs were perfused with PBS and cut into small pieces in 5 ml R10 supplemented with 2 mg collagenase A (Sigma Aldrich), 250 µg/ml DNase I and 25 mM Hepes (Invitrogen). Digestion was done for 45 min at 37°C under agitation and stopped with 5mM EDTA (5 min at 37°C). Tissue was filtered through a 70 µm cell strained and separated by Percoll (2590 rpm, 30 min, 4°C).

Small intestines were cleaned of feces and mesenteric fat tissue, then opened longitudinally and cut into 1-2 cm pieces. These were incubated in 30 mM EDTA solution (Ca^{2+} and Mg^{2+} free PBS) for 30 min on ice and then washed in PBS until solution was clear. Tissues were cut into smaller pieces and digested with 1 mg/ml collagenase D and 25 µg/ml DNase I in DMEM for 15 min at 37°C under agitation. After addition of DMEM, pieces were homogenized using 1 ml pipette

(tip cut smaller in every step), supernatant was collected and procedure was repeated 3x with addition of fresh collagenase. Digested tissue was mashed through a 70 µm strainer and subjected to Percoll separation (1800 rpm, 30 min, RT) to isolate the lamina propria (LP) leukocytes. Prior to sort splenocytes were depleted of $CD19^+/CD14^+/CD4^+/CD8^+$ cells using microbeads (Miltenyi), tonsillar cells as indicated in Table 2, whereas LP cells were not MACS-separated.

Flow Cytometry and cell sorting

All antibodies used for flow cytometric analysis are listed in Table 3. Dead cells were excluded with LIVE/DEAD Fixable Aqua or Near-IR kit (Invitrogen), 7-AAD (Biolegend) or TO-PRO-3-Iodide (ThermoFisher). For surface markers, cells were stained for 20 min on ice. For cytokine/granzymeB/perforin detection, cells were fixed and permeabilized with Cytofix/Cytoperm Kit from BD Biosciences and stained for 30 min on ice. For intranuclear stainings, Foxp3/Transcription Factor Staining Buffer Set from eBiosciences was used and cells were stained for 45 min at RT or ON at 4°C. Data was acquired on FACSCanto or LSR II Fortessa cytometers (BD Biosciences). For cell sorting FACSAria III instrument (BD Biosciences) was used. Fresh innate lymphoid cells were sorted as shown in Figure 1A from tonsils (from individual subjects), humanized mouse-derived splenocytes or LP cells (both pooled from several animals reconstituted with $CD34^+$ HPCs from the same donor). Expanded ILC3s were purified as live $CD117^+CD94^-$ cells. Analysis was performed using FlowJo software (TreeStar).

Table 3

Marker	Fluorochrome	Company	Cat No	clone	isotype
CD107a	FITC	BD	555800	H4A3	Mouse IgG1, κ
CD117	BV605	Biolegend	313218	104D2	Mouse IgG1, κ
CD117	PE	Biolegend	313204	104D2	Mouse IgG1, κ
CD127	PerCP-Cy5.5	eBioscience	45-1278-41	eBioRDR5	Mouse IgG1, κ
CD127	PE-Dazzle-594	Biolegend	351336	A019D5	Mouse IgG1, κ
CD14	BV510	Biolegend	301842	M5E2	Mouse IgG2a, κ
CD14	AF700	Biolegend	325614	HCD14	Mouse IgG1, κ
CD14	FITC	BD	561712	M5E2	Mouse IgG2a
CD158a	FITC	Biolegend	339503	HP-MA4	Mouse IgG2b, κ
CD158b	FITC	Biolegend	312603	DX27	Mouse IgG2a, κ
CD16	BV785	Biolegend	302045	3G8	Mouse IgG1, κ
CD16	BV510	Biolegend	302047	3G8	Mouse IgG1, κ
CD16	APC-Cy7	Biolegend	302018	3G8	Mouse IgG1, κ
CD161	BV711	BD	563865	DX12	Mouse IgG1, κ
CD19	BV510	Biolegend	302242	HIB19	Mouse IgG1, κ
CD19	AF700	eBioscience	56-0199-41	HIB19	Mouse IgG1, κ
CD19	PE-Cy7	Biolegend	302216	HIB19	Mouse IgG1, κ
CD19	BV785	Biolegend	302239	HIB19	Mouse IgG1, κ
CD19	FITC	Biolegend	302205	HIB19	Mouse IgG1, κ
CD196 (CCR6)	AF647	BD	560466	11A9	Mouse IgG1, κ
CD294 (CRTH2)	PerCP-Cy5.5	BD	561660	BM16	**Rat** WI IgG2a, κ
CD294 (CRTH2)	BIOT	eBioscience	13-2949-80	BM16	**Rat** IgG2a
CD3	BV510	Biolegend	300447	UCHT1	Mouse IgG1, κ
CD3	PE-CF594	BD	562310	UCHT1	Mouse IgG1, κ
CD3	PerCP-Cy5.5	Biolegend	300429	UCHT1	Mouse IgG1, κ
CD3	PB	Invitrogen	MHCD0328	S4.1	Mouse IgG1, κ
CD3	PE	Biolegend	300408	UCHT1	Mouse IgG1, κ
CD3	BV785	Biolegend	317330	OKT3	Mouse IgG1, κ
CD303 (BDCA-2)	FITC	Miltenyi	130-090-510	AC144	Mouse IgG1, κ
CD314 (NKG2D)	PE-CF594	BD	562498	1D11	Mouse IgG1, κ
CD335 (NKp46)	PE-Cy7	BD	562101	9E2	Mouse IgG1, κ
CD335 (NKp46)	APC	BD	558051	9E2	Mouse IgG1, κ
CD335 (NKp46)	BV650	Biolegend	331928	9E2	Mouse IgG1, κ
CD336 (NKp44)	PE	Biolegend	325108	P44-8	Mouse IgG1, κ
CD336 (NKp44)	APC	Biolegend	325109	P44-8	Mouse IgG1, κ
CD34	BV510	Biolegend	343528	581	Mouse IgG1, κ
CD34	APC	Invitrogen	CD34-581-05	581	Mouse IgG1, κ
CD38	PE	Biolegend	303506	HIT2	Mouse IgG1, κ
CD4	APC-Cy7	Biolegend	300518	RPA-T4	Mouse IgG1, κ
CD45	PB	Biolegend	304029	HI30	Mouse IgG1, κ
CD56	PE-Cy7	BD	335826	NCAM16	Mouse IgG2b, κ
CD62L	FITC	BD	561914	DREG-56	Mouse IgG1, κ
CD69	FITC	Invitrogen	MHCD6901	CH/4	Mouse IgG2a
CD8	PerCP	Biolegend	344708	SK1	Mouse IgG1, κ
CD94	APC-Vio770	Miltenyi	130-101-146	REA113	recomb **Human** IgG1
CD94	FITC	Biolegend	305504	DX22	Mouse IgG1, κ
CD94	PE	BD	555889	HP-3D9	Mouse IgG1, κ
EOMES	FITC	eBioscience	11-4877-41	WD1928	Mouse IgG1, κ
EOMES	PerCP-eFluor710	eBioscience	46-4877-42	WD1928	Mouse IgG1, κ
FceR1	BV510	Biolegend	334626	AER-37	Mouse IgG2b, κ
Granzyme B	AF700	BD	561016	GB11	Mouse IgG1, κ
HLA-A2	FITC	Biolegend	343303	BB7.2	Mouse IgG2b, κ
HLA-DR	APC	Biolegend	307610	L243	Mouse IgG2a, κ
HLA-DR	FITC	Biolegend	307604	L243	Mouse IgG2a, κ
IFNg	APC	eBioscience	17-7319-82	4S.B3	Mouse IgG1, κ
IL-22	PE-Cy7	eBioscience	25-7229-41	22URTI	Mouse IgG1, κ
KI67	AF647	BD	558615	B56	Mouse IgG1, κ
mCD45	AF700	BioLegend	103127	30-F11	Rat IgG2b, κ
Perforin	AF488	BD	563764	δG9	Mouse IgG2b, κ
RORgt	APC	eBioscience	17-6988-82	AFKJS9	**Rat** IgG2a
streptavidin	BV510	Biolegend	405233		
T-bet	BV650	BD	564142	O4-46	Mouse IgG1, κ
T-bet	PE	eBioscience	12-5825-80	eBio4B10	Mouse IgG1, κ
T-bet	PerCP-Cy5.5	eBioscience	45-5825-80	eBio4B10	Mouse IgG1
T-bet	PE-CF594	BD	562467	O4-46	Mouse IgG1, κ
TCRab	BIOT	Biolegend	306703	IP26	Mouse IgG1, κ
TCRab	PerCP-Cy5.5	Biolegend	306723	IP26	Mouse IgG1, κ
TCRgd	BV510	Biolegend	331219	B1	Mouse IgG1, κ
TCRgd	PerCP-Cy5.5	Biolegend	331223	B1	Mouse IgG1, κ
TNFa	PE-Cy7	BD	560923	MAb11	Mouse IgG1, κ

Table 3 List of antibodies used in flow cytometry

Expansion of ILCs

ILCs were seeded with irradiated allogeneic peripheral blood mononuclear cells (PBMCs) and B-lymphoblastoid cell line (LCL) 721.221 (details in Tables 1 and 2) in the presence of phytohemagglutinin (PHA-L) (2.5 µg/ml, EMD Millipore) and cytokines (Peprotech); the latter were replenished every 3-4 days from day 5. ILCs were stimulated with IL-2 (600 U/ml), IL-7 (10 ng/ml), IL-12 (50 ng/ml), IL-15 (20 ng/ml), IL-18 (50 ng/ml), or combinations thereof as described in the figures. Cytokine mixes stated in Figure 2A are shown in Table 4. Medium for NK cells was supplemented with IL-15; IL-12 was added in the initial experiments but it diminished their viability. Cultures were maintained in RPMI + 10% human serum AB (Bioconcept) + L-glutamine (2 mM, Gibco) + gentamicin (20 µg/ml) at 37°C with 5% CO_2 for 2-6 weeks as indicated in the figures. For the clonal assay, ILC3s were single-cell sorted into 96-well plates preseeded with irradiated Cell Trace Violet-labeled feeders, expanded with IL-2 + IL-7 or IL-12 + IL-15 and analyzed after 21 days.

Cytokine production, degranulation and cytotoxicity assays

The human erythroleukemia cell line K562 served as target in all functional assays. For flow cytometric analyses, K562 cells were labeled with Cell Trace Violet (Invitrogen), according to the manufacturers instructions, in order to distinguish them from ILCs.

For cytokine production or cytotoxic effector molecule release, cultured ILCs were stimulated with K562 cells at an effector to target ratio of 1:1 or with 10 ng/ml PMA and 500 ng/ml ionomycin (both from Sigma Aldrich) for 4 hours. After 45 minutes 2 µM monensin (eBioscience) and 5 µg/ml Brefeldin A (Sigma Aldrich) were added.

For degranulation assays, cultured ILCs were co-incubated with K562 cells at a ratio of 1:1 in the presence of FITC-conjugated anti-CD107a mAb. After 1 hour degranulation was blocked by addition of GolgiStop (BD Biosciences) according to manufacturer's protocol and after a total of 4 hrs CD107a surface expression on effector cells was assessed.

To detect spontaneous degranulation or constitutive expression of cytokines/cytotoxic effectors, a control without target cells was included.

For cytotoxicity evaluated by flow cytometry, target cells were labeled with Cell Trace Violet and plated (1×10^4 cells/well) with effectors at the indicated ratios for 4 or 18 hours. Cells were then stained with 0.1 µM TO-PRO-3, a membrane impermeable DNA dye, and analyzed by flow cytometry. Spontaneous lysis was determined from target only wells. Percent specific lysis was calculated according to the formula:

$$\% \text{ Specific lysis} = \left(1 - \frac{\% \text{ alive cells at end}}{\% \text{ alive cells at start}}\right) \times 100$$

% alive cells at start = average % alive cells in target only wells

For cytolytic activity determined by LDH assay (ThermoFisher), K562 cells (2×10^3 cells/well) were incubated with effectors at the indicated ratios for 4 and/or 18 hours. Percent cytotoxicity was calculated according to the formula:

$$\% \text{ Cytotoxicity} = \left(\frac{\text{Experimental value - Effector Cells Spontaneous Control - Target Cells Spontaneous Control}}{\text{Target Cell Maximum Control - Target Cells Spontaneous Control}}\right) \times 100$$

EBV production and infection

293/EBV-wt cells were seeded onto poly-D-lysine (Sigma Aldrich) pre-coated 10 cm^2 plates (CORNING) at high density (3×10^6 cells) and maintained ON in antibiotic-free medium. They were then lytically induced by transfection with p509 (carrying *BZLF1*) and p2670 (carrying *BALF4*) plasmids using Metafectene PRO (Biontex). Plasmids (1.5 µg each/plate/600 µl RPMI) were mixed with Metafectene (16 µl /plate/600 µl RPMI) and after 15-min incubation at RT added to the cells. The medium was replaced after 4-5 hours. After 3 days supernatants were harvested, centrifuged (2000 g, 10 min), filtered (0.45 µm), concentrated via ultra-centrifugation (30 000 g, 2 hrs) and stored at 4°C. The virus was titered on Raji cells and infection assessed after 2 days by expression of GFP (encoded on p2089 (Delecluse et al., 1998)). Humanized mice were infected via intraperitoneal injection of $1\text{-}2 \times 10^5$ Raji-infecting units (RIUs).

Lentiviral vector production and infection

GFP-encoding lenvirus was produced by transient transfection of 293T cells with the self-inactivating pCLX-UBI-GFP, psPAX2 (encoding gag/pol), and pCAG-VSVG (encoding the G protein of vesicular stomatitis virus glycoprotein (VSV-G)) as described previously (Giry-Laterrière et al., 2011). The following modifications were made – 4.6 x 10^6 cells were seeded per 10 cm^2 plate, 0.25 M $CaCl_2$ was used for transfection, plasmid concentration per plate was 5 µg for pCAG-VSVG and 10 µg of the other two, and supernatant was collected 30-32 hours after addition of fresh medium. Virus was concentrated the next day using Vivapure Lentiselect 40 (Sartorius stedim) according to manufacturers instructions and stored at -80°C. Plasmids (Figure 13) and protocols were kindly provided by Dr. Renier Myburgh and Prof. Roberto Speck. ILC3s were transduced ON (MOI not determined). After circa 6 weeks expansion cells were sorted as live $CD117^+CD94^-$ cells and GFP expression was assessed.

Adoptive transfer experiments

ILC3s defined as $CD45^+Lin^-CD127^+CD117^+$($NKp44^+$ or NCR^-) cells were sorted from pooled spleens.

For short-term experiments freshly isolated ILC3s were labeled with Cell Trace Violet and injected intravenously into recipient mice from the same HFL cohort (Table 2). Cells were injected at steady state, at week 4 post EBV infection (1×10^5 RIU/mouse) or 14 hours after treatment with polyICLC (Hiltonol, kindly provided by Andres Salazar, Oncovir). PolyICLC was injected according to supplier's recommendation – twice at 24 hours interval, 50 µg/mouse per shot, intraperitoneal. After 4 days mice were sacrificed and organs (PB, spleen, liver, lung, LNs) were harvested for analyses.

For long-term experiments ILC3s were expanded with IL-2 and IL-7 for 5-6 weeks, re-sorted as $CD117^+CD94^-$ cells and injected intravenously at 1×10^6 cells/mouse, one day before EBV injection ($1\text{-}2 \times 10^5$ RIU/mouse). For autologous I and II experiments recipient mice were from the same HFL cohort, in the latter 11.6% of ILC3 were GFP^+. For the allogeneic experiment ILC3s derived from HLA-$A2^+$ reconstitutions were transferred in mice engrafted with $CD34^+$ HPCs from HLA-$A2^-$ donors. Body weight (BW) measurements were performed at 3 day intervals as weight loss is associated with symptomatic EBV

infection (Chijioke et al., 2013). Mice were sacrificed circa 6 weeks after virus inoculation and organs (PB, spleen, liver, lung, LNs and small intestine) were collected for analyses. Splenomegaly (ratio spleen to BW) was assessed, as an indicator for $CD8^+$ T cell expansion in response to EBV (Chijioke et al., 2013); inversion of the CD4:CD8 ratio was evaluated by flow cytometry. Tumor burden was determined macroscopically.

Quantification of viral load

DNA from whole blood was extracted using NucliSENS (bioMérieux) and from splenic tissue with QIAamp tissue Kit (QIAGEN) according to the manufacturers protocols. Quantification of EBV DNA was performed by TaqMan (Applied Biosystems) real-time PCR as previously described (Berger et al., 2001), with modified primers for the *Bam*H1 W fragment (5′-CTTCTCAGTCCAGCGCGTTT-3′ and 5′-CAGTGGTCCCCCTCCCTAGA-3′) and a fluorogenic probe (5′-(FAM)-CGTAAGCCAGACAGCAGCCAATTGTCAG-(TAMRA)-3′). The amplification was performed using ABI Prism 7700 Sequence Detector (Applied Biosystems). Mice were considered uninfected if EBV DNA was below detection limit in blood and spleen during the course of infection.

RNA sequencing

Total RNA was isolated using PicoPure RNA isolation kit (ThermoFisher) by Dr. Frank Lehmann. $NKp44^+$ ILC3s were either transferred to lysis buffer right after sorting or differentially cultured for 3 weeks. Samples were stored at -80°C until use. 2 000 – 15 000 freshly isolated spleen ILC3s, 900 – 9 000 tonsil ILC3s and 10 000 expanded cells were used for RNA isolation. Quality control and sequencing was performed by the Genomics Facility Basel (Department of Biosystems Science and Engineering, ETH). Data was analyzed by Dr. Robert Ivanek.

Statistical analysis

Comparison between differentially cultured ILCs was done via paired t-test. Spearman coefficient was used to determine correlation between cytotoxicity (LDH assay) and expression of NK markers. Data from adoptive transfer experiments was analyzed using Mann-Whitney test. p-values below 0.05 were

considered statistically significant (* $p < 0.05$, ** $p < 0.01$, *** $p < 0.001$). Statistical analysis was performed using Prism software (GraphPad). Data is displayed as mean ± standard deviation (SD), unless otherwise stated.

Appendix

Figure 13

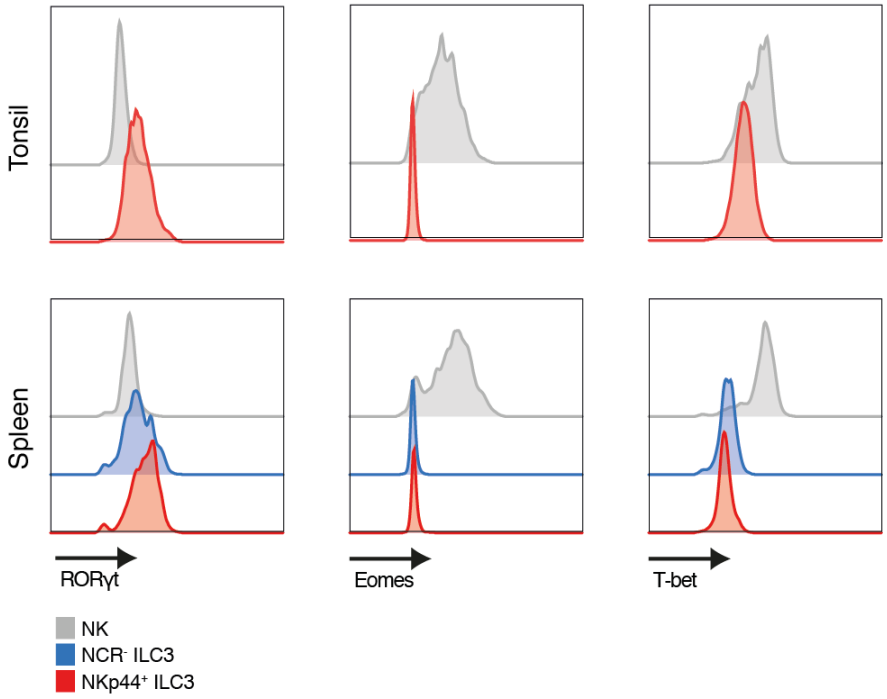

Figure 13 Expression of lineage-specific transcription factors in the purified ILC populations

Figure 14

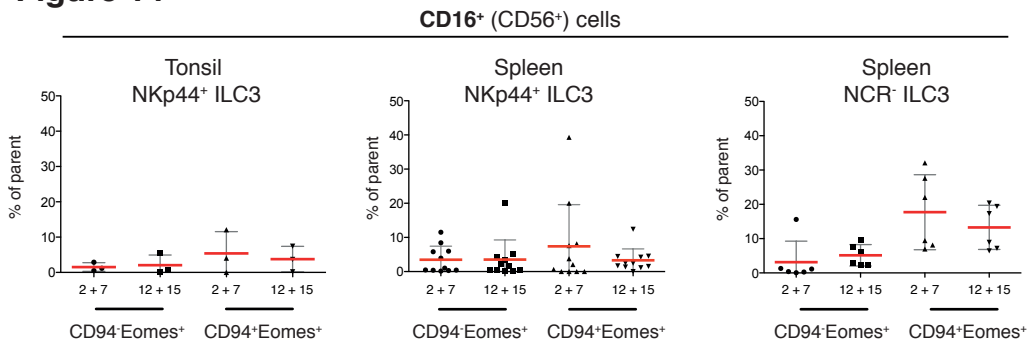

Figure 14 Frequency of CD16⁺CD56⁺ among Eomes-expressing CD94⁺ or CD94⁻ cells

ILC3s were cultured for 3 weeks and analyzed for expression of NK markers.

Figure 15

gsea_camera_Hallmark Signatures_(groupTo_c - groupTo_b) - (groupSp_c - groupSp_b)

GeneSet	NGenes	Correlation	Direction	absLog2FC	PValue	adj.P.Val
HALLMARK_E2F_TARGETS	200	0.01	Up	0.82448184	1.64E-27	8.22E-26
HALLMARK_G2M_CHECKPOINT	197	0.01	Up	0.78250316	2.70E-20	6.76E-19
HALLMARK_MYC_TARGETS_V1	200	0.01	Up	0.35807237	1.45E-10	2.42E-09
HALLMARK_MITOTIC_SPINDLE	196	0.01	Up	0.63574302	0.0004397	0.004397
HALLMARK_SPERMATOGENESIS	86	0.01	Up	0.64825292	0.0005636	0.004621
HALLMARK_INTERFERON_ALPHA_RESPONSE	96	0.01	Up	0.5557815	0.000647	0.004621
HALLMARK_DNA_REPAIR	147	0.01	Up	0.40146496	0.01157	0.04133
HALLMARK_MTORC1_SIGNALING	200	0.01	Up	0.45739145	0.01293	0.0431
HALLMARK_OXIDATIVE_PHOSPHORYLATION	199	0.01	Up	0.24835189	0.02028	0.06337
HALLMARK_MYC_TARGETS_V2	58	0.01	Up	0.37628488	0.02302	0.06495
HALLMARK_PANCREAS_BETA_CELLS	21	0.01	Up	0.53144877	0.0261	0.06869
HALLMARK_UNFOLDED_PROTEIN_RESPONSE	112	0.01	Up	0.33872813	0.1267	0.2346
HALLMARK_FATTY_ACID_METABOLISM	138	0.01	Up	0.47480136	0.1653	0.2786
HALLMARK_PI3K_AKT_MTOR_SIGNALING	94	0.01	Up	0.37509976	0.3861	0.5905
HALLMARK_PROTEIN_SECRETION	90	0.01	Up	0.28419781	0.3897	0.5905
HALLMARK_TGF_BETA_SIGNALING	52	0.01	Up	0.48719748	0.5838	0.7484
HALLMARK_PEROXISOME	90	0.01	Up	0.44483689	0.5995	0.7493
HALLMARK_ADIPOGENESIS	184	0.01	Up	0.4596987	0.7835	0.8903
HALLMARK_INTERFERON_GAMMA_RESPONSE	196	0.01	Up	0.5571115	0.9532	0.9645
HALLMARK_ESTROGEN_RESPONSE_LATE	155	0.01	Up	0.74612191	0.9596	0.9645
HALLMARK_GLYCOLYSIS	177	0.01	Up	0.56568199	0.9645	0.9645

gsea_camera_Immunologic Signatures_(groupTo_c - groupTo_b) - (groupSp_c - groupSp_b)

GeneSet	NGenes	Correlation	Direction	absLog2FC	PValue	adj.P.Val
GSE15750_DAY6_VS_DAY10_TRAF6KO_EFF_CD8_TCELL_UP	194	0.01	Up	1.10161779	7.88E-32	3.84E-28
GSE15750_DAY6_VS_DAY10_EFF_CD8_TCELL_UP	194	0.01	Up	1.09683414	1.78E-26	4.34E-23
GSE13547_CTRL_VS_ANTI_IGM_STIM_BCELL_12H_UP	178	0.01	Up	1.03497816	4.48E-22	7.27E-19
GSE39556_CD8A_DC_VS_NK_CELL_MOUSE_3H_POST_POLYIC_INJ_UP	197	0.01	Up	0.86805312	1.74E-21	2.12E-18
GSE30962_PRIMARY_VS_SECONDARY_ACUTE_LCMV_INF_CD8_TCELL_UP	190	0.01	Up	0.9778937	4.44E-21	4.33E-18
GSE36476_CTRL_VS_TSST_ACT_72H_MEMORY_CD4_TCELL_YOUNG_DN	200	0.01	Up	0.90828096	4.16E-19	3.38E-16
GSE37532_WT_VS_PPARG_KO_VISCERAL_ADIPOSE_TISSUE_TREG_UP	196	0.01	Up	0.76230229	2.94E-18	2.05E-15
GSE27241_WT_VS_RORGT_KO_TH17_POLARIZED_CD4_TCELL_UP	144	0.01	Up	0.95613779	3.61E-18	2.20E-15
GSE14415_TCONV_VS_FOXP3_KO_INDUCED_TREG_DN	181	0.01	Up	0.7930824	5.33E-18	2.89E-15
GSE18893_TCONV_VS_TREG_24H_TNF_STIM_UP	200	0.01	Up	0.68155295	2.70E-17	1.20E-14

gsea_camera_Immunologic Signatures_groupTo_c - groupTo_a

GeneSet	NGenes	Correlation	Direction	absLog2FC	PValue	adj.P.Val
GSE15750_DAY6_VS_DAY10_EFF_CD8_TCELL_UP	194	0.01	Up	2.61790282	2.49E-33	1.21E-29
GSE15750_DAY6_VS_DAY10_TRAF6KO_EFF_CD8_TCELL_UP	194	0.01	Up	2.6106981	7.23E-33	1.76E-29
GSE36476_CTRL_VS_TSST_ACT_72H_MEMORY_CD4_TCELL_YOUNG_DN	200	0.01	Up	2.23779927	1.53E-31	2.48E-28
GSE36476_CTRL_VS_TSST_ACT_72H_MEMORY_CD4_TCELL_OLD_DN	200	0.01	Up	2.05298697	5.54E-31	6.75E-28
GSE22886_UNSTIM_VS_IL15_STIM_NKCELL_DN	199	0.01	Up	1.54045808	7.83E-31	7.63E-28
GSE36476_CTRL_VS_TSST_ACT_40H_MEMORY_CD4_TCELL_YOUNG_DN	199	0.01	Up	2.14358688	1.14E-27	9.23E-25
GSE21063_WT_VS_NFATC1_KO_8H_ANTI_IGM_STIM_BCELL_UP	199	0.01	Up	2.25222054	3.19E-26	2.17E-23
GSE13547_2H_VS_12_H_ANTI_IGM_STIM_BCELL_DN	180	0.01	Up	1.89269583	3.56E-26	2.17E-23
GSE13547_CTRL_VS_ANTI_IGM_STIM_BCELL_12H_UP	178	0.01	Up	2.39952657	6.60E-26	3.25E-23
GSE36476_CTRL_VS_TSST_ACT_40H_MEMORY_CD4_TCELL_OLD_DN	200	0.01	Up	1.87616796	6.68E-26	3.25E-23

gsea_camera_Immunologic Signatures_groupTo_c - groupTo_b

GeneSet	NGenes	Correlation	Direction	absLog2FC	PValue
GSE22886_UNSTIM_VS_IL15_STIM_NKCELL_DN	199	0.01	Up	0.86622923	1.31E-30
GSE3982_MEMORY_CD4_TCELL_VS_TH1_DN	199	0.01	Up	1.05812425	5.67E-27
GSE22886_UNSTIM_VS_IL2_STIM_NKCELL_DN	200	0.01	Up	0.83524491	3.08E-26
GSE32986_UNSTIM_VS_GMCSF_AND_CURDLAN_LOWDOSE_STIM_DC_UP	197	0.01	Up	1.02023062	6.27E-26
GSE13547_2H_VS_12_H_ANTI_IGM_STIM_BCELL_DN	180	0.01	Up	1.01848291	8.61E-24
GSE36476_CTRL_VS_TSST_ACT_72H_MEMORY_CD4_TCELL_YOUNG_DN	200	0.01	Up	1.05137605	1.43E-23
GSE22886_NAIVE_CD4_TCELL_VS_48H_ACT_TH1_DN	200	0.01	Up	0.77705095	4.94E-23
GSE2770_IL12_AND_TGFB_ACT_VS_ACT_CD4_TCELL_6H_DN	194	0.01	Up	0.95170777	2.58E-22
GSE28726_NAIVE_CD4_TCELL_VS_NAIVE_VA24NEG_NKTCELL_UP	196	0.01	Up	0.97631202	3.26E-22
GSE3982_MEMORY_CD4_TCELL_VS_TH2_DN	199	0.01	Up	0.94394918	5.83E-22

Figure 15 GSEA analysis for tonsillar NKp44⁺ ILC3s

To address the enhanced cytotoxicity over controls in tonsil (To)- but not spleen (Sp)-derived NKp44⁺ ILC3s we assessed differential expression of IL-12 plus IL-15 (c) and IL-2 plus IL-7 (b) treated cells between the tissues. To c-a indicates up-regulated gene signatures in IL-12 and IL-15 cultures relative to freshly sorted cells, whereas To c-b relative to the IL-2 and IL-7 condition

Figure 16

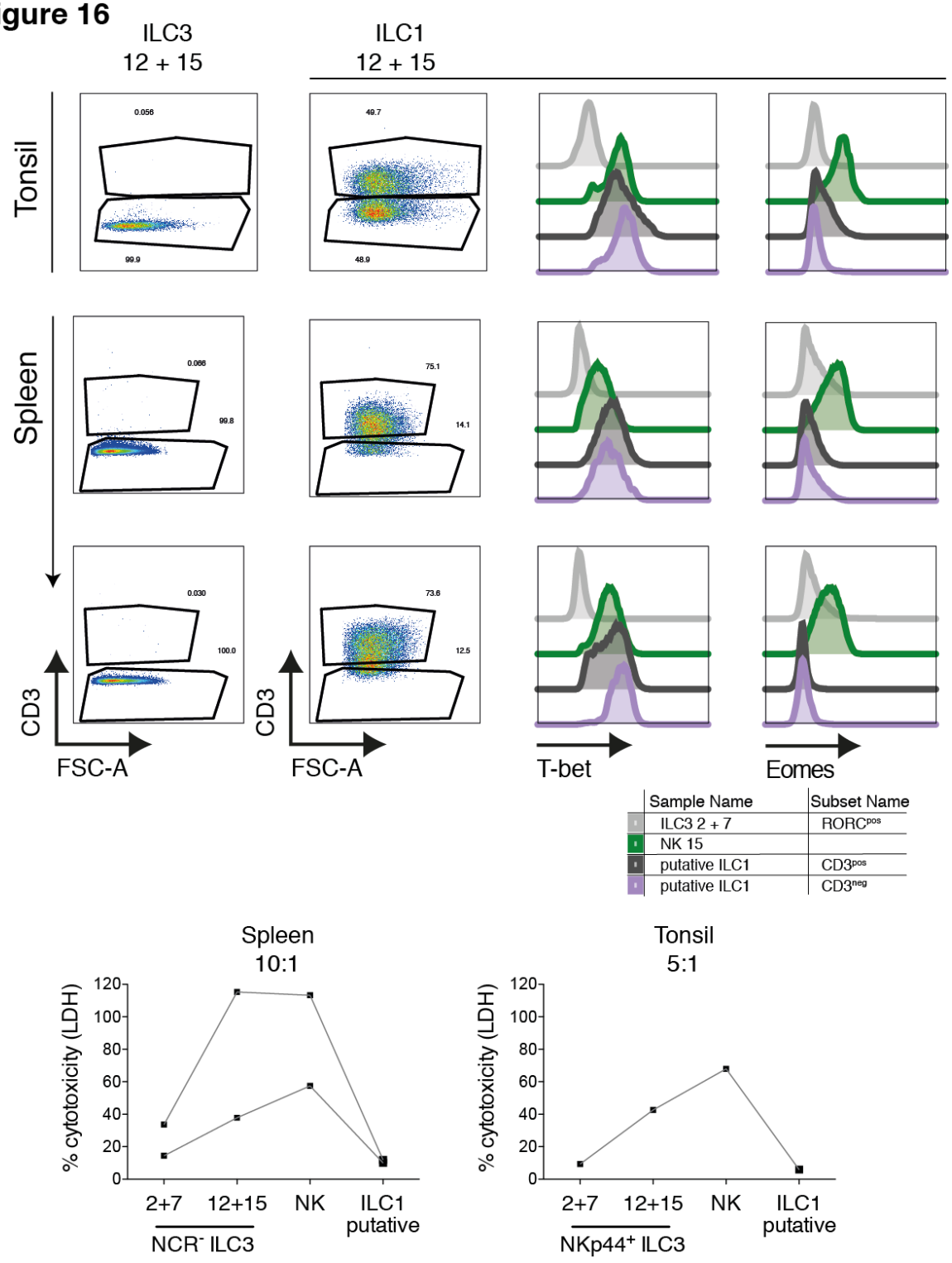

Figure 16 Analysis of putative ILC1s
Putative ILC1s sorted as viable CD45⁺ Lin⁻CD94⁻CD127⁺CD117⁻NKp44⁻ cells were cultured for 3 weeks with IL-12 and IL-15 and analyzed for CD3 and T-box transcription factors. Cytolytic activity determined though LDH release was compared to the ILC3 differential cultures in an 18-hour assay against K562 cells.

Abbreviations

EBV	Epstein Barr Virus
ILC	innate lymphoid cell
cNK	conventional natural killer cell
TCR	T cell receptor
CLP	common lymphoid progenitor
RAG	recombination-activating genes
Lin	lineage
Th	T helper
PB	peripheral blood
BM	bone marrow
ieILC1	intraepithelial ILC1
HSC	hematopoietic stem cells
αLP	$\alpha4\beta7^+$ lymphoid progenitor
Flt3	FMS-like tyrosine kinase 3
EILP	early ILC progenitor
FL	fetal liver
CHILP	common helper-like ILC precursor
PLZF	promyelocytic leukemia zinc finger
LTi	lymphoid tissue inducer cells
RORγt	RAR-related orphan receptor gamma
LN	lymph node
PP	Peyer's patches
fm	fate map
LP	lamina propria
Eomes	eomesodermin
hILC1	helper ILC1
DC	dendritic cell
NKP	NK precursor
TNF	tumor necrosis factor
TRAIL	tumor necrosis factor (TNF)–related apoptosis-inducing ligand

KO	knock-out
Tg	transgenic
HPC	hematopoietic progenitor cell
UCB	umbilical cord blood
AHR	aryl hydrocarbon receptor
SCF	stem cell factor
NSG	NOD/SCIDγc^{null} mice
SCID	severe combined immunodeficiency
Gzm	granzyme
KIR	killer immunoglobulin-like receptor
NKG2	natural-killer group 2 (receptor)
HLA	human leukocyte antigen
MICA	MHC class I chain-related protein A
ULBP	UL-16 binding proteins
HCMV	human cytomegalovirus
ADCC	antibody-dependent cellular cytotoxicity
DNAM-1	DNAX Accessory Molecule-1
SLT	secondary lymphoid tissues
S1P	sphingosine 1-phosphate
HVEM	herpes virus entry mediator
TLR	Toll-like receptor
IFN	interferon
CRTH2	prostaglandin D2 receptor 2
HSCT	hematopoietic stem cell transplantation

Declaration

Herewith I declare that I have written this thesis myself and have only used the stated references.
Zürich, Switzerland 25.04.2017

_____

Ana Raykova

References

Appay, V., Zaunders, J.J., Papagno, L., Sutton, J., Jaramillo, A., Waters, A., Easterbrook, P., Grey, P., Smith, D., McMichael, A.J., et al. (2002). Characterization of CD4(+) CTLs ex vivo. J. Immunol. *168*, 5954–5958.

Azzi, T., Lünemann, A., Murer, A., Ueda, S., Béziat, V., Malmberg, K.-J., Staubli, G., Gysin, C., Berger, C., Münz, C., et al. (2014). Role for early-differentiated natural killer cells in infectious mononucleosis. Blood *124*, 2533–2543.

Bal, S.M., Bernink, J.H., Nagasawa, M., Groot, J., Shikhagaie, M.M., Golebski, K., van Drunen, C.M., Lutter, R., Jonkers, R.E., Hombrink, P., et al. (2016). IL-1β, IL-4 and IL-12 control the fate of group 2 innate lymphoid cells in human airway inflammation in the lungs. Nat Immunol *17*, 636–645.

Balfour, H.H., Odumade, O.A., Schmeling, D.O., Mullan, B.D., Ed, J.A., Knight, J.A., Vezina, H.E., Thomas, W., and Hogquist, K.A. (2013). Behavioral, virologic, and immunologic factors associated with acquisition and severity of primary Epstein-Barr virus infection in university students. J. Infect. Dis. *207*, 80–88.

Berger, C., Day, P., Meier, G., Zingg, W., Bossart, W., and Nadal, D. (2001). Dynamics of Epstein-Barr virus DNA levels in serum during EBV-associated disease. J. Med. Virol. *64*, 505–512.

Bernink, J.H., Krabbendam, L., Germar, K., de Jong, E., Gronke, K., Kofoed-Nielsen, M., Munneke, J.M., Hazenberg, M.D., Villaudy, J., Buskens, C.J., et al. (2015). Interleukin-12 and -23 Control Plasticity of CD127(+) Group 1 and Group 3 Innate Lymphoid Cells in the Intestinal Lamina Propria. Immunity *43*, 146–160.

Bernink, J.H., Peters, C.P., Munneke, M., Velde, te, A.A., Meijer, S.L., Weijer, K., Hreggvidsdottir, H.S., Heinsbroek, S.E., Legrand, N., Buskens, C.J., et al. (2013). Human type 1 innate lymphoid cells accumulate in inflamed mucosal tissues. Nat Immunol *14*, 221–229.

Béziat, V., Dalgard, O., Asselah, T., Halfon, P., Bedossa, P., Boudifa, A., Hervier, B., Theodorou, I., Martinot, M., Debré, P., et al. (2012). CMV drives clonal expansion of NKG2C+ NK cells expressing self-specific KIRs in chronic hepatitis patients. European Journal of Immunology *42*, 447–457.

Béziat, V., Descours, B., Parizot, C., Debré, P., and Vieillard, V. (2010). NK cell terminal differentiation: correlated stepwise decrease of NKG2A and acquisition of KIRs. PLoS ONE *5*, e11966.

Björkström, N.K., Ljunggren, H.-G., and Michaëlsson, J. (2016). Emerging insights into natural killer cells in human peripheral tissues. Nat. Rev. Immunol. *16*, 310–320.

Björkström, N.K., Riese, P., Heuts, F., Andersson, S., Fauriat, C., Ivarsson, M.A., Björklund, A.T., Flodström-Tullberg, M., Michaëlsson, J., Rottenberg, M.E., et al. (2010). Expression patterns of NKG2A, KIR, and CD57 define a process of CD56dim NK-cell differentiation uncoupled from NK-cell education. Blood *116*, 3853–3864.

Bjorklund, A.K., Forkel, M., Picelli, S., Konya, V., Theorell, J., Friberg, D., Sandberg, R., Mjosberg, J. (2016). The heterogeneity of human CD127(+) innate lymphoid cells

revealed by single-cell RNA sequencing. Nat Immunol 1–13.

Boyman, O., Ramsey, C., Kim, D.M., Sprent, J., and Surh, C.D. (2008). IL-7/anti-IL-7 mAb complexes restore T cell development and induce homeostatic T Cell expansion without lymphopenia. J. Immunol. *180*, 7265–7275.

Bryceson, Y.T., Ljunggren, H.-G., and Long, E.O. (2009). Minimal requirement for induction of natural cytotoxicity and intersection of activation signals by inhibitory receptors. Blood *114*, 2657–2666.

Buonocore, S., Ahern, P.P., Uhlig, H.H., Ivanov, I.I., Littman, D.R., Maloy, K.J., and Powrie, F. (2010). Innate lymphoid cells drive interleukin-23-dependent innate intestinal pathology. Nature *464*, 1371–1375.

Burkhard, S.H., Mair, F., Nussbaum, K., Hasler, S., and Becher, B. (2014). T cell contamination in flow cytometry gating approaches for analysis of innate lymphoid cells. PLoS ONE *9*, e94196.

Cao, Z., Xiong, J., Takeuchi, M., Kurama, T., and Goeddel, D.V. (1996). TRAF6 is a signal transducer for interleukin-1. Nature *383*, 443–446.

Carrega, P., Loiacono, F., Di Carlo, E., Scaramuccia, A., Mora, M., Conte, R., Benelli, R., Spaggiari, G.M., Cantoni, C., Campana, S., et al. (2015). ILC3 concentrate in human lung cancer and associate with intratumoral lymphoid structures. Nature Communications *6*, 1–13.

Cella, M., and Colonna, M. (2010). Expansion of human NK-22 cells with IL-7, IL-2, and IL-1β reveals intrinsic functional plasticity. Pnas 1–6.

Cella, M., Fuchs, A., Vermi, W., Facchetti, F., Otero, K., Lennerz, J.K.M., Doherty, J.M., Mills, J.C., and Colonna, M. (2008). A human natural killer cell subset provides an innate source of IL-22 for mucosal immunity. Nature *457*, 722–725.

Chan, A., Hong, D.-L., Atzberger, A., Kollnberger, S., Filer, A.D., Buckley, C.D., McMichael, A., Enver, T., and Bowness, P. (2007). CD56bright human NK cells differentiate into CD56dim cells: role of contact with peripheral fibroblasts. J. Immunol. *179*, 89–94.

Cherrier, M., Sawa, S., and Eberl, G. (2012). Notch, Id2, and RORγt sequentially orchestrate the fetal development of lymphoid tissue inducer cells. J Exp Med *209*, 729–740.

Chijioke, O., Müller, A., Feederle, R., Barros, M.H.M., Krieg, C., Emmel, V., Marcenaro, E., Leung, C.S., Antsiferova, O., Landtwing, V., et al. (2013). Human Natural Killer CellsPrevent Infectious Mononucleosis Features by Targeting Lytic Epstein-Barr Virus Infection. Cell Reports *5*, 1489–1498.

Collins, A., Rothman, N., Liu, K., and Reiner, S.L. (2017). Eomesodermin and T-bet mark developmentally distinct human natural killer cells. JCI Insight *2*, e90063.

Constantinides, M.G., McDonald, B.D., Verhoef, P.A., and Bendelac, A. (2015). A committed precursor to innate lymphoid cells. Nature *508*, 397–401.

Crellin, N.K., Trifari, S., Kaplan, C.D., Cupedo, T., and Spits, H. (2010). Human NKp44 +IL-22 +cells and LTi-like cells constitute a stable RORC+ lineage distinct from conventional natural killer cells. J Exp Med *207*, 281–290.

Cruz-Guilloty, F., Pipkin, M.E., Djuretic, I.M., Levanon, D., Lotem, J., Lichtenheld, M.G., Groner, Y., and Rao, A. (2009). Runx3 and T-box proteins cooperate to establish the transcriptional program of effector CTLs. J Exp Med *206*, 51–59.

Cupedo, T., Crellin, N.K., Papazian, N., Rombouts, E.J., Weijer, K., Grogan, J.L., Fibbe, W.E., Cornelissen, J.J., and Spits, H. (2008). Human fetal lymphoid tissue–inducer cells are interleukin 17–producing precursors to RORC+ CD127+ natural killer–like cells. Nat Immunol *10*, 66–74.

Daussy, C., Faure, F., Mayol, K., Viel, S., Gasteiger, G., Charrier, E., Bienvenu, J., Henry, T., Debien, E., Hasan, U.A., et al. (2014). T-bet and Eomes instruct the development of two distinct natural killer cell lineages in the liver and in the bone marrow. J Exp Med *211*, 563–577.

de Saint Basile, G., Ménasché, G., and Fischer, A. (2010). Molecular mechanisms of biogenesis and exocytosis of cytotoxic granules. Nature Publishing Group *10*, 568–579.

Delecluse, H.J., Hilsendegen, T., Pich, D., Zeidler, R., and Hammerschmidt, W. (1998). Propagation and recovery of intact, infectious Epstein-Barr virus from prokaryotic to human cells. Proc. Natl. Acad. Sci. U.S.a. *95*, 8245–8250.

Di santo, J.P. (2006). Natural killer cell developmental pathways: a question of balance. Annu. Rev. Immunol. *24*, 257–286.

Dimova, D.K., and Dyson, N.J. (2005). The E2F transcriptional network: old acquaintances with new faces. Oncogene *24*, 2810–2826.

Eberl, G., Marmon, S., Sunshine, M.-J., Rennert, P.D., Choi, Y., and Littman, D.R. (2004). An essential function for the nuclear receptor RORgamma(t) in the generation of fetal lymphoid tissue inducer cells. Nat Immunol *5*, 64–73.

Eidenschenk, C., Dunne, J., Jouanguy, E., Fourlinnie, C., Gineau, L., Bacq, D., McMahon, C., Smith, O., Casanova, J.-L., Abel, L., et al. (2006). A novel primary immunodeficiency with specific natural-killer cell deficiency maps to the centromeric region of chromosome 8. Am. J. Hum. Genet. *78*, 721–727.

Eisenman, J., Ahdieh, M., Beers, C., Brasel, K., Kennedy, M.K., Le, T., Bonnert, T.P., Paxton, R.J., and Park, L.S. (2002). Interleukin-15 interactions with interleukin-15 receptor complexes: characterization and species specificity. Cytokine *20*, 121–129.

Eisenring, M., Berg, vom, J., Kristiansen, G., Saller, E., and Becher, B. (2010). IL-12 initiates tumor rejection via lymphoid tissue-inducer cells bearing the natural cytotoxicity receptor NKp46. Nat Immunol *11*, 1030–1038.

Endt, J., Eissmann, P., Hoffmann, S.C., Meinke, S., Giese, T., and Watzl, C. (2007). Modulation of 2B4 (CD244) activity and regulated SAP expression in human NK cells. European Journal of Immunology *37*, 193–198.

Facchetti, F., Blanzuoli, L., Ungari, M., Alebardi, O., and Vermi, W. (1998). Lymph node pathology in primary combined immunodeficiency diseases. Springer Semin. Immunopathol. *19*, 459–478.

Fathman, J.W., Bhattacharya, D., Inlay, M.A., Seita, J., Karsunky, H., and Weissman, I.L. (2011). Identification of the earliest natural killer cell-committed progenitor in murine bone marrow. Blood *118*, 5439–5447.

Ferlazzo, G., Pack, M., Thomas, D., Paludan, C., Schmid, D., Strowig, T., Bougras, G., Muller, W.A., Moretta, L., and Münz, C. (2004). Distinct roles of IL-12 and IL-15 in human natural killer cell activation by dendritic cells from secondary lymphoid organs. Proc. Natl. Acad. Sci. U.S.a. *101*, 16606–16611.

Fischer, A. (2007). Human primary immunodeficiency diseases. Immunity *27*, 835–845.

Foley, B., Cooley, S., Verneris, M.R., Curtsinger, J., Luo, X., Waller, E.K., Anasetti, C., Weisdorf, D., and Miller, J.S. (2012). Human cytomegalovirus (CMV)-induced memory-like NKG2C(+) NK cells are transplantable and expand in vivo in response to recipient CMV antigen. The Journal of Immunology *189*, 5082–5088.

Freud, A.G., Becknell, B., Roychowdhury, S., Mao, H.C., Ferketich, A.K., Nuovo, G.J., Hughes, T.L., Marburger, T.B., Sung, J., Baiocchi, R.A., et al. (2005). A human CD34(+) subset resides in lymph nodes and differentiates into CD56bright natural killer cells. Immunity *22*, 295–304.

Freud, A.G., Keller, K.A., Scoville, S.D., Mundy-Bosse, B.L., Cheng, S., Youssef, Y., Hughes, T., Zhang, X., Mo, X., Porcu, P., et al. (2016). NKp80 Defines a Critical Step during Human Natural Killer Cell Development. Cell Reports *16*, 379–391.

Freud, A.G., Yokohama, A., Becknell, B., Lee, M.T., Mao, H.C., Ferketich, A.K., and caligiuri, M.A. (2006). Evidence for discrete stages of human natural killer cell differentiation in vivo. J Exp Med *203*, 1033–1043.

Fuchs, A. (2005). Paradoxic inhibition of human natural interferon-producing cells by the activating receptor NKp44. Blood *106*, 2076–2082.

Fuchs, A., Vermi, W., Lee, J.S., Lonardi, S., Gilfillan, S., Newberry, R.D., Cella, M., and Colonna, M. (2013). Intraepithelial Type 1 Innate Lymphoid CellsAre a Unique Subset of IL-12- and IL-15-Responsive IFN-g-Producing Cells. Immunity *38*, 769–781.

Geremia, A., Arancibia-Cárcamo, C.V., Fleming, M.P.P., Rust, N., Singh, B., Mortensen, N.J., Travis, S.P.L., and Powrie, F. (2011). IL-23–responsive innate lymphoid cells are increased in inflammatory bowel disease. J Exp Med *208*, 1127–1133.

Gineau, L., Cognet, C., Kara, N., Lach, F.P., Dunne, J., Veturi, U., Picard, C., Trouillet, C., Eidenschenk, C., Aoufouchi, S., et al. (2012). Partial MCM4 deficiency in patients with growth retardation, adrenal insufficiency, and natural killer cell deficiency. J. Clin. Invest. *122*, 821–832.

Giry-Laterrière, M., Verhoeyen, E., and Salmon, P. (2011). Lentiviral Vectors. In Viral Vectors for Gene Therapy (Springer), pp. 183–209.

Glatzer, T., Killig, M., Meisig, J., Ommert, I., Luetke-Eversloh, M., Babic, M., Paclik, D., Blüthgen, N., Seidl, R., Seifarth, C., et al. (2013). Innate Lymphoid Cells Acquirea Proinflammatory Program upon Engagement of the Activating Receptor NKp44. Immunity *38*, 1223–1235.

Gordon, S.M., Chaix, J., Rupp, L.J., Wu, J., Madera, S., Sun, J.C., Lindsten, T., and Reiner, S.L. (2012). The Transcription Factors T-bet and Eomes Control Key Checkpoints of Natural Killer Cell Maturation. Immunity *36*, 55–67.

Goudy, K., Aydin, D., Barzaghi, F., Gambineri, E., Vignoli, M., Ciullini Mannurita, S., Doglioni, C., Ponzoni, M., Cicalese, M.P., Assanelli, A., et al. (2013). Human IL2RA null

mutation mediates immunodeficiency with lymphoproliferation and autoimmunity. Clin. Immunol. *146*, 248–261.

Gronke, K., Kofoed-Nielsen, M., and Diefenbach, A. (2016). Innate lymphoid cells, precursors and plasticity. Immunology Letters *179*, 9–18.

Gujer, C., Chatterjee, B., Landtwing, V., Raykova, A., McHugh, D., and Münz, C. (2015). Animal models of Epstein Barr virus infection. Curr Opin Virol *13*, 6–10.

Hazenberg, M.D., and Spits, H. (2014). Human innate lymphoid cells. Blood *124*, 700–709.

Hendricks, D.W., Balfour, H.H., Dunmire, S.K., Schmeling, D.O., Hogquist, K.A., and Lanier, L.L. (2014). Cutting Edge: NKG2ChiCD57+ NK Cells Respond Specifically to Acute Infection with Cytomegalovirus and Not Epstein-Barr Virus. The Journal of Immunology *192*, 4492–4496.

Hirschhorn-Cymerman, D., Budhu, S., Kitano, S., Liu, C., Zhao, F., Zhong, H., Lesokhin, A.M., Avogadri-Connors, F., Yuan, J., Li, Y., et al. (2012). Induction of tumoricidal function in CD4+ T cells is associated with concomitant memory and terminally differentiated phenotype. J Exp Med *209*, 2113–2126.

Hodgson, P.D., Grant, M.D., and Michalak, T.I. (1999). Perforin and Fas/Fas ligand-mediated cytotoxicity in acute and chronic woodchuck viral hepatitis. Clin. Exp. Immunol. *118*, 63–70.

Hoorweg, K., Peters, C.P., Cornelissen, F., Aparicio-Domingo, P., Papazian, N., Kazemier, G., Mjösberg, J.M., Spits, H., and Cupedo, T. (2012). Functional Differences between Human NKp44(-) and NKp44(+) RORC(+) Innate Lymphoid Cells. Front. Immunol. *3*, 72.

Horowitz, A., Strauss-Albee, D.M., Leipold, M., Kubo, J., Nemat-Gorgani, N., Dogan, O.C., Dekker, C.L., Mackey, S., Maecker, H., Swan, G.E., et al. (2013). Genetic and environmental determinants of human NK cell diversity revealed by mass cytometry. Science Translational Medicine *5*, 208ra145.

Hughes, T., Becknell, B., Freud, A.G., McClory, S., Briercheck, E., Yu, J., Mao, C., Giovenzana, C., Nuovo, G., Wei, L., et al. (2010). Interleukin-1b Selectively Expands and Sustains Interleukin-22. Immunity *32*, 803–814.

Hughes, T., Briercheck, E.L., Freud, A.G., Trotta, R., McClory, S., Scoville, S.D., Keller, K., Deng, Y., Cole, J., Harrison, N., et al. (2014). The Transcription Factor AHR Preventsthe Differentiation of a Stage 3 Innate Lymphoid Cell Subset to Natural Killer Cells. CellReports *8*, 150–162.

Huntington, N.D. (2014). The unconventional expression of IL-15 and its role in NK cell homeostasis. Immunol. Cell Biol. *92*, 210–213.

Huntington, N.D., Legrand, N., Alves, N.L., Jaron, B., Weijer, K., Plet, A., Corcuff, E., Mortier, E., Jacques, Y., Spits, H., et al. (2009). IL-15 trans-presentation promotes human NK cell development and differentiation in vivo. J Exp Med *206*, 25–34.

Katano, I., Takahashi, T., Ito, R., Kamisako, T., Mizusawa, T., Ka, Y., Ogura, T., Suemizu, H., Kawakami, Y., and Ito, M. (2015). Predominant development of mature and functional human NK cells in a novel human IL-2-producing transgenic NOG mouse. The Journal of Immunology *194*, 3513–3525.

Killig, M., Glatzer, T., and Romagnani, C. (2014). Recognition strategies of group 3 innate lymphoid cells. Front. Immunol. *5*, 142.

Klose, C.S.N., Flach, M., Möhle, L., Rogell, L., Hoyler, T., Ebert, K., Fabiunke, C., Pfeifer, D., Sexl, V., Fonseca-Pereira, D., et al. (2014). Differentiation of Type 1 ILCs froma Common Progenitor to All Helper-like Innate Lymphoid Cell Lineages. Cell *157*, 340–356.

Klose, C.S.N., Kiss, E.A., Schwierzeck, V., Ebert, K., Hoyler, T., d'Hargues, Y., Göppert, N., Croxford, A.L., Waisman, A., Tanriver, Y., et al. (2013). A T-bet gradient controls the fate and function of CCR6-RORγt+ innate lymphoid cells. Nature *494*, 261–265.

Kløverpris, H.N., Kazer, S.W., Mjösberg, J., Mabuka, J.M., Wellmann, A., Ndhlovu, Z., Yadon, M.C., Nhamoyebonde, S., Muenchhoff, M., Simoni, Y., et al. (2016). Innate Lymphoid Cells Are Depleted Irreversibly during Acute HIV-1 Infection in the Absence of Viral Suppression. Immunity *44*, 391–405.

Knox, J.J., Cosma, G.L., Betts, M.R., McLane, L.M. (2014). Characterization of T-bet and Eomes in peripheral human immune cells. Front Immunol 1–13.

Kruse, P.H., Matta, J., Ugolini, S., and Vivier, E. (2014). Natural cytotoxicity receptors and their ligands. Immunol. Cell Biol. *92*, 221–229.

Landtwing, V., Raykova, A., Pezzino, G., Béziat, V., Marcenaro, E., Graf, C., Moretta, A., Capaul, R., Zbinden, A., Ferlazzo, G., et al. (2016). Cognate HLA absence in trans diminishes human NK cell education. J. Clin. Invest. *126*, 3772–3782.

Lanier, L.L., and Sun, J.C. (2009). Do the terms innate and adaptive immunity create conceptual barriers? Nat Rev Immunol *9*, 302–303.

Lim, A.I., Li, Y., Lopez-Lastra, S., Stadhouders, R., Paul, F., Casrouge, A., Serafini, N., Puel, A., Bustamante, J., Surace, L., et al. (2017). Systemic Human ILC Precursors Provide a Substrate for Tissue ILC Differentiation. Cell *168*, 1086–1100.e10.

Lim, A.I., Menegatti, S., Bustamante, J., Le Bourhis, L., Allez, M., Rogge, L., Casanova, J.-L., Yssel, H., and Di santo, J.P. (2016). IL-12 drives functional plasticity of human group 2 innate lymphoid cells. J Exp Med *213*, 569–583.

Lomaga, M.A., Yeh, W.C., Sarosi, I., Duncan, G.S., Furlonger, C., Ho, A., Morony, S., Capparelli, C., Van, G., Kaufman, S., et al. (1999). TRAF6 deficiency results in osteopetrosis and defective interleukin-1, CD40, and LPS signaling. Genes Dev. *13*, 1015–1024.

Long, E.O., Kim, H.S., Liu, D., Peterson, M.E., and Rajagopalan, S. (2013). Controlling natural killer cell responses: integration of signals for activation and inhibition. Annu. Rev. Immunol. *31*, 227–258.

Lopez-Vergès, S., Milush, J.M., Pandey, S., York, V.A., Arakawa-Hoyt, J., Pircher, H., Norris, P.J., Nixon, D.F., and Lanier, L.L. (2010). CD57 defines a functionally distinct population of mature NK cells in the human CD56dimCD16+ NK-cell subset. Blood *116*, 3865–3874.

Lünemann, A., Vanoaica, L.D., Azzi, T., Nadal, D., and Münz, C. (2013). A distinct subpopulation of human NK cells restricts B cell transformation by EBV. The Journal of Immunology *191*, 4989–4995.

Mace, E.M., Dongre, P., Hsu, H.-T., Sinha, P., James, A.M., Mann, S.S., Forbes, L.R., Watkin,

L.B., and Orange, J.S. (2014). Cell biological steps and checkpoints in accessing NK cell cytotoxicity. Immunol. Cell Biol. *92*, 245–255.

Magri, G., Miyajima, M., Bascones, S., Mortha, A., Puga, I., Cassis, L., Barra, C.M., Comerma, L., Chudnovskiy, A., Gentile, M., et al. (2014). Innate lymphoid cells integrate stromal and immunological signals to enhance antibody production by splenic marginal zone B cells. Nat Immunol *15*, 354–364.

Marquardt, N., Beziat, V., Nystrom, S., Hengst, J., Ivarsson, M.A., Kekalainen, E., Johansson, H., Mjosberg, J., Westgren, M., Lankisch, T.O., et al. (2015). Cutting Edge: Identification and Characterization of Human Intrahepatic CD49a+ NK Cells. The Journal of Immunology *194*, 2467–2471.

Meixlsperger, S., Leung, C.S., Rämer, P.C., Pack, M., Vanoaica, L.D., Breton, G., Pascolo, S., Salazar, A.M., Dzionek, A., Schmitz, J., et al. (2013). CD141+ dendritic cells produce prominent amounts of IFN-α after dsRNA recognition and can be targeted via DEC-205 in humanized mice. Blood *121*, 5034–5044.

Mjösberg, J., and Spits, H. (2016). Human innate lymphoid cells. Journal of Allergy and Clinical Immunology *138*, 1265–1276.

Mjösberg, J.M., Trifari, S., Crellin, N.K., Peters, C.P., van Drunen, C.M., Piet, B., Fokkens, W.J., Cupedo, T., and Spits, H. (2011). Human IL-25- and IL-33-responsive type 2 innate lymphoid cells are defined by expression of CRTH2 and CD161. Nat Immunol *12*, 1055–1062.

Montaldo, E., Juelke, K., and Romagnani, C. (2015). Group 3 innate lymphoid cells (ILC3s): Origin, differentiation, and plasticity in humans and mice. European Journal of Immunology *45*, 2171–2182.

Montaldo, E., Teixeira-Alves, L.G., Glatzer, T., Durek, P., Stervbo, U., Hamann, W., Babic, M., Paclik, D., Stölzel, K., Gröne, J., et al. (2014). Human RORγt(+)CD34(+) cells are lineage-specified progenitors of group 3 RORγt(+) innate lymphoid cells. Immunity *41*, 988–1000.

Moroso, V., Famili, F., Papazian, N., Cupedo, T., van der Laan, L.J.W., Kazemier, G., Metselaar, H.J., and Kwekkeboom, J. (2011). NK cells can generate from precursors in the adult human liver. European Journal of Immunology *41*, 3340–3350.

Morvan, M.G., and Lanier, L.L. (2016). NK cells and cancer: you can teach innate cells new tricks. Nat. Rev. Cancer *16*, 7–19.

Mrózek, E., Anderson, P., and Caligiuri, M.A. (1996). Role of interleukin-15 in the development of human CD56+ natural killer cells from CD34+ hematopoietic progenitor cells. Blood *87*, 2632–2640.

Murphy, K., and Weaver, C. (2016). Janeway's Immunobiology, 9th edition (Garland Science).

Münz, C. (2015a). Epstein Barr Virus Volume 1 (Springer).

Münz, C. (2015b). Epstein Barr Virus Volume 2 (Springer).

Naito, A., Azuma, S., Tanaka, S., Miyazaki, T., Takaki, S., Takatsu, K., Nakao, K., Nakamura, K., Katsuki, M., Yamamoto, T., et al. (1999). Severe osteopetrosis, defective interleukin-1

signalling and lymph node organogenesis in TRAF6-deficient mice. Genes Cells *4*, 353–362.

Nikiforow, S., Bottomly, K., Miller, G., and Münz, C. (2003). Cytolytic CD4(+)-T-cell clones reactive to EBNA1 inhibit Epstein-Barr virus-induced B-cell proliferation. J. Virol. *77*, 12088–12104.

O'Donnell, K.A., Wentzel, E.A., Zeller, K.I., Dang, C.V., and Mendell, J.T. (2005). c-Myc-regulated microRNAs modulate E2F1 expression. Nature *435*, 839–843.

Ohne, Y., Silver, J.S., Thompson-Snipes, L., Collet, M.A., Blanck, J.P., Cantarel, B.L., Copenhaver, A.M., Humbles, A.A., and Liu, Y.-J. (2016). IL-1 is a critical regulator of group 2 innate lymphoid cell function and plasticity. Nat Immunol *17*, 646–655.

Ohs, I., van den Broek, M., Nussbaum, K., Münz, C., Arnold, S.J., Quezada, S.A., Tugues, S., and Becher, B. (2016). Interleukin-12 bypasses common gamma-chain signalling in emergency natural killer cell lymphopoiesis. Nature Communications *7*, 13708.

Okada, S., Markle, J.G., Deenick, E.K., Mele, F., Averbuch, D., Lagos, M., Alzahrani, M., Al-Muhsen, S., Halwani, R., Ma, C.S., et al. (2015). IMMUNODEFICIENCIES. Impairment of immunity to Candida and Mycobacterium in humans with bi-allelic RORC mutations. Science *349*, 606–613.

Orange, J.S. (2006). Human natural killer cell deficiencies. Curr Opin Allergy Clin Immunol *6*, 399–409.

Paludan, C., Bickham, K., Nikiforow, S., Tsang, M.L., Goodman, K., Hanekom, W.A., Fonteneau, J.-F., Stevanović, S., and Münz, C. (2002). Epstein-Barr nuclear antigen 1-specific CD4(+) Th1 cells kill Burkitt's lymphoma cells. J. Immunol. *169*, 1593–1603.

Pappworth, I.Y., Wang, E.C., and Rowe, M. (2007). The switch from latent to productive infection in Epstein-Barr virus-infected B cells is associated with sensitization to NK cell killing. J. Virol. *81*, 474–482.

Parolini, S., Bottino, C., Falco, M., Augugliaro, R., Giliani, S., Franceschini, R., Ochs, H.D., Wolf, H., Bonnefoy, J.Y., Biassoni, R., et al. (2000). X-linked lymphoproliferative disease. 2B4 molecules displaying inhibitory rather than activating function are responsible for the inability of natural killer cells to kill Epstein-Barr virus-infected cells. J Exp Med *192*, 337–346.

Pearce, E.L., Mullen, A.C., Martins, G.A., Krawczyk, C.M., Hutchins, A.S., Zediak, V.P., Banica, M., DiCioccio, C.B., Gross, D.A., Mao, C.-A., et al. (2003). Control of effector CD8+ T cell function by the transcription factor Eomesodermin. Science *302*, 1041–1043.

Pearce, E.L., Walsh, M.C., Cejas, P.J., Harms, G.M., Shen, H., Wang, L.-S., Jones, R.G., and Choi, Y. (2009). Enhancing CD8 T-cell memory by modulating fatty acid metabolism. Nature *460*, 103–107.

Pearson, C., Thornton, E.E., McKenzie, B., Shaupp, A.L., Huskens, N., Griseri, T., West, N>, Tung, S., Seddon, B.P., Uhlig, H.H., Powrie, F. (2016). ILC3 GM-CSF production and mobilisation orchestrate acute intestinal inflammation. eLife 1–21.

Pegram, H.J., Andrews, D.M., Smyth, M.J., Darcy, P.K., and Kershaw, M.H. (2011). Activating and inhibitory receptors of natural killer cells. Immunol. Cell Biol. *89*, 216–224.

Pelengaris, S., Khan, M., and Evan, G. (2002). c-MYC: more than just a matter of life and death. Nat. Rev. Cancer *2*, 764–776.

Pikovskaya, O., Chaix, J., Rothman, N.J., Collins, A., Chen, Y.-H., Scipioni, A.M., Vivier, E., and Reiner, S.L. (2016). Cutting Edge: Eomesodermin Is Sufficient To Direct Type 1 Innate Lymphocyte Development into the Conventional NK Lineage. The Journal of Immunology *196*, 1449–1454.

Pipkin, M.E., Sacks, J.A., Cruz-Guilloty, F., Lichtenheld, M.G., Bevan, M.J., and Rao, A. (2010). Interleukin-2 and inflammation induce distinct transcriptional programs that promote the differentiation of effector cytolytic T cells. Immunity *32*, 79–90.

Poluektova, L.Y., Garcia-Martinez, J.V., Koyanagi, Y., Manz, M.G., and Tager, A.M. (2015). Humanized Mice for HIV Research (Springer)

Possot, C., Schmutz, S., Chea, S., Boucontet, L., Louise, A., Cumano, A., and Golub, R. (2011). Notch signaling is necessary for adult, but not fetal, development of RORγt+ innate lymphoid cells. Nat Immunol *12*, 949–958.

Puel, A., Ziegler, S.F., Buckley, R.H., and Leonard, W.J. (1998). Defective IL7R expression in T(-)B(+)NK(+) severe combined immunodeficiency. Nat. Genet. *20*, 394–397.

Rajagopalan, S. and Long, E.O. (2012). KIR2DL4 (CD158d): an activation receptor for HLA-G. Front. Imunol. 1–6.

Raveney, B.J.E., Oki, S., Hohjoh, H., Nakamura, M., Sato, W., Murata, M., and Yamamura, T. (2015). Eomesodermin-expressing T-helper cells are essential for chronic neuroinflammation. Nature Communications *6*, 8437.

Renoux, V.M., Zriwil, A., Peitzsch, C., Michaëlsson, J., Friberg, D., Soneji, S., and Sitnicka, E. (2015). Identification of a Human Natural Killer Cell Lineage- Restricted Progenitor in Fetal and Adult Tissues. Immunity *43*, 394–407.

Romagnani, C., Juelke, K., Falco, M., Morandi, B., D'Agostino, A., Costa, R., Ratto, G., Forte, G., Carrega, P., Lui, G., et al. (2007). CD56brightCD16- Killer Ig-Like Receptor- NK Cells Display Longer Telomeres and Acquire Features of CD56dim NK Cells upon Activation. The Journal of Immunology *178*, 4947–4955.

Rosmaraki, E.E., Douagi, I., Roth, C., Colucci, F., Cumano, A., Di santo, J.P. (2001). Identification of committed NK cell progenitorsin adult murine bone marrow. European Journal of Immunology 1–10.

Satoh-Takayama, N., Lesjean-Pottier, S., Vieira, P., Sawa, S., Eberl, G., Vosshenrich, C.A.J., and Di santo, J.P. (2010). IL-7 and IL-15 independently program the differentiation of intestinal CD3 −NKp46 +cell subsets from Id2-dependent precursors. J Exp Med *207*, 273–280.

Satoh-Takayama, N., Vosshenrich, C.A.J., Lesjean-Pottier, S., Sawa, S., Lochner, M., Rattis, F., Mention, J.-J., Thiam, K., Cerf-Bensussan, N., Mandelboim, O., et al. (2008). Microbial Flora Drives Interleukin 22 Production in Intestinal NKp46+ cells that provide innate mucosal immune defense. Immunity *29*, 958–970.

Sawa, S., Cherrier, M., Lochner, M., Satoh-Takayama, N., Fehling, H.J., Langa, F., Di santo, J.P., and Eberl, G. (2010). Lineage relationship analysis of RORγt+ innate lymphoid cells. Science *330*, 665–669.

Scoville, S.D., Mundy-Bosse, B.L., Zhang, M.H., Chen, L., Zhang, X., Keller, K.A., Hughes, T., Chen, L., Cheng, S., Bergin, S.M., et al. (2016). A Progenitor Cell Expressing Transcription Factor RORγt Generates All Human Innate Lymphoid Cell Subsets. Immunity *44*, 1140–1150.

Shaw, R.K., Issekutz, A.C., Fraser, R., Schmit, P., Morash, B., Monaco-Shawver, L., Orange, J.S., and Fernandez, C.V. (2012). Bilateral adrenal EBV-associated smooth muscle tumors in a child with a natural killer cell deficiency. Blood *119*, 4009–4012.

Silver, J.S., Kearley, J., Copenhaver, A.M., Sanden, C., Mori, M., Yu, L., Pritchard, G.H., Berlin, A.A., Hunter, C.A., Bowler, R., et al. (2016). Inflammatory triggers associated with exacerbations of COPD orchestrate plasticity of group 2 innate lymphoid cells in the lungs. Nat Immunol *17*, 626–635.

Simoni, Y., Fehlings, M., Kløverpris, H.N., McGovern, N., Koo, S.-L., Loh, C.Y., Lim, S., Kurioka, A., Fergusson, J.R., Tang, C.-L., et al. (2017). Human Innate Lymphoid Cell Subsets Possess Tissue-Type Based Heterogeneity in Phenotype and Frequency. Immunity *46*, 148–161.

Song, C., Lee, J.S., Gilfillan, S., Robinette, M.L., Newberry, R.D., Stappenbeck, T.S., Mack, M., Cella, M., and Colonna, M. (2015). Unique and redundant functions of NKp46 +ILC3s in models of intestinal inflammation. J Exp Med *212*, 1869–1882.

Spits, H., Bernink, J.H., and Lanier, L. (2016). NK cells and type 1 innate lymphoid cells: partners in host defense. Nat Immunol *17*, 758–764.

Stegmann, K.A., Robertson, F., Hansi, N., Gill, U., Pallant, C., Christophides, T., Pallett, L.J., Peppa, D., Dunn, C., Fusai, G., et al. (2016). CXCR6 marks a novel subset of T-bet(lo)Eomes(hi) natural killer cells residing in human liver. Sci Rep 1–10.

Strowig, T., Chijioke, O., Carrega, P., Arrey, F., Meixlsperger, S., Ramer, P.C., Ferlazzo, G., and Munz, C. (2010). Human NK cells of mice with reconstituted human immune system components require preactivation to acquire functional competence. Blood *116*, 4158–4167.

Strowig, T., Brilot, F., Arrey, F., Bougras, G., Thomas, D., Muller, W.A., and Münz, C. (2008). Tonsilar NK cells restrict B cell transformation by the Epstein-Barr virus via IFN-gamma. PLoS Pathog. *4*, e27.

Suwanai, H., Wilcox, M.A., Mathis, D., and Benoist, C. (2010). A defective Il15 allele underlies the deficiency in natural killer cell activity in nonobese diabetic mice. Proceedings of the National Academy of Sciences *107*, 9305–9310.

Takeda, K., Cretney, E., Hayakawa, Y., Ota, T., Akiba, H., Ogasawara, K., Yagita, H., Kinoshita, K., Okumura, K., and Smyth, M.J. (2005). TRAIL identifies immature natural killer cells in newborn mice and adult mouse liver. Blood *105*, 2082–2089.

Theocharides, A.P.A., Rongvaux, A., Fritsch, K., Flavell, R.A., and Manz, M.G. (2016). Humanized hemato-lymphoid system mice. Haematologica *101*, 5–19.

Tugues, S., Burkhard, S.H., Ohs, I., Vrohlings, M., Nussbaum, K., Berg, vom, J., Kulig, P., and Becher, B. (2014). New insights into IL-12-mediated tumor suppression. Cell Death and Differentiation *22*, 237–246.

Vély, F., Barlogis, V., Vallentin, B., Neven, B., Piperoglou, C., Ebbo, M., Perchet, T., Petit, M.,

Yessaad, N., Touzot, F., et al. (2016a). Evidence of innate lymphoid cell redundancy in humans. Nat Immunol *17*, 1291–1299.

Vély, F., Golub, R., and Vivier, E. (2016b). HLA-Fatal attraction. Nat Immunol *17*, 1012–1014.

Vivier, E., Di Santo, J., and Moretta, A. (2016). Natural Killer Cells (Springer).

Vivier, E., Tomasello, E., Baratin, M., Walzer, T., and Ugolini, S. (2008). Functions of natural killer cells. Nat Immunol *9*, 503–510.

Vonarbourg, C., Mortha, A., Bui, V.L., Hernández, P.P., Kiss, E.A., Hoyler, T., Flach, M., Bengsch, B., Thimme, R., Hölscher, C., et al. (2010). Regulated Expression of Nuclear Receptor RORγt Confers Distinct Functional Fates to NK Cell Receptor-Expressing RORγt. Immunity *33*, 736–751.

Vosshenrich, C.A.J., Ranson, T., Samson, S.I., Corcuff, E., Colucci, F., Rosmaraki, E.E., and Di santo, J.P. (2005). Roles for common cytokine receptor gamma-chain-dependent cytokines in the generation, differentiation, and maturation of NK cell precursors and peripheral NK cells in vivo. J. Immunol. *174*, 1213–1221.

Wu, C., Li, B., Lu, R., Koelle, S.J., Yang, Y., Jares, A., Krouse, A.E., Metzger, M., Liang, F., Loré, K., et al. (2014). Clonal Tracking of Rhesus Macaque Hematopoiesis Highlights a Distinct Lineage Origin for Natural Killer Cells. Stem Cell *14*, 486–499.

Wu, H.-H., Hwang-Verslues, W.W., Lee, W.-H., Huang, C.-K., Wei, P.-C., Chen, C.-L., Shew, J.-Y., Lee, E.Y.-H.P., Jeng, Y.-M., Tien, Y.-W., et al. (2015). Targeting IL-17B-IL-17RB signaling with an anti-IL-17RB antibody blocks pancreatic cancer metastasis by silencing multiple chemokines. J Exp Med *212*, 333–349.

Yagi, R., Zhong, C., Northrup, D.L., Yu, F., Bouladoux, N., Spencer, S., Hu, G., Barron, L., Sharma, S., Nakayama, T., et al. (2014). The transcription factor GATA3 is critical for the development of all IL-7Rα-expressing innate lymphoid cells. Immunity *40*, 378–388.

Yang, Q., Li, F., Harly, C., Xing, S., Ye, L., Xia, X., Wang, H., Wang, X., Yu, S., Zhou, X., et al. (2015). TCF-1 upregulation identifies early innate lymphoid progenitors in the bone marrow. Nat Immunol *16*, 1044–1050.

Yasukawa, M., Ohminami, H., Arai, J., Kasahara, Y., Ishida, Y., and Fujita, S. (2000). Granule exocytosis, and not the fas/fas ligand system, is the main pathway of cytotoxicity mediated by alloantigen-specific CD4(+) as well as CD8(+) cytotoxic T lymphocytes in humans. Blood *95*, 2352–2355.

Yu, J., Freud, A.G., and caligiuri, M.A. (2013). Location and cellular stages of natural killer cell development. Trends in Immunology *34*, 573–582.

Yu, J., Mao, H.C., Wei, M., Hughes, T., Zhang, J., Park, I.-K., Liu, S., McClory, S., Marcucci, G., Trotta, R., et al. (2010). CD94 surface density identifies a functional intermediary between the CD56bright and CD56dim human NK-cell subsets. Blood *115*, 274–281.

Zhang, Z., Cheng, L., Zhao, J., Li, G., Zhang, L., Chen, W., Nie, W., Reszka-Blanco, N.J., Wang, F.-S., and Su, L. (2015). Plasmacytoid dendritic cells promote HIV-1–induced group 3 innate lymphoid cell depletion. Journal of Clinical Investigation *125*, 3692–3703.

Acknowledgements

First of all, I would like to thank Christian for giving me the chance to pursue a PhD in his lab. It was a tough path but I learned a lot. Thank you for your support and for staying positive even when I was not. I extend my thanks to my PhD committee, in particular Burkhard for his good suggestions, and the newest member Maries for jumping in the day before I had to submit this thesis.

I extend my gratitude to all current and former members of the lab. I would like to thank the humanized mouse team. It is not easy to share a responsibility with so many people but it always worked out and thanks to all who in the last year of my project gave me the better mice. I am especially grateful to Anita, Nici and Julia who helped me when I most needed it and Obi for always showing interest in my project even after he left the lab and finding time in his busy schedule to proofread my thesis. I would like to thank Flo for sorting when needed even when it conflicted his schedule and for introducing me together with Sabi to climbing. I especially appreciate Kathrin, just for being there, the whole time, suffering with me. Thanks for all your help.

I'm grateful to Olya, Kris, Nathi, Rosa, Migi, Iva, Tom, Margit, Mario and Isaak for all the good times outside the lab and keeping my mental health in check. I'm especially thankful to Isaak for his valuable input in all my projects and technical help. And of course to Vanessa for being a shoulder to lean on in hard times and making the good ones better.

I would like to thank my family who encouraged me all my life and always helped me when I was feeling lost.

Most of all, I thank Flavio for his patience and understanding when I was most frustrated, for being able to cheer me up no matter how hopeless I felt and for always being there when I needed him, also when that meant coming to lab after midnight to help me out.

Curriculum Vitae

Ana Plamenova Raykova

Address	Mattengasse 11 8005 Zurcih Switzerland
E-mail	raykova@immunology.uzh.ch
Telephone	+41 767 098922
Date of birth	27/03/1988
Place of birth	Sofia, Bulgaria
Nationality	Bulgarian

Education

University of Zurich 05/2011 – 06/2017
Institute of Experimental Immunology
Laboratory of Prof. Christian Münz
PhD student
Thesis title – *Type 3 Innate Lymphoid Cells Acquire a Cytotoxic Program upon Stimulation with Interleukins 12 and 15*

University of Oxford 10/2009 – 01/2011
Oxford, United Kingdom
Master of Science in Integrated Immunology
Thesis title – *Phenotype and function of γδ T cells pre- and post-vaccination with BCG and MVA85A TB vaccine candidate*

Jacobs University 09/2006 – 06/2009
Bremen, Germany
Bachelor of Science in Biochemistry and Cell Biology
Graduated with overall GPA of 1.54 on a scale of 1 to 5, where 1 is the best grade possible. Thesis title – *Tapasin role in MHC Class I peptide loading and the distribution of cathepsin B in cells are decisive factors in pathological condition*s. Mark given 1.00.

Sofia High School of Mathematics 09/2001 – 06/2006
Sofia, Bulgaria
High School Diploma
Graduated with overall GPA of 5.75 on a scale of 2 to 6, where 6 is the best grade possible.

Practical Experience

Jacobs University 09/2008 – 05/2009
Bremen, Germany
Teaching Assistant in the Advanced Biochemistry and Molecular Biology I and II Courses
Responsible for correcting and grading written assignments and examinations for second year students.

Research Experience

The Jenner Institute 04/2010 – 07/2010
Oxford, United Kingdom
MSc project in the group of Dr. Helen McShane
Studied γδ T cell phenotype and function pre- and post-vaccination with MVA85A TB vaccine candidate.

Ludwig Institute for Cancer Research 06/2009 – 07/2009
Brussels, Belgium
Internship in the group of Prof. Benoît Van den Eynde
Worked on TAP-independent presentation of tumour antigens

Jacobs University 02/2009 - 04/2009
Bremen, Germany
Guided Research in the group of Prof. Klaudia Brix
Investigated the localization of Cathepsin B in thyroid carcinoma cell lines in the presence or absence of thyroid stimulating hormone.

Jacobs University 09/2008 - 11/2008
Bremen, Germany
Guided Research in the group of Prof. Sebastian Springer
Studied the role of tapasin in peptide loading on MHC Class I molecules.

Ludwig Institute for Cancer Research 06/2008 – 07/2008
Brussels, Belgium
Internship in the group of Prof. Benoît Van den Eynde
Worked on tumour antigen processing, with focus on TAP, and the induction of anti-tumour immune responses in tumour-bearing mice.

International Conferences

16th meeting of the Society for Natural Immunity 10/2016
Taormina, Sicily, Italy
presentation

EMBO conference on Innate Lymphoid Cells 09/2014
Paris, France
attendance

RCAI International Summer Program (RISP) 06/2013
Yokohama, Japan
poster and presentation

International Symposium on Immunology 2013 06/2013
Yokohama, Japan
attendance

Publications

Cognate HLA absence in trans diminishes human NK cell education.
Landtwing V, **Raykova A**, Pezzino G, Béziat V, Marcenaro E, Graf C, Moretta A, Capaul R, Zbinden A, Ferlazzo G, Malmberg KJ, Chijioke O, Münz C.
J Clin Invest. 2016 Oct 3;126(10):3772-3782

Animal models of Epstein Barr virus infection.
Gujer C, Chatterjee B, Landtwing V, **Raykova A**, McHugh D, Münz C.
Curr Opin Virol. 2015 Aug;13:6-10. doi: 10.1016/j.coviro.2015.03.014. Epub 2015 Apr 2. Review.

Adoptive transfer of EBV specific CD8+ T cell clones can transiently control EBV infection in humanized mice.
Antsiferova O, Müller A, Rämer PC, Chijioke O, Chatterjee B, **Raykova A**, Planas R, Sospedra M, Shumilov A, Tsai MH, Delecluse HJ, Münz C.
PLoS Pathog. 2014 Aug 28;10(8):e1004333.

Dendritic cell-mediated immune humanization of mice: implications for allogeneic and xenogeneic stem cell transplantation.
Salguero G, Daenthanasanmak A, Münz C, **Raykova A**, Guzmán CA, Riese P, Figueiredo C, Länger F, Schneider A, Macke L, Sundarasetty BS, Witte T, Ganser A, Stripecke R.
J Immunol. 2014 May 15;192(10):4636-47

Spontaneous lytic replication and epitheliotropism define an Epstein-Barr virus strain found in carcinomas.
Tsai MH, **Raykova A**, Klinke O, Bernhardt K, Gärtner K, Leung CS, Geletneky K, Sertel S, Münz C, Feederle R, Delecluse HJ.
Cell Rep. 2013 Oct 31;5(2):458-70

Infectious diseases in humanized mice.
Leung C, Chijioke O, Gujer C, Chatterjee B, Antsiferova O, Landtwing V, McHugh D, **Raykova A**, Münz C.
Eur J Immunol. 2013 Sep;43(9):2246-54